

VATNAJÖKULL: Mass balance, meltwater drainage and surface velocity of the glacial year 2023_24



Institute of Earth Sciences
University of Iceland
and
National Power Company

Finnur Pálsson
Andri Gunnarsson
Eyjólfur Magnússon
Sveinbjörn Steinþórsson
Hlynur Skagfjörð Pálsson

RH-09-24

Contents:

1. Introduction
2. Diary
3. Mass balance measurements
 - 3.1 Methods
 - 3.2 Results of mass balance measurements
 - 3.2.1. Tungnaárfjökkull
 - 3.2.2. Köldukvíslarjökkull
 - 3.2.3. Dyngjujökkull
 - 3.2.4. Brúarfjökkull
 - 3.2.5. Eyjabakkajökkull
 - 3.2.6. Breiðamerkurjökkull
 - 3.2.7. Skeiðarárjökkull
 - 3.2.8. Síðujökkull
 - 3.2.9. Grímsvötn
 - 3.3. The mass balance record for Vatnajökkull
4. Surface velocity measurements
5. Melt water runoff
6. Conclusions

Figures:

- Figure 1. Outlets of Vatnajökkull and location of mass balance sites in 2023_24.
- Figure 2. Maps showing point values of specific in m water equivalent (m_{we}), 2023_24.
- Figure 3. a. Specific point mass balance (m_{we}), along all mass balance profiles 2023_24.
b. Specific point mass balance as a function of elevation on central flow lines on Vatnajökkull outlets.
- Figure 4. Specific mass balance of Vatnajökkull (m_{we}) 2023_24. Top: winter, Centre: summer Bottom: net balance.
- Figure 5. Top left: The difference between winter balance in 2023_24 and the average winter balance 1995_96 to 2022_23. Top right: The difference between summer balance in 2024 and the average summer balance 1996 to 2023. Lower left: The difference between net balance in 2023_24 and the average net balance 1995_96 to 2022_23. (Blue is higher than average balance and red lower than average).
- Figure 6. Mass balance at a central flow line on Tungnaárfjökkull 2023_24, and average mass balance 1991_92 to 2021_22 (*the horizontal red lines indicate st. dev. of the variability at the survey site during the survey period*).
- Figure 7. Specific mass balance at a central flow line on Köldukvíslarjökkull 2023_24, and average mass balance 1991_92 to 2021_22.
- Figure 8. Mass balance at a central flow line on Dyngjujökkull 2023_24, and average mass balance 1992_93 to 2021_22.
- Figure 9. Mass balance at two flow lines on Brúarfjökkull 2023_24, and average mass balance 1992_93 to 2021_22.
- Figure 10. Mass balance at a central flow line on Eyjabakkajökkull 2023_24, and average mass balance 1995_96 to 2021_22.
- Figure 11. Mass balance at a central flow line on Breiðamerkurjökkull 2023_24, and average mass balance 1995_96 to 2021_22.
- Figure 12. Mass balance at a central flow line on Skeiðarárjökkull 2023_24, and average mass balance 2004_05 to 2021_22.
- Figure 13. Mass balance at a central flow line on Síðujökkull 2023_24, and average mass balance 2004_05 to 2021_22.

- Figure 14. Mass balance at a central flow line towards Grímsvötn 2023_24, and average mass balance 1991_92 to 2021_22.
- Figure 15. Vatnajökull winter (left) and summer (right) mass balance plotted against net mass balance for the survey period 1991_92 to 2023_24.
- Figure 16. Specific mass balance record for Vatnajökull (top), and selected Vatnajökull outlets 1991_92 - 2023_24.
- Figure 17. Cumulative specific surface mass balance Vatnajökull and selected Vatnajökull outlets 1991_92 – 2023_24.
- Figure 18. The relation between net annual balance (bn) and accumulation area ratio (AAR) and bn and equilibrium line altitude (ELA), for Vatnajökull outlets during the survey period.
- Figure 19. Average summer surface velocity at survey sites in 2024.
- Figure 20. Surface elevation change relative to spring 2010 (upper panel) and average surface velocity (lower panel) at mb sites on Dyngjujökull in 1992 to 2024.
- Figure 21. Surface elevation change relative to spring 2010 (upper panel) and average surface velocity (lower panel) at mb sites on Eyjabakkajökull in 1995 to 2024.
- Figure 22. Location of surface elevation profiles surveyed in field trips on Vatnajökull in 2024.
- Figure 23. Water divides and drainage basins of selected rivers draining water from Vatnajökull, Súla is since summer 2016 diverted to Gígja.
- Figure 24. The temporal variation of the average annual meltwater runoff to selected river catchments.

Tables:

Table I. Melt water drainage to selected rivers.

Appendices:

- Appendix A: Surface mass balance at survey sites 2023_24.
- Appendix B: Surface mass balance distribution by elevation in 2023_24.
- Appendix C: Coordinates at velocity measurement sites surveyed in 2024.
- Appendix D: Measured surface velocity on Vatnajökull in 2023_24.
- Appendix E: Melt water runoff to selected rivers in summer 2024 derived from summer ablation.
- Appendix F: Records of surface elevation change and surface velocity at mass balance survey sites on Vatnajökull.

1. INTRODUCTION

In 1992 (glacial year 1991_92) a program of surface mass balance measurements was started for Vatnajökull by the Science Institute University of Iceland (now Institute of Earth Sciences, IES) in collaboration with the National Power Company (NPC). For the first year the program was limited to the western part of the glacier but then expanded to include the northern outlets as well. In 1996 this study was further expanded to include southern outlets, with support from The European Union (Framework IV - Environment and Climate, TEMBA project 1996-1997). This program was extended 1998–2000 with further support from EU (Framework IV - Environment and Climate, ICEMASS project, 1998-2000). In 2000-2002 NPC and IES continued the program. In 2003-2005 IES participated in a multinational research project, which was financially supported by The European Union (EVK2-CT-2002-00152 SPICE). IES was responsible for obtaining data sets for calibration of models of the mass balance and dynamics of Vatnajökull. This work was also supported by The National Power Company of Iceland and The National Road Authority and was a continuation of the TEMBA-project of 1996-97 and ICEMASS project 1998-2001.

Since then, IES and NPC have continued a similar program. Mass balance measurements on the southeast outlet Breiðamerkurjökull is financially supported by the National Road Authority.

The aim of the collaborative work of NPC and IES is to improve understanding of the mass balance and melt water runoff from glaciers. This work in combination with energy balance measurements by NPC and IES on Vatnajökull will be used for calibration of models of the surface energy and mass balance of Vatnajökull.

This report describes the field measurements, mass balance, melt water runoff and GNSS survey, for the glaciological year 2023_24.

2. DIARY

April 30 – May 5, June 9-12: measurements of the winter balance, setup of AWSs.

June 11-12: installation of melt wires and maintenance of the lower AWS on Breiðamerkurjökull.

September 25-28, November 21- 23: summer balance measurements, take down of AWSs.

In all expeditions the locations of mass balance stakes were measured with Kinematic GNSS (or fast static GNSS) for surface velocity calculation.

The following members of staff of the Institute of Earth Sciences, University of Iceland, carried out the fieldwork on Vatnajökull: Finnur Pálsson, Sveinbjörn Steinþórsson, Eyjólfur Magnússon, with Andri Gunnarsson and Franz Fredriksson (National Power Company), Hlynur Skagfjörð (Reykjavík Rescue Team) and Eiríkur Finnur Sigursteinsson.

Volunteers in the Iceland Glaciological Society Spring expedition to Vatnajökull helped in the field work in June.

Field work in spring was done in favorable conditions, except that this time “Svítan” (the cabin on skis) was recently destroyed, so accommodation was the snow track and a pop-up kitchen in a container. The extraordinary autumn weather, dry and at times with high northern wind, set conditions such that the autumn field work was postponed till late November as a last resort. In 4 days of temperatures \sim 15 - -20 °C and similar numbers ms^{-1} for wind speed most of the sites were visited, but 8 sites at lower elevation were left out due to lack of snow (not secure for travel). The leftover sites will be visited in early 2025.

3. MASS BALANCE MEASUREMENTS

The purpose of the mass balance measurements is to describe the temporal and spatial distribution of the components of the mass balance. The mean annual values of the components and their variation from year to year are analyzed and related to meteorological conditions and climatic variability. The results are used in studies of changes in the glacier volume, estimates of meltwater contribution to glacial rivers, mass balance modeling, evaluation of altitudinal and regional variations of mass balance in response to climatic variations, and to assess the hydrometeorological and dynamic response of the ice cap to climate change.

The mass balance was determined by a stratigraphic method, measuring changes in thickness and density relative to the summer surface. The winter balance was estimated by drilling ice cores through the winter layer in the spring. Ablation was monitored from markers; snow stakes were put up on the glacier and wires were drilled down in the ablation area. The summer balance was measured in the autumn.

3.1 Methods

Measurements of the surface mass balance on a large ice cap like Vatnajökull are impractical in terms of cost with conventional techniques and sampling density that are typically used on small glaciers. The spatial variability of the mass balance may, however, be predictable on the flat large outlets of such an ice cap given data on several profiles extending over the elevation range of the glacier. The precipitation generally increases with elevation and decreases with the distance from the coast, but both the

distribution of snowfall and redistribution of snow by drift depend on the prevailing wind direction during the winter. The summer melting depends mainly on the altitude and the albedo of the glacier surface. Therefore, we have used observations along a limited number of flowlines which span the elevation ranges of the outlets. Each profile describes the variation with elevation, but together they also describe the lateral variation of the mass balance. Recently, modern over-snow vehicles and helicopters have allowed fast traverses to ensure successful fieldwork despite frequently poor weather conditions. The error for individual point measurement is estimated ~ 30 cm^{we} for both summer and winter balance. The error for the glacier wide specific mass balance, based on area integral of mass balance, is however considered smaller, since the error for individual survey sites is independent.

The winter mass balance (b_w) is defined as the mass of snow accumulated during the winter months, the summer balance (b_s) is the mass balance during the summer, and the net balance (b_n) is defined as their sum. The specific mass balance is expressed in terms of the equivalent thickness of water. All mass balance components apply to a time interval between given measurement dates, which are not fixed from one year to another. The dates in the autumn are separated by approximately one calendar year, which roughly coincides with the glaciological year defined as October 1st to September 30th. Snow cores are drilled in April-May through the winter layer and profiles of the density are measured. The summer balance is derived in the autumn from measurements of the changes in the snow core density during the summer in the accumulation area and from readings at stakes and wires drilled into the ice in the ablation areas.

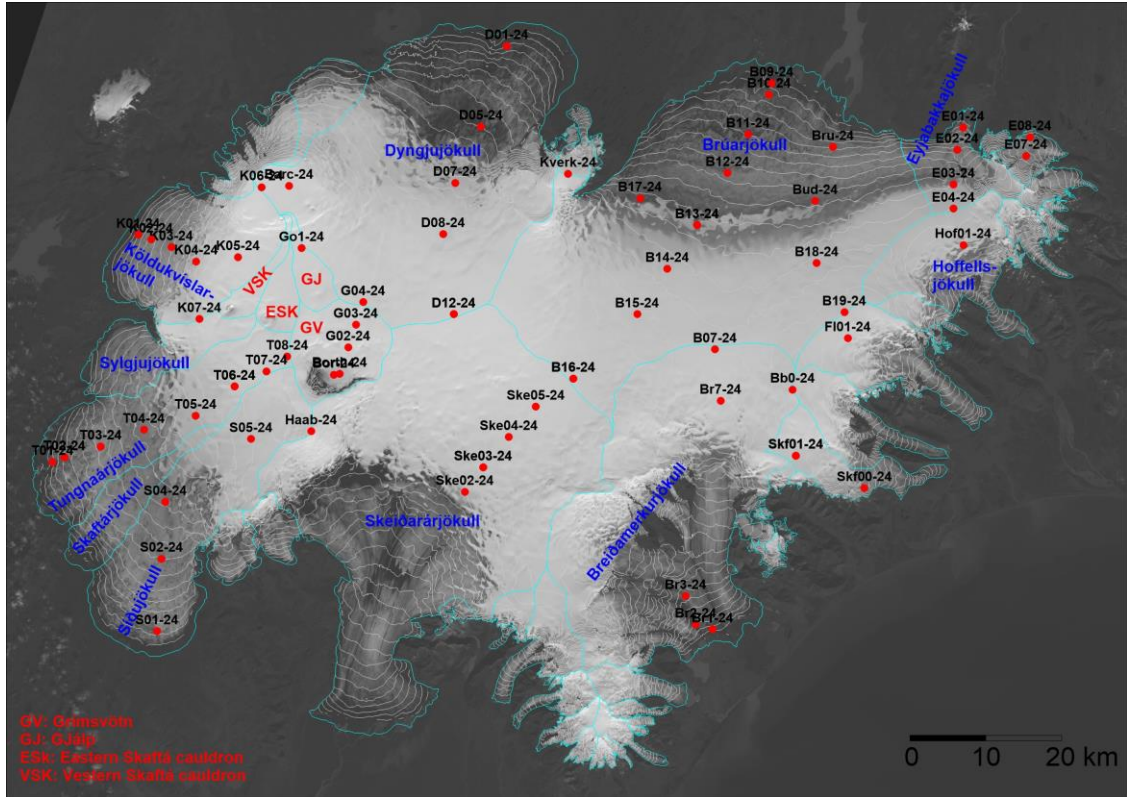


Figure 1. Outlets of Vatnajökull and location of mass balance survey sites 2023_24.

Digital maps are created for winter, summer and net balance for the whole ice cap based on the in-situ measurements. The mass balance is calculated over both the ice and water drainage basins. The summer balance over the water basin is an estimate of meltwater contribution to rivers and groundwater storage. This estimate, however, does not include precipitation that falls as rain on the glacier or snow, which falls and melts during the summer. As conventional for the north hemisphere we define the glaciological year from the start of October to the end of September next year and the period draining meltwater from the glacier during the summer from start of June through September. It would be misleading to include May in the summer period because runoff from the glacier melt in May is delayed due to refreezing during the elimination of the frost in the surface layer.

3.2 Results of mass balance measurements.

Winter mass balance measurements were done at 68 sites in spring 2023 (Fig. 1). The specific mass balance at individual sites is shown in Fig. 2. Most survey sites are on approximate central flow lines at individual outlets. The specific mass balance along the flow lines is given in Fig 3. for the glacier outlets: Síðujökull, Tungnaárjökull, Köldukvíslarjökull, Dyngjujökull, Brúarjökull (west and east), Eyjabakkajökull, Breiðamerkurjökull, SE-Vatnajökull, Skeiðarárjökull accumulation zone and the ice catchment of Grímsvötn.

Digital maps for winter, summer and net balance are shown in Figure 4. The mass balance of individual outlet is discussed in the following subsections.

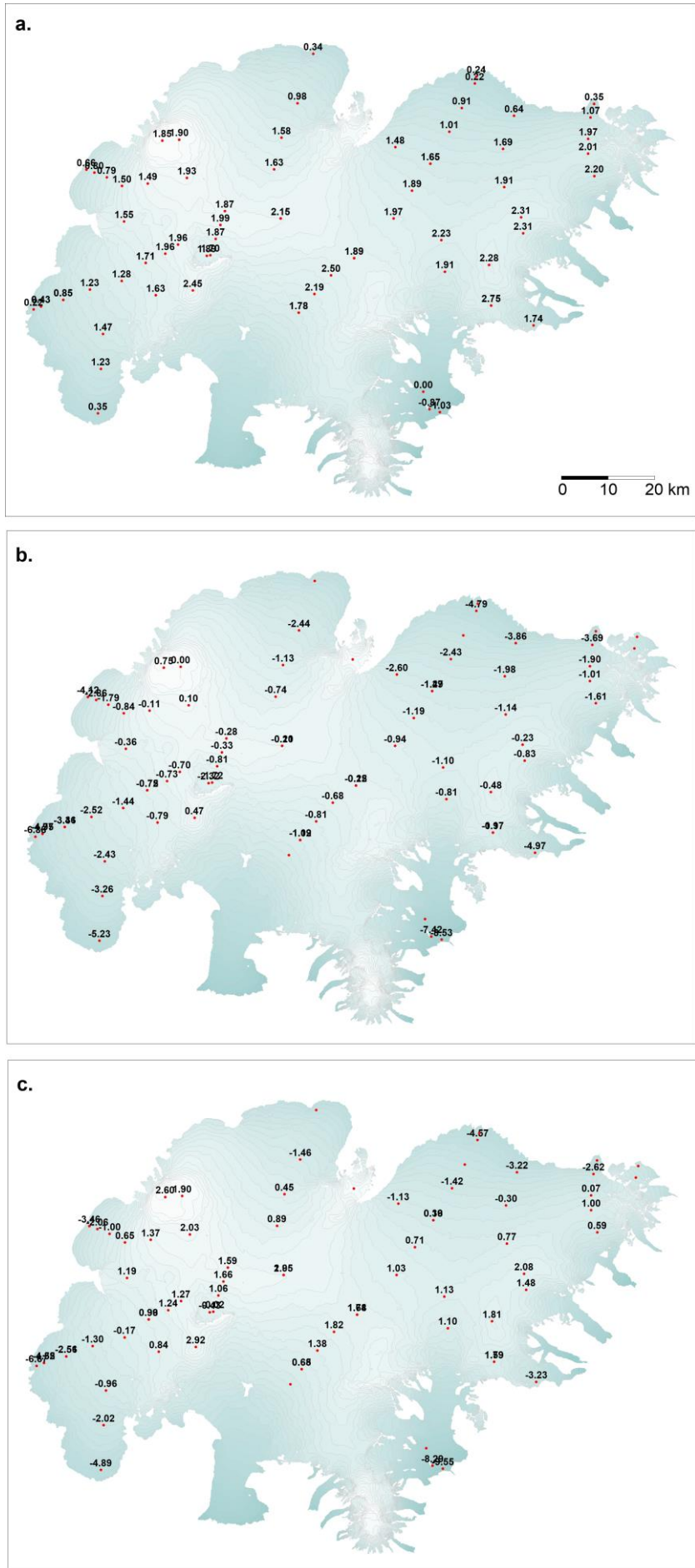


Figure 2. Maps showing point values of specific surface mass balance in m water equivalent (m_{we}), 2023_24. a. winter, b. summer, c. net balance.

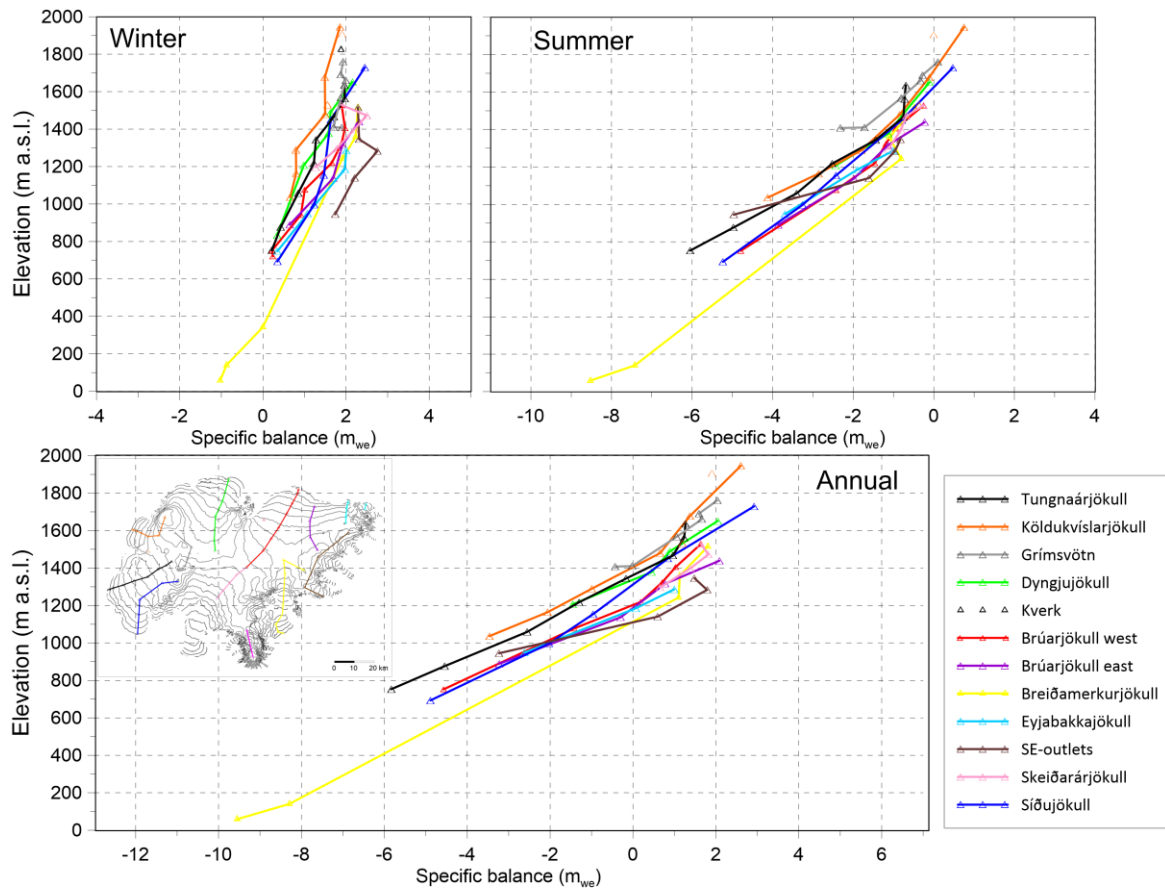


Figure 3. a. Specific mass balance (m_{we}), at survey sites along all mass balance profiles 2023_24.

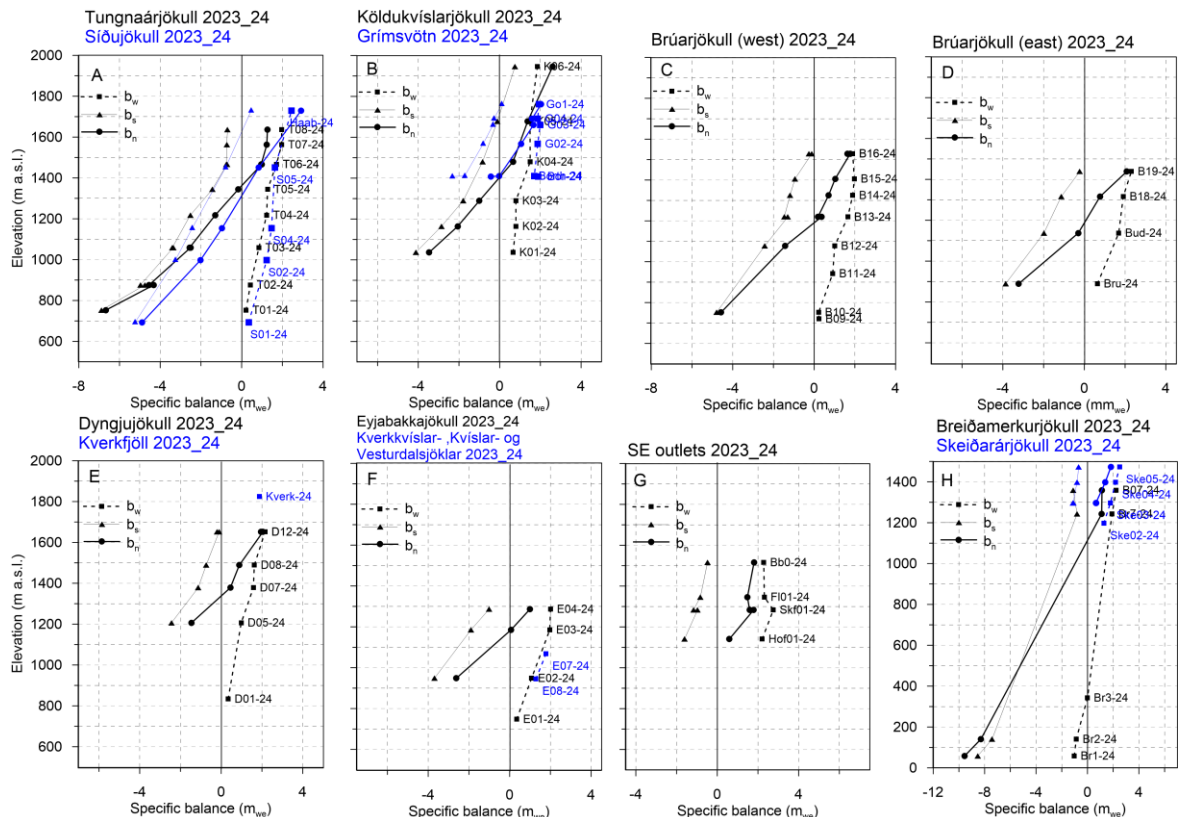
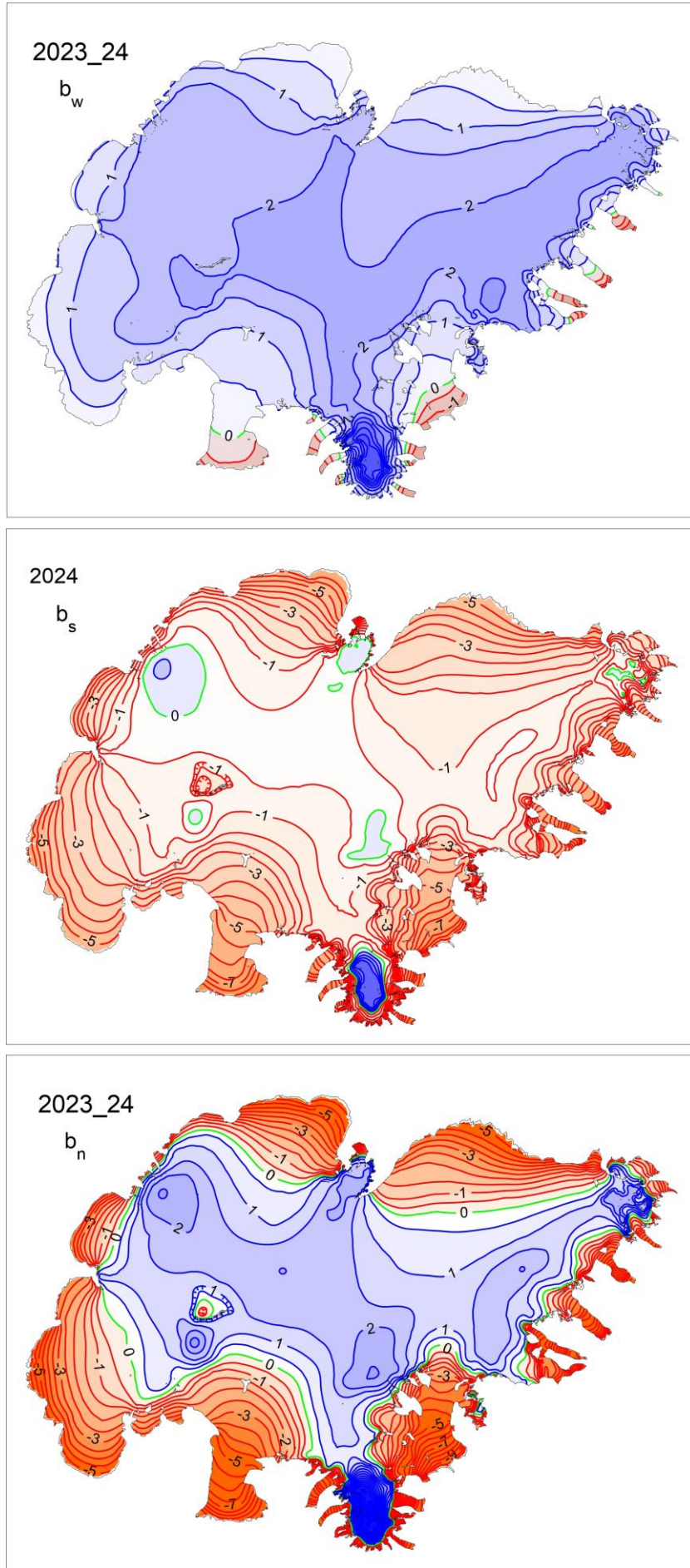


Figure 3. b. Specific point mass balance (m_{we}) 2023_24 as a function of elevation on central flow lines on Vatnajökull outlets.



*Figure 4. Specific mass balance (m_{we}) maps of Vatnajökull 2023_24.
Top: winter, Centre: summer, Bottom: net balance.*

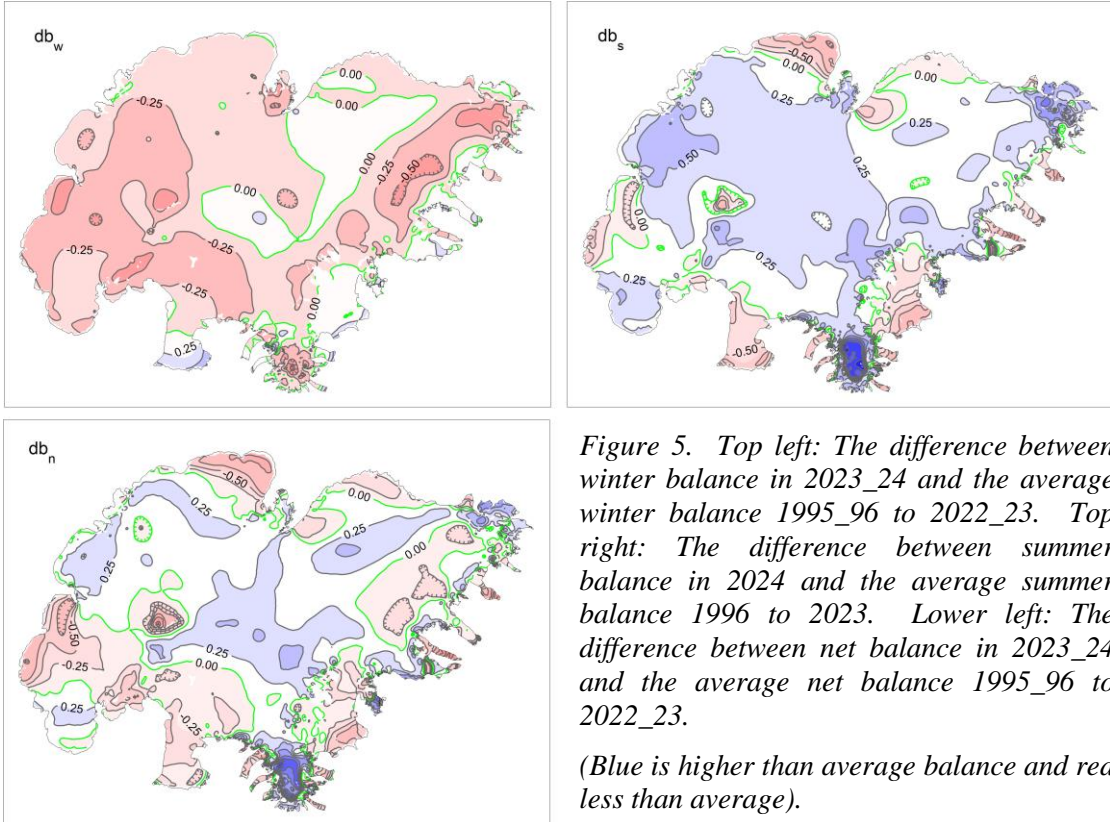


Figure 5. Top left: The difference between winter balance in 2023_24 and the average winter balance 1995_96 to 2022_23. Top right: The difference between summer balance in 2024 and the average summer balance 1996 to 2023. Lower left: The difference between net balance in 2023_24 and the average net balance 1995_96 to 2022_23.

(Blue is higher than average balance and red less than average).

A surface DEM is needed for surface area distribution and delineation of ice divides for individual outlets and catchments. The currently used surface DEM is mostly based on LiDAR survey 2010, -11 and -12 (**Jóhannesson et al. 2013), but the large set of GNSS profiles measured in spring 2023 were used to update the DEM to the 2023 elevation. That DEM cut to the glacier terminus of autumn 2023, was used in all area distributions; ice and water divides were not reworked. Although of variable accuracy locally the DEM reflects fairly accurate elevation distribution.

The winter of 2023-2024 was rather cold, with winter precipitation less than average, very little until end of December 2023.

Distribution of the winter snow was not typical (see fig. 5). In general, there was by far less snow than average in the accumulation zones of the ice cap, and by far less than average at all elevations in the west. Winter melting at the low-lying S-outlets was less than average. The beginning of summer was cold, with

snowfall reducing melting, relatively sunny July, but cold and wet August. The autumn months were very dry, most of the N-Atlantic low-pressure systems passed far south of Iceland. Warm and windy days in the autumn contributed markedly to the total melt. In all this resulted in less average summer melting, especially in above ~1000 m elevation, and above ~1650 m the summer balance was positive. The resulting annual balance was close to average in the ~1000-1500 m range, slightly above average above that, but lower than average in many of the ablation zone regions. In total the mass loss was ~60 % of the average since 1995.

**Jóhannesson, T., Björnsson, H., Magnússon, E., Guðmundsson, S., Pálsson, F., Sigurðsson, O., Thorsteinsson, T., and Berthier, E.:
Ice-volume changes, bias estimation of mass-balance measurements and changes in subglacial lakes derived by lidar mapping of the surface Icelandic glaciers, Ann. Glaciol., 54, 63–74, doi:10.3189/2013AoG63A422, 2013.

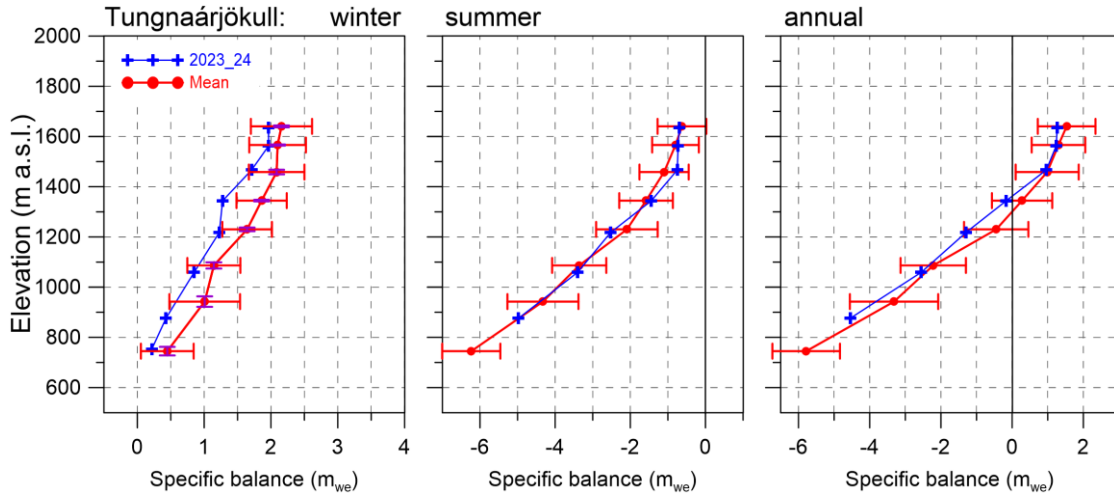


Figure 6. Mass balance at a central flow line of Tungnaárjökull 2023_24 and average mass balance 1991_92 to 2021_22 (the horizontal red lines indicate std. dev of the variability at the survey site during the survey period).

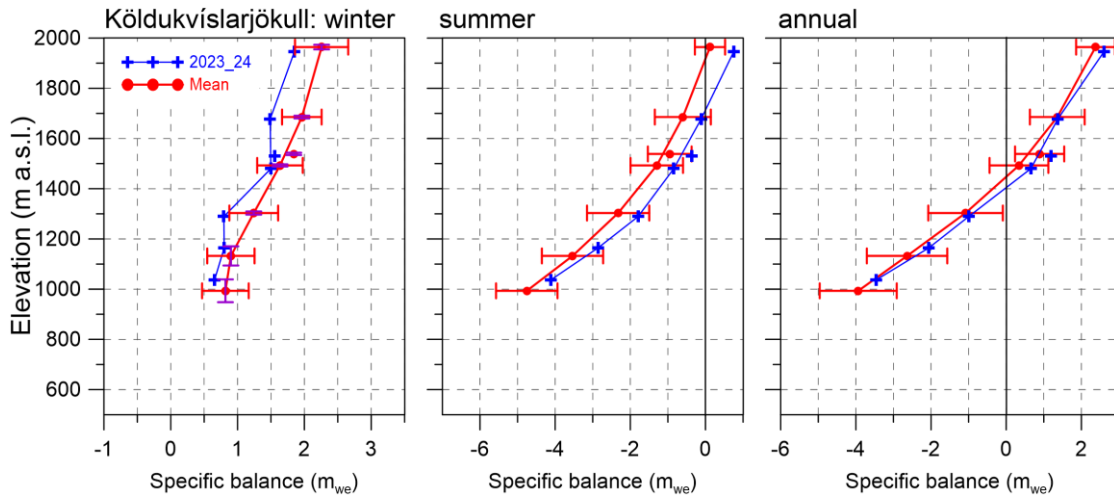


Figure 7. Mass balance at a central flow line of Köldukvíslarjökull 2023_24 and average mass balance 1991_92 to 2021_22.

3.2.1 Tungnaárjökull.

Area = 323 km²

$B_w = 0.37 \text{ km}^3 \text{ we}$; $b_w = 1.15 \text{ m}_\text{we}$

$B_s = -0.81 \text{ km}^3 \text{ we}$; $b_s = -2.52 \text{ m}_\text{we}$

$B_n = -0.44 \text{ km}^3 \text{ we}$; $b_n = -1.37 \text{ m}_\text{we}$

ELA = 1365 m a.s.l. (at profile)

AAR = 35 %

(The terms are defined at the foot of this page)

Variation of mass balance along a central flow line on Tungnaárjökull is shown in Fig. 6. The winter accumulation was under the average at all survey sites, by far so, in the ablation zone. The total winter balance was only 77% of the average. Summer mass loss was not far from average at all survey sites, in total 5% less than

For each ice catchment basin, B_w , B_s and B_n are water equivalent volumes of winter, summer and net balance, ELA the equilibrium line altitude, and AAR is the accumulation area ratio.

average. This year is the 29th year out of the 32 surveyed with negative net balance on Tungnaárjökull catchment, this time 20 % more mass was lost than at average in the survey period.

3.2.2 Köldukvíslarjökull

Area = 284 km²

$B_w = 0.36 \text{ km}^3 \text{ we}$; $b_w = 1.28 \text{ m}_\text{we}$

$B_s = -0.38 \text{ km}^3 \text{ we}$; $b_s = -1.36 \text{ m}_\text{we}$

$B_n = -0.02 \text{ km}^3 \text{ we}$; $b_n = -0.08 \text{ m}_\text{we}$

ELA = 1405 m a.s.l. (at profile)

AAR = 58 %

Variation of mass balance along a central flow line on Köldukvíslarjökull is shown in Fig. 7. The winter accumulation was less than average in the accumulation zone by about 1. Std.

close to average at close to the ELA zone, but almost $\frac{1}{2}$ std. in the ablation zone. The total winter accumulation was $\sim 86\%$ of the average. Summer mass loss was ~ 1 std. less than average in the accumulation zone, but by $\frac{1}{2}$ to $\frac{1}{4}$ std. in the ablation zone. In total summer mass loss was $\sim 70\%$ of the average. This year Kóldukvíslarjökull net balance was negative, as have been 27 years of the 33 surveyed, now only 17% of the mass loss in an average year since 1991-92.

3.2.3 Dyngjujökull

Area = 1026 km²

$B_w = 1.49 \text{ km}^3 \text{ we}$; $b_w = 1.45 \text{ m we}$

$B_s = -1.54 \text{ km}^3 \text{ we}$; $b_s = -1.50 \text{ m we}$

$B_n = -0.05 \text{ km}^3 \text{ we}$; $b_n = -0.05 \text{ m we}$

ELA = 1340 m a.s.l. (at profile)

AAR = 47 %

Variation of mass balance along a flow line on Dyngjujökull is shown on Fig. 8. At the highest accumulation zone sites snow accumulation was ~ 1.25 std. under average, but close to average at all other. In the ablation zone snow collection was close to average. The total winter accumulation is estimated 91% of the average of the survey

period.

Summer mass loss was almost at average at all survey sites but by about 1 std. under average at the top site. The lowest site has not been visited yet when the report is written.

The net balance was slightly negative, by -0.05 m we not far from the average for Dyngjujökull that is only slightly negative (-0.03 m we).

Dyngjujökull has often had mass balance close to zero, and the net balance has been estimated positive in at least 12 years of the three-decade period of almost continuous mass loss for Vatnajökull as a whole. The inland Dyngjujökull, is the outlet of Vatnajökull closest to mass equilibrium during the survey period.

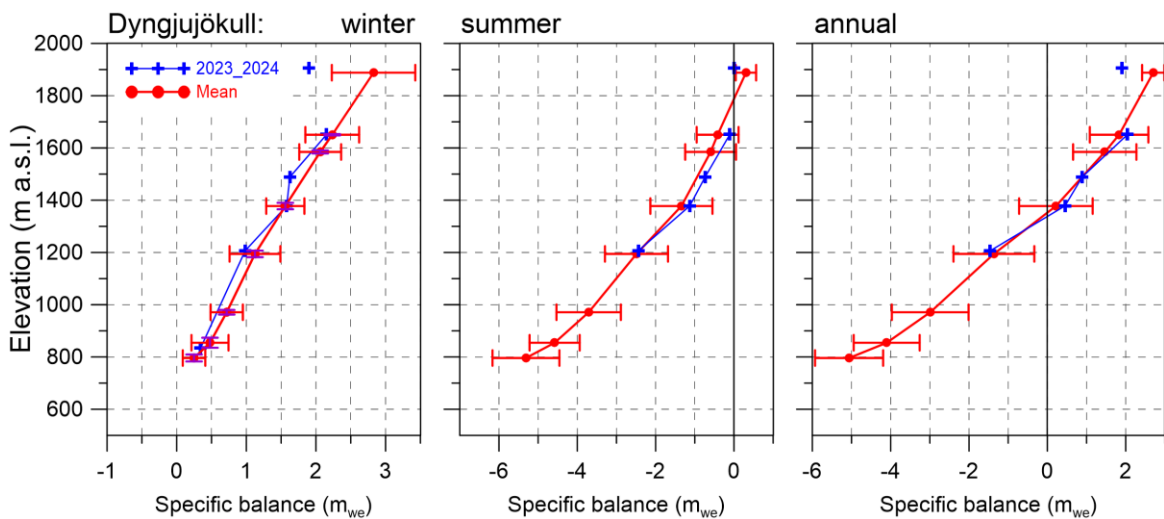


Figure 8. Mass balance at a central flow line on Dyngjujökull 2023_24 and average mass balance 1991_92 to 2021_22 (except 1998_99 – 2003_04 at all but the top elevation).

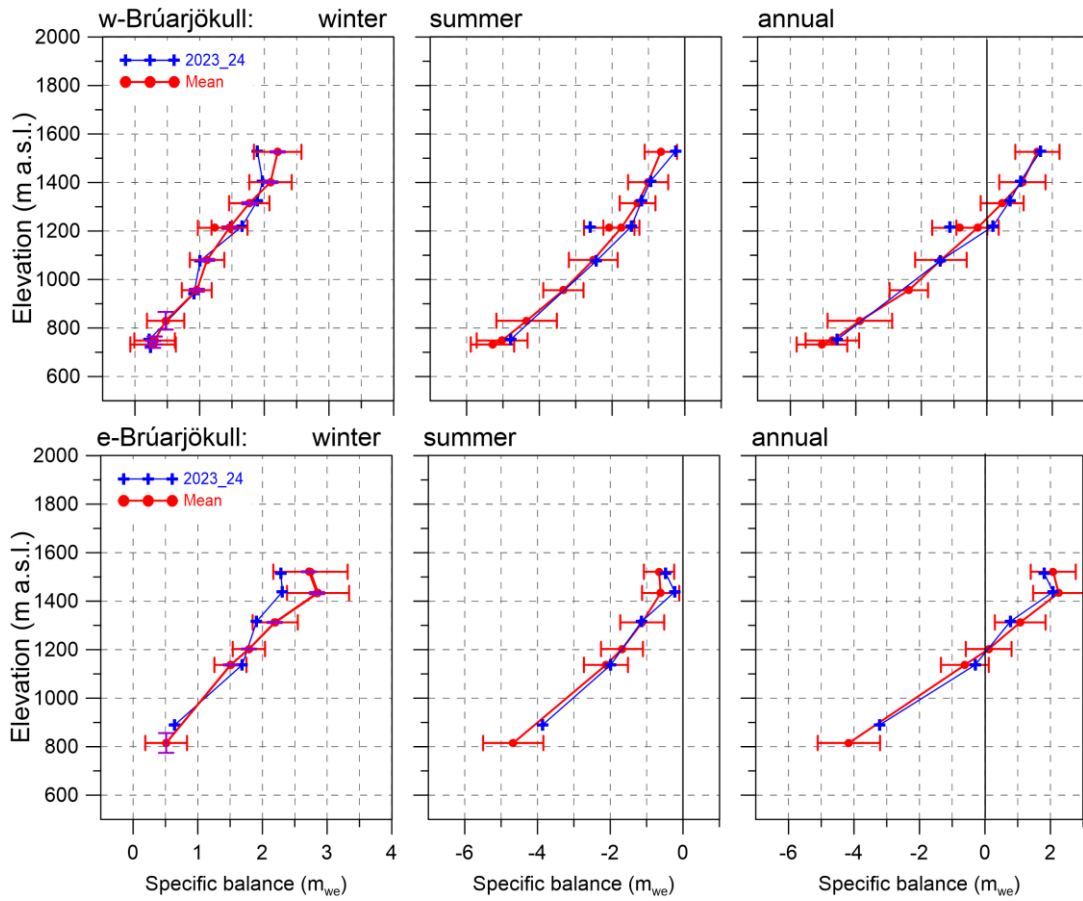


Figure 9. Mass balance at two flow lines on Brúarjökull 2023_24 and average mass balance 1992_93 to 2021_22.

3.2.4 Brúarjökull

Area = 1481 km²
 $B_w = 2.40 \text{ km}^3_{\text{we}}$; $b_w = 1.62 \text{ m}_{\text{we}}$
 $B_s = -2.49 \text{ km}^3_{\text{we}}$; $b_s = -1.68 \text{ m}_{\text{we}}$
 $B_n = -0.09 \text{ km}^3_{\text{we}}$; $b_n = -0.06 \text{ m}_{\text{we}}$
ELA = 1280 m a.s.l. (western flow line)
ELA = 1205 m a.s.l. (eastern flow line)
AAR = 53 %

Variation of mass balance along the flow lines on Brúarjökull is shown in Fig. 9. On Brúarjökull winter snow collection was not far from average at most survey sites, except in upper accumulation zone, where it was ~1 std. less than average. The winter accumulation was in total at average. Summer mass loss was close to average at the survey sites below 1400 m elevation, but less than 1 std. over average at sites above. In total the

mass loss in summer was 87% of the average.

The net balance was close to average at all survey sites. In total the net balance was slightly negative by ~20% of the average. During the survey period, there have been 9 years of positive balance and 23 years with negative net balance.

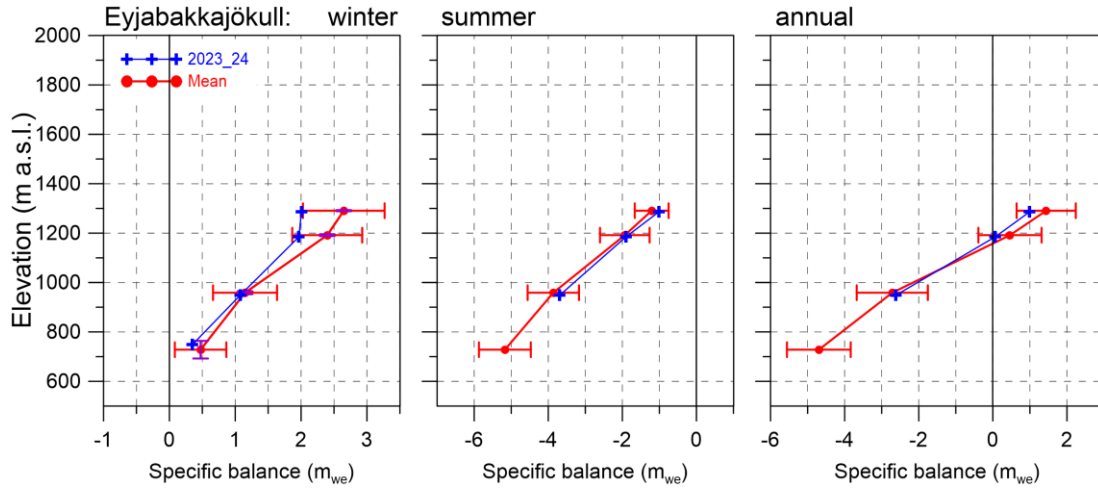


Figure 10. Mass balance at a central flow line of Eyjabakkajökull 2023_24 and average mass balance 1995_96 to 2021_22.

3.2.5 Eyjabakkajökull

Area = 104 km²
 $B_w = 0.17 \text{ km}^3 \text{ we}$; $b_w = 1.62 \text{ m}_\text{we}$
 $B_s = -0.22 \text{ km}^3 \text{ we}$; $b_s = -2.14 \text{ m}_\text{we}$
 $B_n = -0.05 \text{ km}^3 \text{ we}$; $b_n = -0.51 \text{ m}_\text{we}$
ELA = 1180 m a.s.l. (at profile)
AAR = 46 %

Variation of mass balance along a central flow line on Eyjabakkajökull is shown in Fig. 10. Like Brúarjökull the winter accumulation here was at average at the lower sites but 1 std. less at the higher. The total winter accumulation is estimated 89% of the survey period average. Summer mass loss was slightly less than average at all survey sites. The total summer

mass loss was 80% of the average. The net balance was negative by 60% of the average of the survey period and has been negative for all but 3 years of the 29 years of survey.

3.2.6 Breiðamerkurjökull

Area = 875 km²
 $B_w = 1.33 \text{ km}^3 \text{ we}$; $b_w = 1.52 \text{ m}_\text{we}$
 $B_s = -1.98 \text{ km}^3 \text{ we}$; $b_s = -2.27 \text{ m}_\text{we}$
 $B_n = -0.65 \text{ km}^3 \text{ we}$; $b_n = -0.74 \text{ m}_\text{we}$
ELA = 1150 m a.s.l. (at profile)
AAR = 58%

Variation of surface mass balance along a central flow line on Breiðamerkurjökull is shown in Fig. 11. Winter accumulation was less than average at the survey sites in the

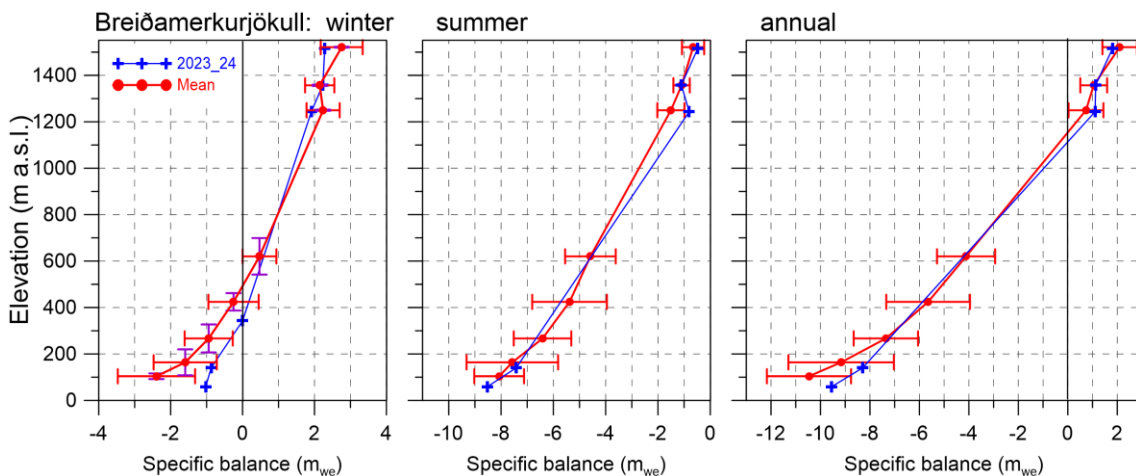


Figure 11. Mass balance at a central flow line of Breiðamerkurjökull 2023_24 and average mass balance 1995_96 to 2021_22.

accumulation zone, but at the lower sites in the ablation zone mass loss in winter was more 1 std. less than average. This led to the total winter balance close to average (2% higher) of the survey period average.

Summer mass loss was not far from the average in the accumulation zone) at all survey sites. The total summer mass loss is estimated 14% less than the average during the survey period. The net surface mass loss this year is estimated about 66% of an average year.

In addition to mass loss due to surface melt Breiðamerkurjökull loses in the order of 0.5 km^3 ($\sim 0.6 \text{ m}$) annually via calving into the marginal lake Jökulsárlón; this mass loss is not accounted for here.

3.2.7 Skeiðarárjökull

$$\text{Area} = 1346 \text{ km}^2$$

$$B_w = 1.98 \text{ km}^3 \text{ we}; b_w = 1.47 \text{ m}_\text{we}$$

$$B_s = -2.68 \text{ km}^3 \text{ we}; b_s = -1.99 \text{ m}_\text{we}$$

$$B_n = -0.70 \text{ km}^3 \text{ we}; b_n = -0.52 \text{ m}_\text{we}$$

$$\text{ELA} = \sim 1190 \text{ m a.s.l. (at profile)}$$

$$\text{AAR} = 58$$

The surface mass balance of Skeiðarárjökull is only measured in the accumulation zone due to almost impassable terrain in the ablation zone both in autumn and spring.

The mb-survey program here was initiated in 2002, although sporadic measurements were conducted in the 1990s. Estimation of mb in the ablation zone for the creation of the mb-maps is based on the survey of the neighboring Breiðamerkurjökull in the east (with similar elevation span) and western neighboring outlet Síðujökull.

Variation of mass balance along the survey profile on Skeiðarárjökull is shown in Fig. 12. Winter snow accumulation was 1 std. under average at the lower accumulation zone, but at average at the higher.

Summer mass loss was far less than average at the upper sites, at average at 1250 m but the lowest was not reachable in the autumn due to crevasses.

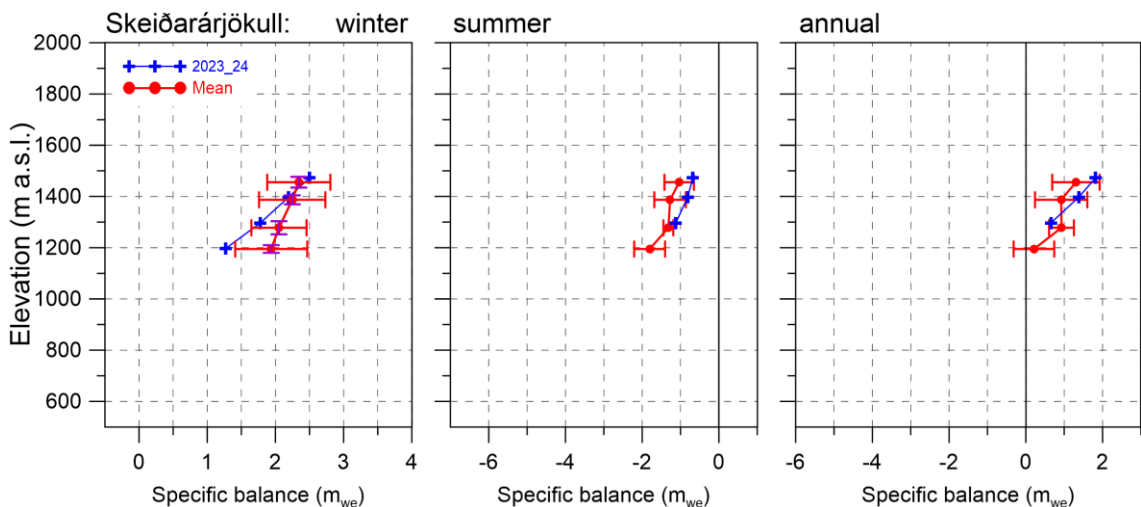


Figure 12. Mass balance at a central flow line of Skeiðarárjökull 2023_24 and average mass balance 2016_17 to 2021_22.

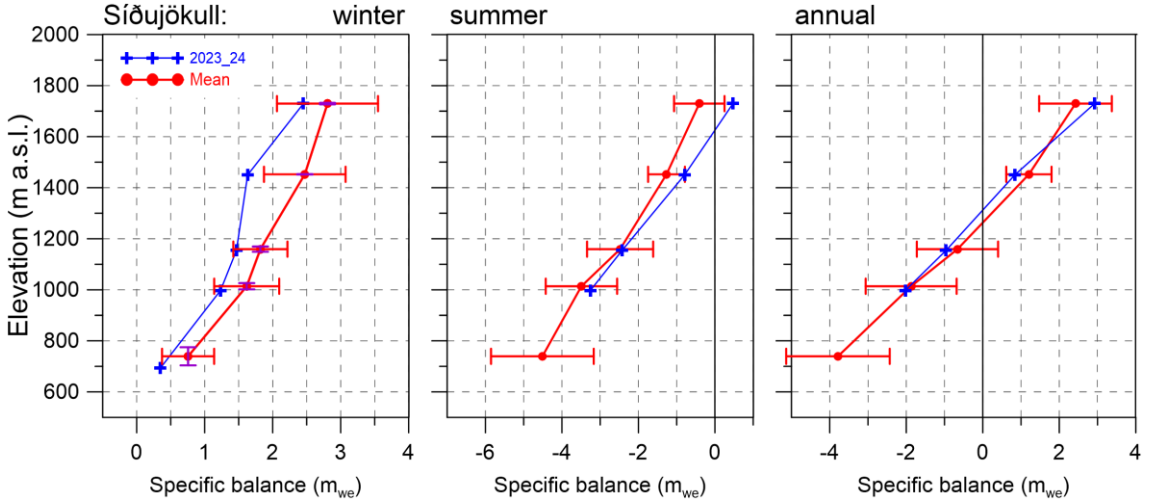


Figure 13. Mass balance at a central flow line of Síðujökull 2023_24 and average mass balance 2004_05 to 2021_22.

3.2.8 Síðujökull

Area = 400 km²

$B_w = 0.52 \text{ km}^3 \text{ we}$; $b_w = 1.30 \text{ m}_\text{we}$

$B_s = -1.00 \text{ km}^3 \text{ we}$; $b_s = -2.51 \text{ m}_\text{we}$

$B_n = -0.48 \text{ km}^3 \text{ we}$; $b_n = -1.20 \text{ m}_\text{we}$

ELA = 1310 m a.s.l. (at profile)

AAR = 37 %

Variation of mass balance along a central flow line on Síðujökull is shown in Fig. 13.

The winter snow accumulation was between $\frac{1}{2}$ - 1 std. under average at all survey sites. The total winter balance was 82% of the average (since

2004_05). Summer mass loss was at average at the lower sites, but far less at the upper sites, even net mass gain at the summit of Háabunga. (In autumn the route to the lowest site was impassable). The total summer mass loss was 85% of the average of the survey period. Total mass loss was ~90 % of the average during the 19-year survey period. At Síðujökull the only year of surveyed positive net balance was 2014_2015.

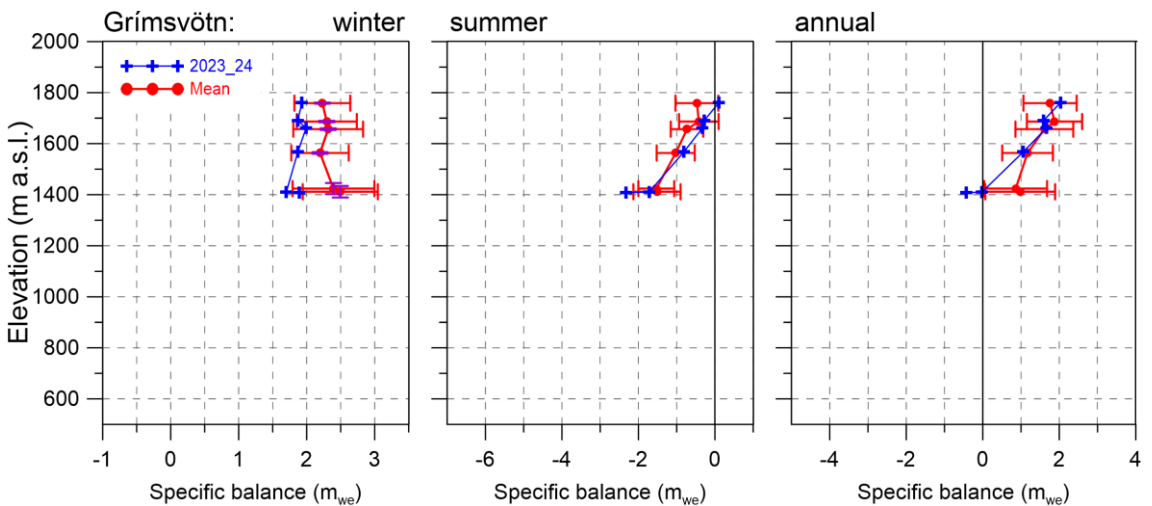


Figure 14. Mass balance at a flow line towards Grímsvötn 2023_24 and average mass balance 1991_92 to 2021_22.

3.2.9 Grímsvötn-Gjálp

Area = 173 km²

$B_w = 0.34 \text{ km}^3 \text{ we}$; $b_w = 1.92 \text{ m we}$

$B_s = -0.12 \text{ km}^3 \text{ we}$; $b_s = -0.70 \text{ m we}$

$B_n = 0.21 \text{ km}^3 \text{ we}$; $b_n = 1.21 \text{ m we}$

Variation of mass balance at sites close to a flow line from Bárðarbunga towards Grímsvötn center is shown in Fig. 14. Snow accumulation at the survey sites was between $\frac{1}{2}$ - 1 std. less than average, and total winter accumulation 12% less than average. Summer mass loss was at average at the sites on the ice-shelf of Grímsvötn, but far less at the upper sites, even net mass gain at the slopes of Bárðarbunga. Total summer mass loss was ~85 % of the average. Net balance was at average at the survey sites except the one at the center of the ice shelf. As always (except 2010) the total surface balance is positive, now ~82 % of the average.

In addition to surface mass loss in summer, geothermal melt in the Grímsvötn catchment area is on the order of 0.2 km³ annually. This mass loss is about 1.21 m evenly distributed over the ice catchment, or approximately equal to this year net surface balance. This means that the total balance for the catchment of Grímsvötn is close to zero this year.

The average surface mass balance in the survey period (since 1991-92) is +1.50 m, so assuming the annual 1.21 m loss due to geothermal melt yields an annual surplus of ~0.3 m (0.052 km³) on average, or ~1.6 km³. In the Gjálp eruption, within the Grímsvötn ice catchment, over 3.5 km³ of ice was melted and some, although much less, in the 1998, 2004 and 2011 Grímsvötn eruptions. About half of this has been compensated for by the average total positive surface balance.

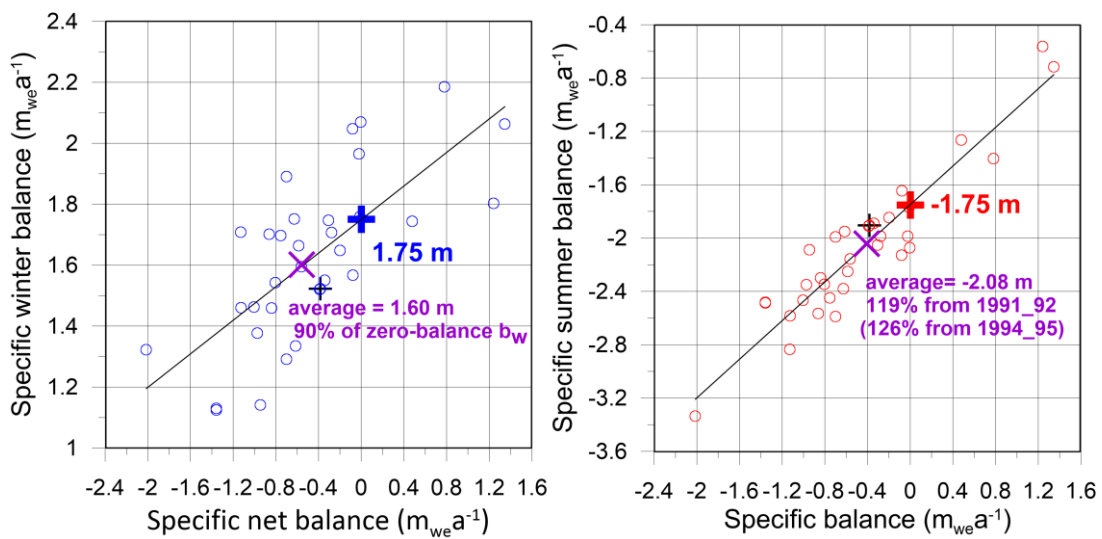


Figure 15. Vatnajökull winter (left) and summer (right) mass balance plotted against net mass balance for the survey period 1991_92 to 2023_24, current point marked with +. The + and + and the accompanying numbers, mark the zero-mass balance mass turnover for Vatnajökull (current topography) as estimated from the linear trends shown with thin black lines.

3.3 Vatnajökull: Surface mass balance record

From the digital mb maps (Fig. 4) the glacier wide volumes of winter, summer and net balances for Vatnajökull have been calculated by integration and are as follows:

Area = 7593 km²

B_w = 11.50 km³we ; b_w = 1.52 m_{we}

B_s = -14.39 km³we ; b_s = -1.90 m_{we}

B_n = -2.88 km³we ; b_n = -0.38 m_{we}

AAR = 58%;

(balance values as a function of elevation are tabulated in appendix D)

The winter of 2023-2024 was rather cold, with winter precipitation less than average, very little until end of December 2023.

Distribution of the winter snow was not typical (see fig. 5). In general, there was by far less snow than average in the accumulation zones of the ice cap, and by far less than average at all elevations in the west. Winter melting at the low-lying S-outlets was less than average. The total mass collection in winter was ~95% of the average since 1995.

Early summer was cold with occasional snowfall, reducing melting, relatively sunny July, but cold and wet August. The autumn months were very dry, most of the N-Atlantic low-pressure systems passed far south of Iceland. Warm and windy days in the autumn contributed markedly to the total melt. In all this resulted in less average summer melting, especially in above ~1000 m elevation, and above ~1650 m the summer balance was positive. This resulted in a summer mass loss ~86% of the average since 1995.

The resulting annual balance was close to average in the ~1000-1500 m range, slightly above average above that, but lower than average in many of the ablation zone regions. In total the mass loss was ~62 % of the average since 1995.

The zero-mass balance mass turnover (mbt) for Vatnajökull (current topography) is estimated from the zero net balance crossover of the linear trend of b_w plotted against b_n and equivalently b_s against b_n (see fig 15.) and found to be close to 1.75 m_{we} (13.4 km³we). The winter balance 2023_24 is ~93% of the estimated zero-mass balance turnover (0-mbt), while the average b_w of the survey period is ~92% of the 0-mbt.

The summer balance of 2024 is -0.19 m (or 22%) more negative than 0-mbt. On average the summer mass loss has been 19% (average of summers 1992-2022) higher than 0-mbt, (27% for the period of 1995-2023).

This clearly shows that the high mass loss of the past 3 decades is governed by too much mass loss during summer rather than too little snow accumulation during winter.

Since 2010, after the 15-year period of high mass loss, the summer and net balance have been highly variable (figure 16.), one year with definite positive mass balance, 2014_15, and a few close to zero or slightly positive: 2010_11, 2016_17, 2017_18 and 2021_22.

The variability of the winter balance is by far more prominent for the outlets closest to sea. That section of the glacier receives precipitation in all south and east wind directions and thus has high snow accumulation in winters when prevailing paths of the North Atlantic low-pressure systems are just south and east of Iceland.

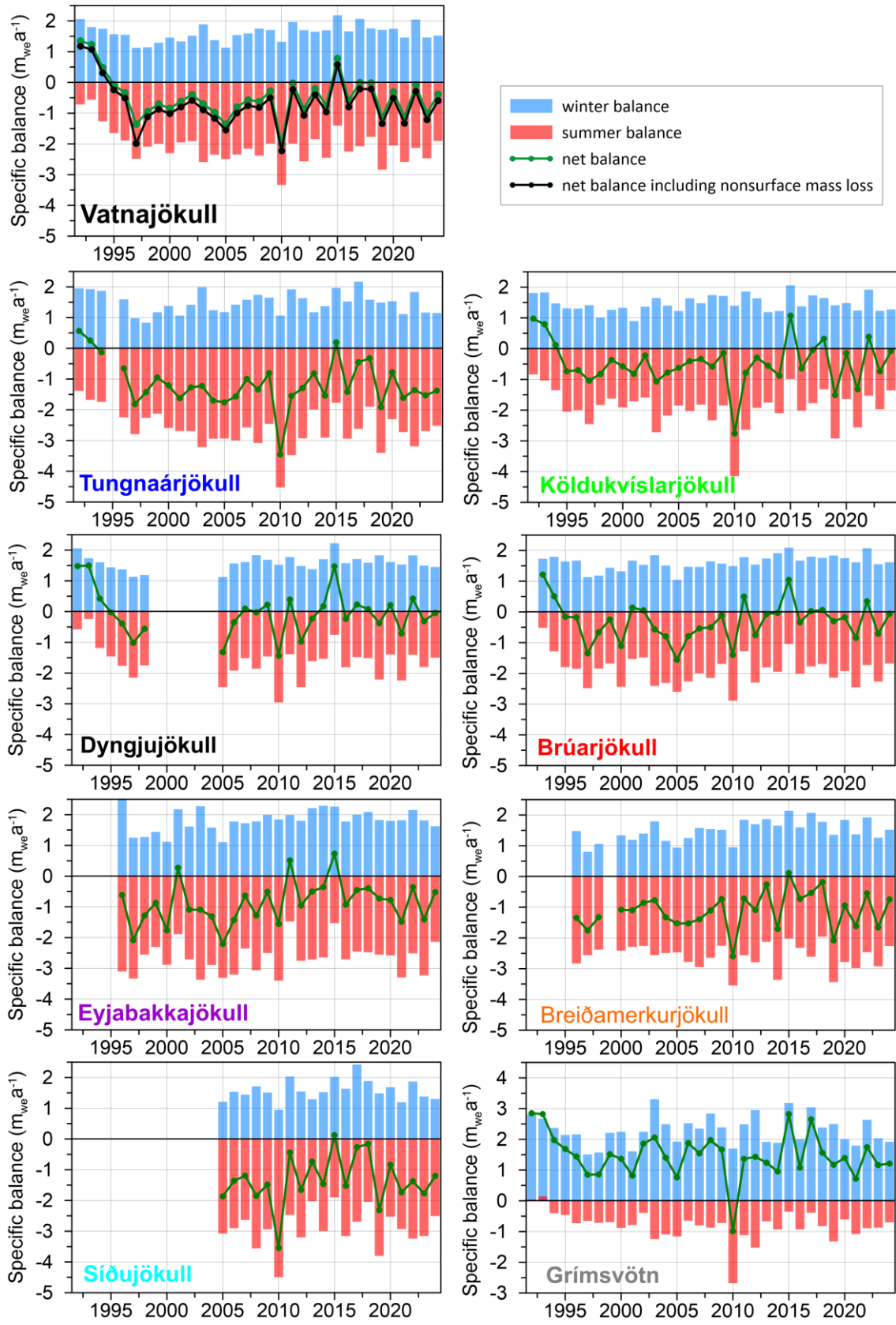


Figure 16. Specific mass balance record for Vatnajökull (top), and selected Vatnajökull outlets 1991-92-2023-24.

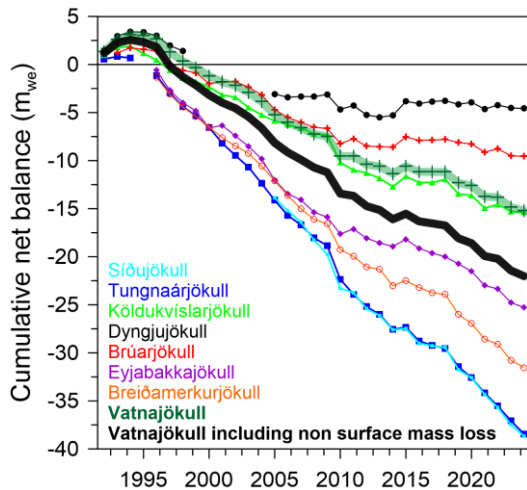


Figure 17. Cumulative specific surface mass balance Vatnajökull and selected Vatnajökull outlets 1991_92 – 2023_24.

The cumulative net balance curves for the outlets of Vatnajökull in Fig. 17 show that all outlets have been losing mass since most years since 1994_95. In the period of high mass loss, the loss rate is about -0.5 to -0.6 $\text{m}_{\text{wea}}^{-1}$ for the northern outlets but -1.1 to -1.5 $\text{m}_{\text{wea}}^{-1}$ for the south and western outlets. After 2010 there is a distinct difference between the north inland (Dyngjujökull and Brúarjökull) and the south and west coastal outlets (Breiðamerkurjökull, Tungnaárjökull and Síðujökull) in that there is a sudden change in the mass balance trend for the northern. The trend changes from -0.5 $\text{m}_{\text{wea}}^{-1}$ to about zero for the northern while there is little change for the others. The east outlet Eyjabakkajökull behaves like the coastal and is in fact close to sea, while Köldukvíslarjökull in the NV is more like the northern.

The cumulative mb for Vatnajökull is very similar to Köldukvíslarjökull, with a slope of -0.75 $\text{m}_{\text{wea}}^{-1}$ in the period of high mass loss, but -0.35 $\text{m}_{\text{wea}}^{-1}$ after 2010.

During the survey period starting in 1991_92 Vatnajökull lost $\sim 134 \text{ km}^3$ of ice or thinned $\sim 15 \text{ m}$ due to surface

mass loss (summing from the start of high mass loss in 1994_95 yields 162 km^3 or 19 m thinning).

In addition, non-surface mass loss is estimated (calving, geothermal melt, internal friction, eruptions) $\sim 0.21 \text{ m}_{\text{we}}$ for Vatnajökull in a paper by Tómas Jóhannesson and others (Jóhannesson, T., Pálmarsson, B., Hjartarson, Á., Jarosch, A., Magnússon, E., Belart, J., et al. (2020). Non-surface mass balance of glaciers in Iceland. *J. Glaciol.* 66, 685–697. doi:10.1017/jog.2020.37) which amounts to an ice loss of $\sim 60.3 \text{ km}^3$ or 7.7 m average thinning since 1994_95.

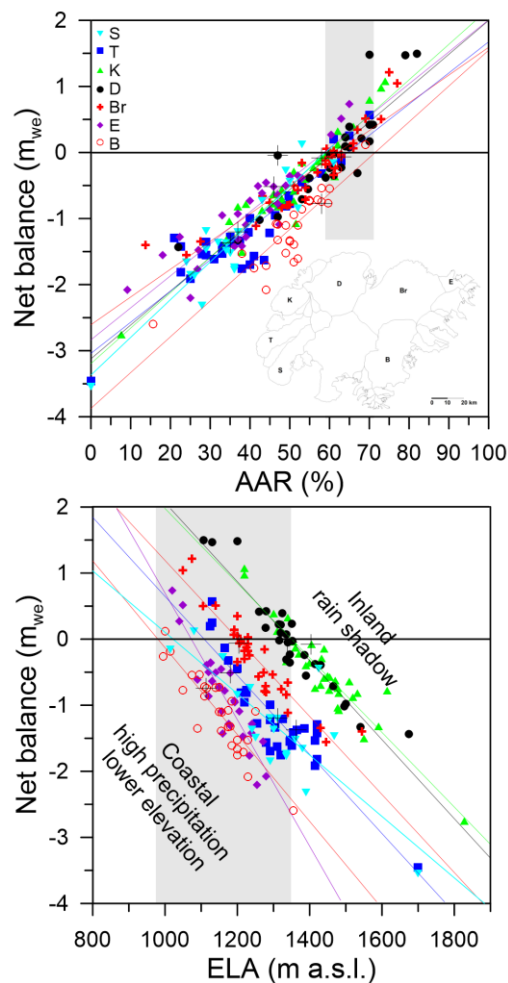


Figure 18. The relation between net annual balance (b_n) and accumulation area ratio (AAR) (upper) and b_n and equilibrium line altitude (ELA), for Vatnajökull outlets during the survey period. (This year's points are marked with a black +).

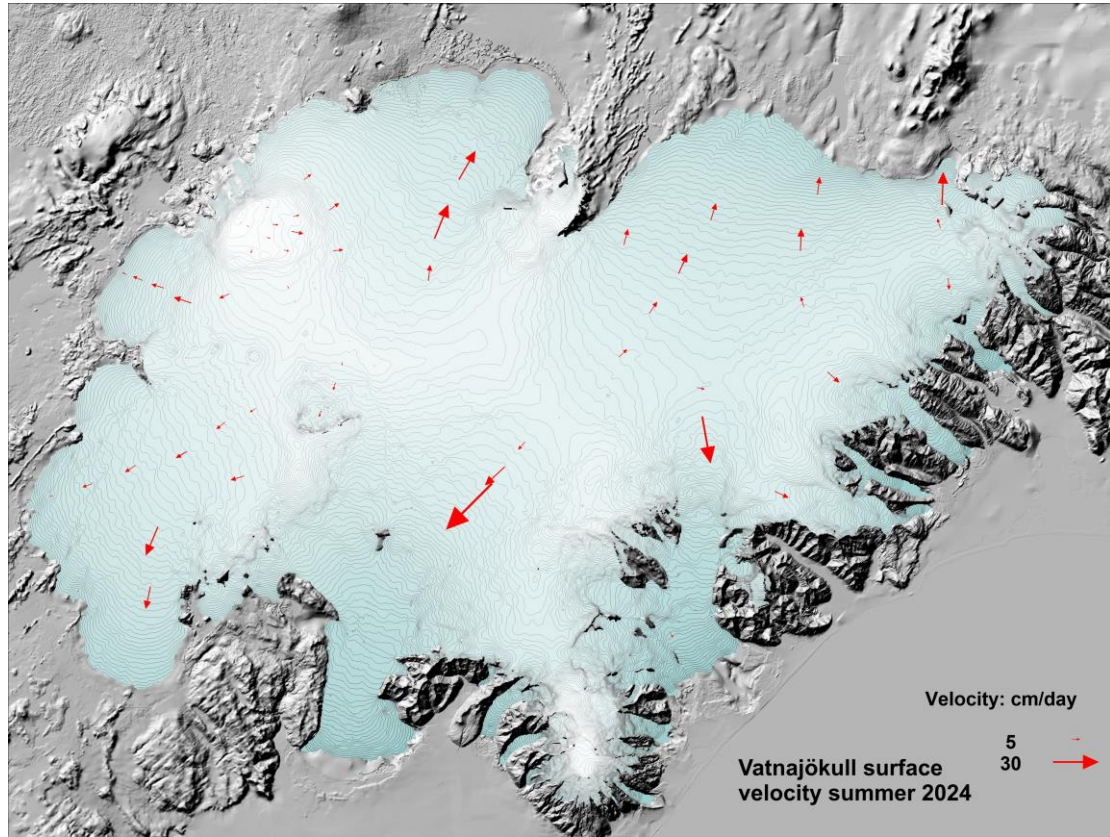


Figure 19. Average summer velocity at survey sites in 2024.

In Fig. 17 the relation of the annual net balance to the accumulation area ratio (AAR) and equilibrium line altitude (ELA) is shown for different outlets over the survey period. The bn-AAR gradient is similar for all outlets, about $0.5 \text{ m}_{\text{we}}$ for 10% change in AAR. The zero-balance AAR varies for different outlets in the range 60–65%, similar for all outlets except for the southern outlet Breiðamerkurjökull. Breiðamerkurjökull is far from equilibrium, the ablation area is too large. A large part of the outlet has carved 200–300 m deep valley into the former sediment bed, and the surface and bed elevation has lowered accordingly. Similarly, the zero-balance ELA varies from about 1000–1100 m a.s.l. for the southern outlets to 1400 m a.s.l. for the NW outlets. The bn-ELA slope is similar for all outlets $-0.6 \text{ m}_{\text{we}}$ per 100 m, except Eyjabakkajökull with a slope of $-1.0 \text{ m}_{\text{we}}$ per 100 m and Síðujökull with a slope of $-0.45 \text{ m}_{\text{we}}$ per 100 m (for Síðujökull possibly due to outliers in the data set).

4. SURFACE VELOCITY MEASUREMENTS

The average summer surface velocity of the glacier surface at the survey sites was calculated from fast static or kinematic GNSS positioning of the ablation stakes/wires (accuracy about $\sim 10 \text{ cm}$). In 2024 nearly all sites were surveyed in spring and autumn and many in June. At a few sites, stakes from previous years were found and resurveyed, making it possible to calculate surface velocity over a year or longer time span. The average summer surface velocity is shown in Figure 19.

At sites close to the glacier terminus very small lateral movement is generally measured. This indicates that the glacier snouts are almost stagnant. In the centre areas of some of the outlets especially close to the equilibrium line, there is an increase in velocity during summer compared to winter. The summer velocity is

typically in the order of two-fold the winter velocity. This suggests that basal sliding is increased in the melting season and is often at the same magnitude as the deformation velocity. To better understand the variable velocity continuous GNSS has been run during summer at several sites. From previous velocity measurements, surging of outlets has been predicted. Currently the increase in velocity at sites D05 and D07 (Fig. 20.) persists and suggests that Dyngjujökull may surge within a few years. The velocity at sites D07 and D05 is now similar to that in 1997 prior to the surge in 1998–2000 and the accumulation zone has thickened. To monitor velocity changes leading up to a surge GNSS instruments were set up in spring to continuously monitor movement at sites D05 and D07.

The data collected allows for post-processing to acquire more accuracy (\sim dm instead of \sim m), but the processing has not been finished when this report is written.

Figure 21. shows the average summer velocity and elevation change record at the survey sites on Eyjabakkajökull. There is a steady increase in velocity at sites E01 and E02 since about 2018. This may be caused by the rapid recession of the glacier snout, and thus steeper surface slopes, formation of a frontal lake and the floating of the ice front. This might be signs of a starting surge, but then speed up at E03 would be expected, which is not the case. Images of velocity and elevation records for other mb survey sites are displayed in Appendix F. Most vehicles used in the survey expeditions are equipped with survey type GNSS instruments that collect data while driving. These are post-processed, to yield surface profiles with an accuracy of \sim dm in horizontal and vertical. Location of all profiles surveyed in 2024 is shown in figure 22. The profiles have proved of high importance to increase accuracy of remote sensing-based surface DEMs.

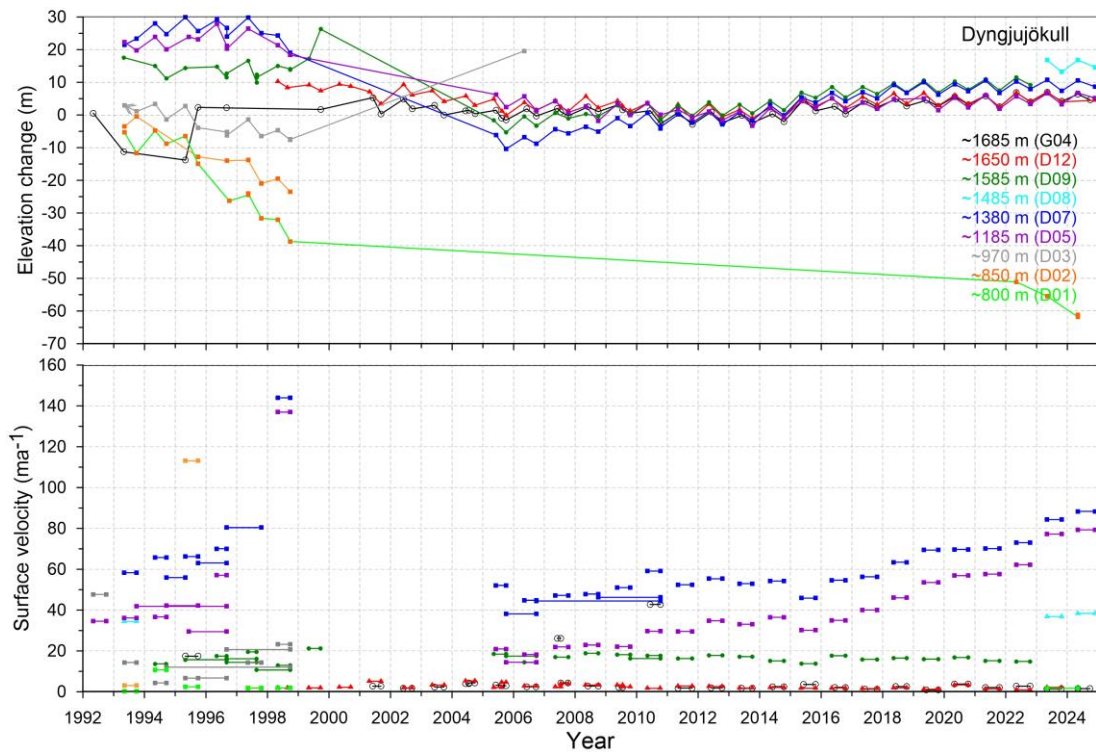


Figure 20. Surface elevation change relative to summer 2011 (upper panel) and average surface velocity (lower panel) at mb sites on Dyngjujökull in 1992 to 2024.

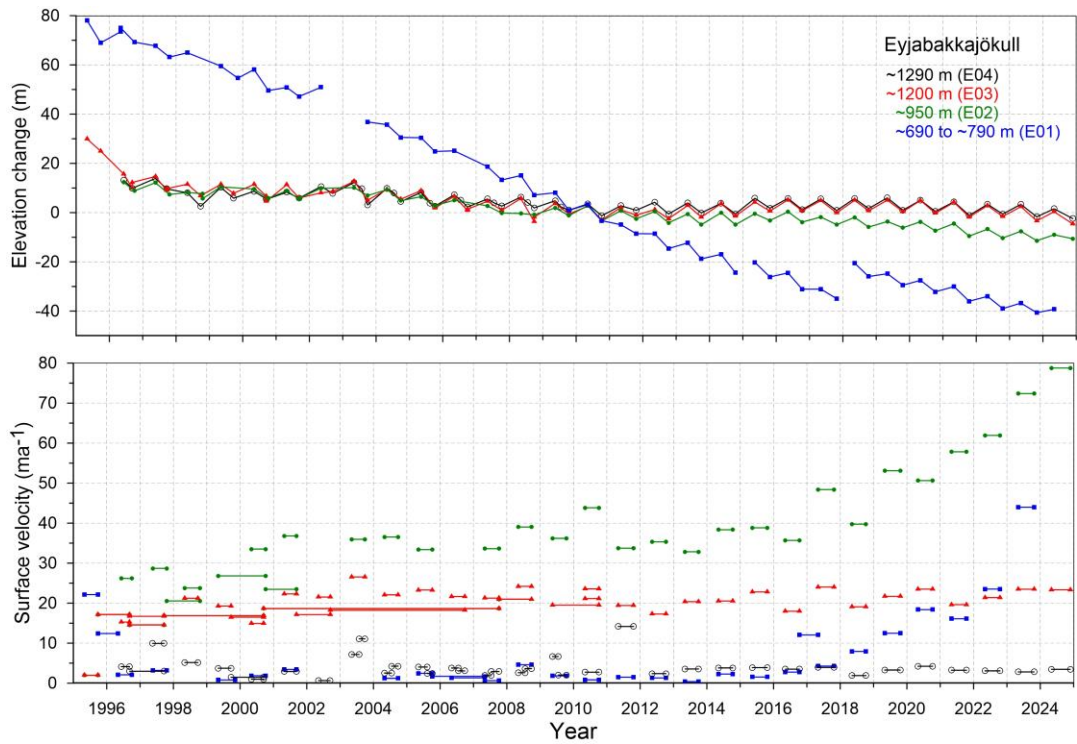


Figure 21. Surface elevation change relative to summer 2010 (upper panel) and average surface velocity (lower panel) at mb sites on Eyjabakkajökull in 1995 to 2024.

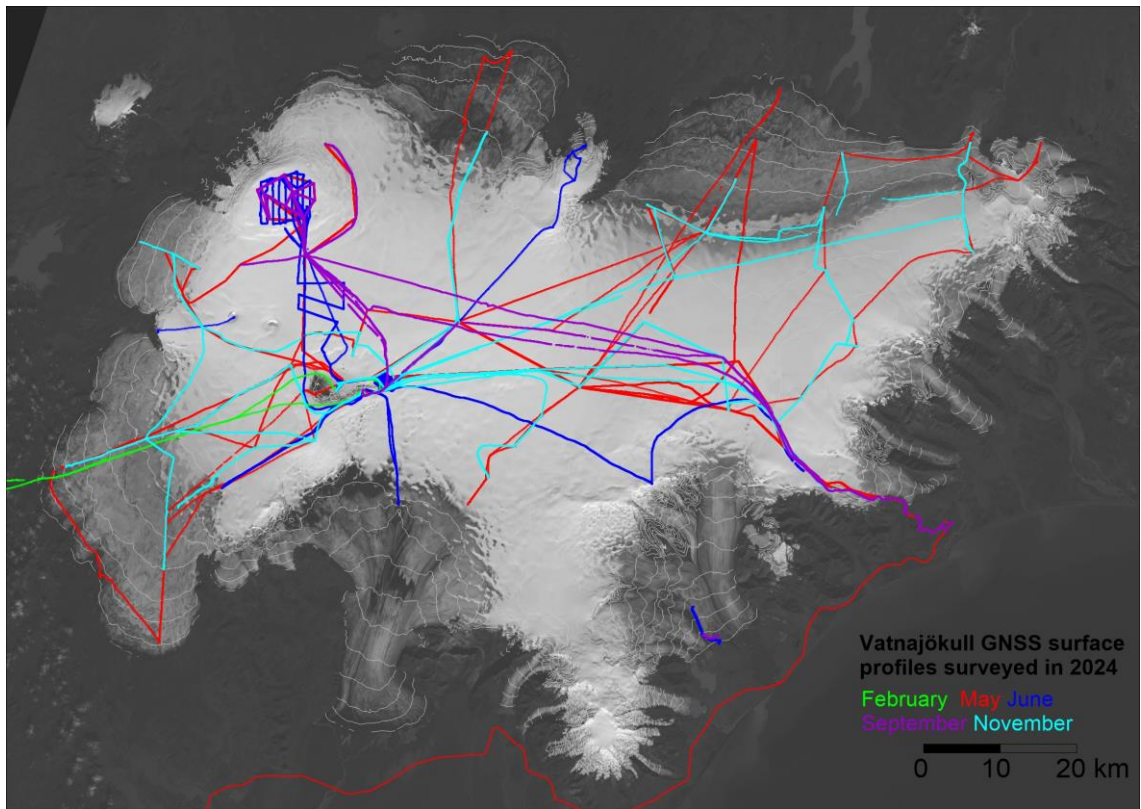


Figure 22. Location of surface elevation profiles surveyed in field trips on Vatnajökull in 2024.

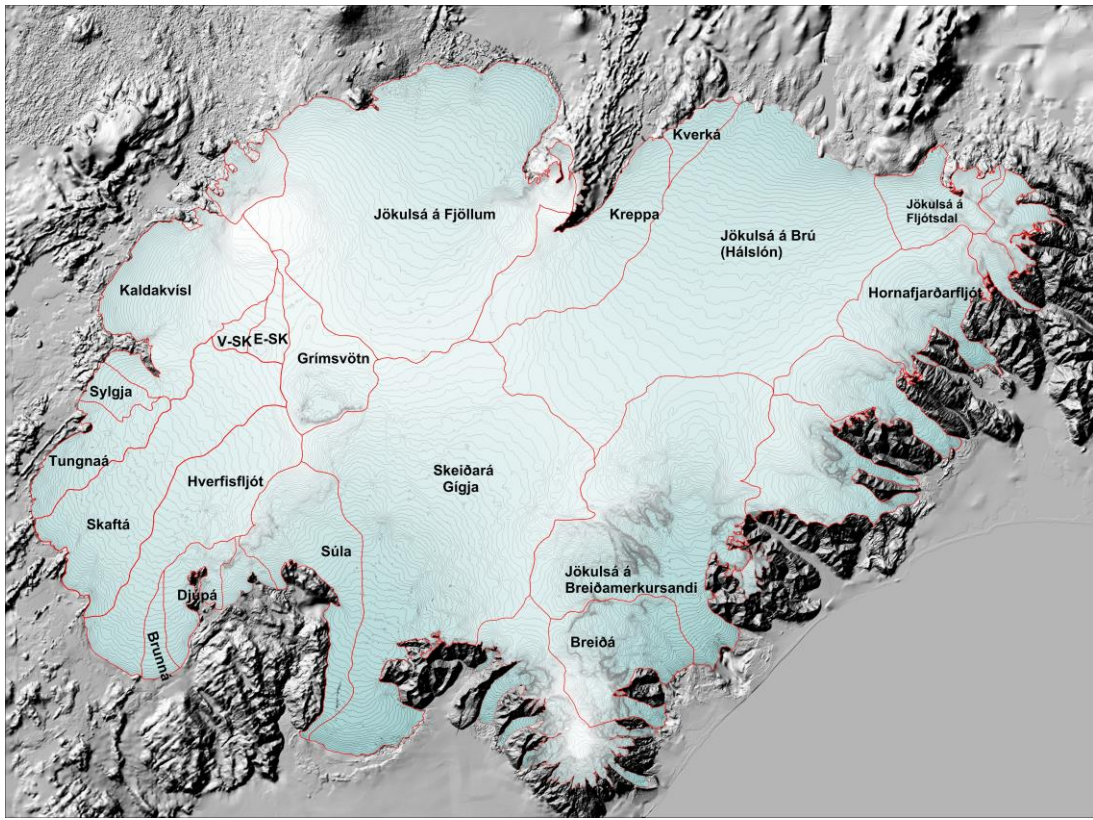


Figure 23. Water divides and drainage basins of selected rivers draining water from Vatnajökull, Súla is since summer 2016 diverted to Gígja.

5. Melt water runoff.

Water divides and drainage basins for rivers draining water from Vatnajökull have been defined from water pressure potential maps. The potential maps were produced from surface (year 2010) and bedrock DEMs.

Figure 23. shows the water divides and drainage areas for selected rivers draining melt water from Vatnajökull. The summer balance over the water basin is an estimate of meltwater contribution to rivers and groundwater storage. This estimate, however, does not include precipitation that falls as rain on the glacier, or snow that falls and melts during the summer. The meltwater contribution can be compared with river runoff at stream flow gauges closest to the glacier. For this comparison, we define the glaciological year from the start of October to the end of September and the period draining meltwater from the

glacier during the summer from June through September. It would be misleading to include May in the summer period because runoff from the glacier melt in May is delayed due

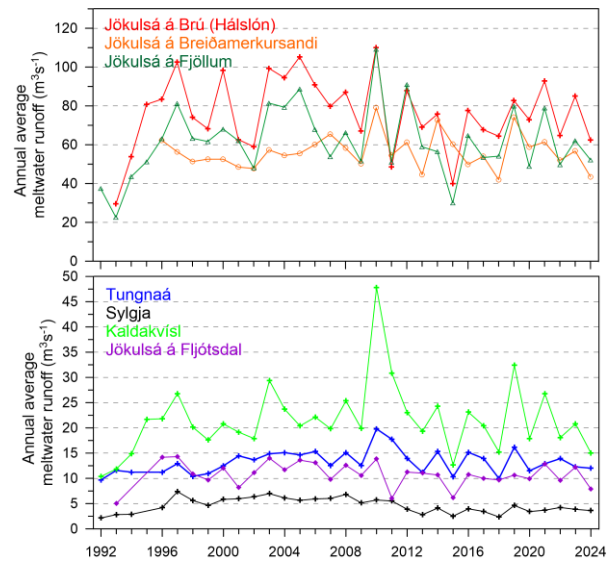


Figure 24. The temporal variation of average annual meltwater runoff to selected river catchments.

Table I. Melt water drainage to selected rivers in summer 2024.

| Water Catchment: | Area (km ²) | ΣQ_s (10 ⁶ m ³) | Q_s (m ³ s ⁻¹) | Q_a (m ³ s ⁻¹) | q_s (ls ⁻¹ km ⁻²) |
|-----------------------------|----------------------------|---|--|--|---|
| Vatnajökull | 7570 | 14545 | 1379.9 | 461.2 | 60.9 |
| Tungnaá | 104 | 379 | 35.9 | 12.0 | 115.0 |
| Sylgja | 38 | 114 | 10.8 | 3.6 | 95.6 |
| Kaldakvísl | 328 | 474 | 45.0 | 15.0 | 45.9 |
| Jökulsá á Fjöllum | 1109 | 1647 | 156.2 | 52.2 | 47.1 |
| Kreppa | 287 | 398 | 37.8 | 12.6 | 44.0 |
| Kverka | 34 | 139 | 13.2 | 4.4 | 129.3 |
| Háslón | 1186 | 1968 | 186.7 | 62.4 | 52.6 |
| Jökulsá á Fljótsdal | 121 | 249 | 23.6 | 7.9 | 65.5 |
| Jökulsá í Lóni | 92 | 179 | 17.0 | 5.7 | 61.6 |
| Hornafjarðarfljót | 227 | 463 | 43.9 | 14.7 | 64.5 |
| Jökulsá á Breiðamerkursandi | 686 | 1371 | 130.1 | 43.5 | 63.4 |
| Breiðá-Fjallsá | 220 | 770 | 73.0 | 24.4 | 110.9 |
| Gígia | 1383 | 2785 | 264.2 | 88.3 | 63.8 |
| Brunná | 30 | 129 | 12.2 | 4.1 | 137.2 |
| Djúpá | 70 | 230 | 21.8 | 7.3 | 104.0 |
| Hverfisfljót | 306 | 617 | 58.5 | 19.6 | 64.0 |
| Skaftá | 380 | 902 | 85.6 | 28.6 | 75.3 |
| Grímsvötn | 171 | 122 | 11.6 | 3.9 | 22.6 |
| Eystri Skaftárketill | 39 | 8 | 0.8 | 0.3 | 6.7 |
| Vestari Skaftárketill | 25 | 5 | 0.5 | 0.2 | 6.5 |
| Hólmsá | 157 | 364 | 34.5 | 11.5 | 73.7 |
| Heinabergsvötn | 214 | 515 | 48.9 | 16.3 | 76.5 |
| Skjálfandafljót | 89 | 79 | 7.4 | 2.5 | 27.9 |

ΣQ_s : total summer melt water; Q_s : average runoff (averaged over summer, 4 months, June – September)
 Q_a : average runoff (averaged over a whole year); q_s : average runoff per km² (averaged over a whole year)

to refreezing during elimination of the cold wave and because of the contribution of the spring snow melt from the highlands to the runoff. Some melting also occurs during winter, especially in the terminus regions of the southern outlets.

Average melt water runoff to different rivers is given in Table I, and temporal variation of the average meltwater runoff in Fig. 24. The average specific runoff (q_s) differs from basin to basin from ~31 to ~176 ls⁻¹km⁻². This is mainly due to different elevation distributions, for example, the water drainage basins for Tungnaá, Brunná and Kverká are within the ablation zone, while that of Grímsvötn and Skaftárkatlar are high in the accumulation zone.

Runoff as function of elevation, estimated from summer balance, is tabulated for individual water catchments in Appendix E.

6. Conclusions

In the glaciological year 2022_23 the winter balance for Vatnajökull was ~90% of the average in the observation period from 1991_92. 11 winters of the survey period have had lower winter balance, but 9 out the 12 recent years have had higher than average winter balance. The average winter balance is 1.6 m_{we} and standard variability is 0.27 m_{we}.

The total summer surface mass loss was 91% of the average since 1995 (86% than average since 1992). During the survey period, only 8 summers have had less surface mass loss. The average summer balance is -2.08 m_{we}, and the standard variability 0.55 m_{we}.

The net balance was negative by 62% of the average since 1995 (83% of the average since 1992), and only 8 glaciological years have had less annual surface mass loss.

The average net balance of the survey period is -0.46 m_{we}, and the standard variability 0.71 m_{we}

Since 2010, after the 15-year period of high mass loss, the summer and net balance have been highly variable, even one year with distinct positive mass balance in 2014_15 and close to zero in 2010_11, 2016_17, 2017_18 and 2021_22.

In contrast 2018_19 and 2020_21 are both among years with highest surface mass loss of the survey period. It is also noteworthy that 4 years of the last decade have had more mass loss than the average of the whole survey period. The cumulative mb for Vatnajökull is very similar to that of Köldukvíslarjökull, with a slope of -0.75 m_{wea}⁻¹ in the period of high mass loss, but -0.35 m_{wea}⁻¹ in the period after 2010.

During the survey period starting in 1991_92 Vatnajökull has lost ~134 km³ of ice or thinned ~15 m due to surface mass loss (summing from the

start of high mass loss in 1994_95 yields 162 km³ or 19 m thinning).

In addition, non-surface mass loss is estimated (calving, geothermal melt, internal friction, eruptions) ~0.21 m_{we} for Vatnajökull in a paper by Tómas Jóhannesson and others (Jóhannesson, T., Pálmarsson, B., Hjartarson, Á., Jarosch, A., Magnússon, E., Belart,J., et al. (2020). Non-surface mass balance of glaciers in Iceland. *J. Glaciol.* 66,685–697. doi:10.1017/jog.2020.37) which amounts to an ice loss of ~60 km³ or 7.7 m average thinning since 1994_95.

Glacier surface meltwater runoff in summer 2024 (estimated from summer surface balance only, summer rain and snow that falls and melts during summer, calving and geothermal and internal melting, is not included):

to Tungnaá 94% of the average, 70% of the average to Kaldakvísl, 88% of the average to Jökulsá á Fjöllum, 88% of the average to Háslón, 78% to Jökulsá í Fljótsdal and 83% to Jökulsá á Breiðamerkursandi.

(Averages refer to the survey period of each outlet.)

Surface velocity measurements suggest that Dyngjujökull is in the first phase of a surge and may complete a surge cycle within the next few years.

Surface mass balance summary 2023_24:

$$B_w = 11.50 \text{ km}^3 \text{ we}$$

$$B_s = -14.39 \text{ km}^3 \text{ we}$$

$$B_n = -2.88 \text{ km}^3 \text{ we}$$

$$AAR = 58\%$$

Specific Values:

$$b_w = 1.52 \text{ m}_w$$

$$b_s = -1.90 \text{ m}_w$$

$$b_n = -0.38 \text{ m}_w$$

$$b_{n(including other mass loss)} = -0.59 \text{ m}_w$$

Appendix A: Surface mass balance at measurement sites 2023_24.

b_w: specific winter balance, **b_s**: specific summer balance, **b_n**: specific net balance,
l_a: new snow in autumn (all in water equivalent).

| Site | Position | | Elévation | Date | Date | b _w | b _s | b _n | l _a |
|----------|----------|-----------|------------|-----------|-----------|----------------|----------------|----------------|----------------|
| | Latitude | Longitude | (m a.s.l.) | in spring | in autumn | (m) | (m) | (m) | (m) |
| B09-23 | 64 | 44.4833 | 16 | 6.1882 | 726.3 | 20230505 | 20231024 | 0.09 | -6.44 |
| B07-24 | 64 | 25.7965 | 16 | 17.4809 | 1358.8 | 20240430 | 20240925 | 2.23 | -1.10 |
| B09-24 | 64 | 44.4841 | 16 | 6.1878 | 720.2 | 20240502 | 20240000 | 0.24 | |
| B10-24 | 64 | 43.6842 | 16 | 6.7027 | 752.2 | 20240502 | 20241001 | 0.22 | -4.79 |
| B11-24 | 64 | 40.9390 | 16 | 10.4800 | 942.0 | 20240501 | 20240000 | 0.91 | |
| B12-24 | 64 | 38.2629 | 16 | 14.1506 | 1077.2 | 20240501 | 20241123 | 1.01 | -2.43 |
| B13-24 | 64 | 34.6584 | 16 | 19.5610 | 1219.2 | 20240502 | 20241001 | 1.65 | -1.47 |
| B14-24 | 64 | 31.6498 | 16 | 24.7708 | 1324.8 | 20240501 | 20241121 | 1.89 | -1.19 |
| B15-24 | 64 | 28.5128 | 16 | 30.0324 | 1405.7 | 20240501 | 20241121 | 1.97 | -0.94 |
| B16-24 | 64 | 24.1239 | 16 | 40.9139 | 1528.9 | 20240501 | 20241001 | 1.89 | -0.25 |
| B17-24 | 64 | 36.7326 | 16 | 28.7959 | 1216.6 | 20240501 | 20241121 | 1.48 | -2.60 |
| B18-24 | 64 | 31.5817 | 16 | 0.1196 | 1316.2 | 20240501 | 20241121 | 1.91 | -1.14 |
| B19-24 | 64 | 28.0098 | 15 | 55.9862 | 1438.6 | 20240501 | 20241121 | 2.31 | -0.23 |
| Barc-24 | 64 | 38.4207 | 17 | 26.7611 | 1906.6 | 20240609 | 20240927 | 1.90 | 0.00 |
| Bb0-24 | 64 | 22.7065 | 16 | 5.0575 | 1515.5 | 20240501 | 20241121 | 2.28 | -0.48 |
| Bor-24 | 64 | 24.9353 | 17 | 20.1523 | 1408.0 | 20240609 | 20241123 | 1.89 | -2.32 |
| Borth-24 | 64 | 24.9910 | 17 | 19.2025 | 1410.4 | 20240502 | 20240930 | 1.70 | -1.72 |
| Br1-24 | 64 | 5.9573 | 16 | 19.8247 | 58.7 | 20240501 | 20240928 | -1.03 | -8.53 |
| Br2-24 | 64 | 6.3538 | 16 | 22.5234 | 140.3 | 20240501 | 20240928 | -0.87 | -7.42 |
| Br3-24 | 64 | 8.4069 | 16 | 23.9626 | 342.9 | 20240501 | 20240000 | 0.00 | |
| Br7-24 | 64 | 22.1413 | 16 | 16.9309 | 1243.1 | 20240501 | 20241121 | 1.91 | -0.81 |
| Bru-24 | 64 | 39.7561 | 15 | 56.5333 | 889.3 | 20240501 | 20241123 | 0.64 | -3.86 |
| Bud-24 | 64 | 35.9920 | 15 | 59.8869 | 1137.4 | 20240501 | 20241121 | 1.69 | -1.98 |
| D01-24 | 64 | 47.8680 | 16 | 49.9738 | 833.7 | 20240503 | 20240000 | 0.34 | |
| D05-24 | 64 | 42.2298 | 16 | 54.6827 | 1206.7 | 20240503 | 20241123 | 0.98 | -2.44 |
| D07-24 | 64 | 38.2946 | 16 | 59.2556 | 1378.4 | 20240503 | 20241123 | 1.58 | -1.13 |
| D08-24 | 64 | 34.6858 | 17 | 1.5208 | 1488.8 | 20240503 | 20241123 | 1.63 | -0.74 |
| D12-24 | 64 | 28.9748 | 17 | 0.1844 | 1651.6 | 20240502 | 20241123 | 2.15 | -0.20 |
| E01-24 | 64 | 40.6633 | 15 | 34.8317 | 747.8 | 20240501 | 20240000 | 0.35 | |
| E02-24 | 64 | 39.1111 | 15 | 36.0021 | 948.5 | 20240501 | 20241123 | 1.07 | -3.69 |
| E03-24 | 64 | 36.6643 | 15 | 36.9262 | 1185.2 | 20240501 | 20241123 | 1.97 | -1.90 |
| E04-24 | 64 | 34.9530 | 15 | 37.1465 | 1286.7 | 20240501 | 20241123 | 2.01 | -1.01 |
| E07-24 | 64 | 38.4128 | 15 | 24.6995 | 1067.9 | 20240501 | 20240000 | 1.78 | |
| E08-24 | 64 | 39.7220 | 15 | 23.8488 | 945.6 | 20240501 | 20240000 | 1.29 | |
| Fl01-24 | 64 | 26.1578 | 15 | 55.6246 | 1346.0 | 20240501 | 20241121 | 2.31 | -0.83 |
| G02-24 | 64 | 26.8495 | 17 | 17.7109 | 1567.5 | 20240503 | 20241121 | 1.87 | -0.81 |
| G03-24 | 64 | 28.4432 | 17 | 16.3317 | 1660.9 | 20240503 | 20241122 | 1.99 | -0.33 |
| G04-24 | 64 | 30.0218 | 17 | 15.0384 | 1690.7 | 20240503 | 20240927 | 1.87 | -0.28 |
| Go1-24 | 64 | 33.9740 | 17 | 24.9254 | 1761.3 | 20240504 | 20240926 | 1.93 | 0.10 |
| Haab-24 | 64 | 20.9661 | 17 | 24.1103 | 1729.6 | 20240504 | 20241122 | 2.45 | 0.47 |
| Hof01-24 | 64 | 32.3434 | 15 | 35.8545 | 1140.6 | 20240501 | 20241123 | 2.20 | -1.61 |

| | | | | | | | | | | | |
|----------|----|---------|----|---------|--------|----------|----------|------|-------|-------|------|
| K01-24 | 64 | 35.1697 | 17 | 51.8566 | 1036.5 | 20240504 | 20241122 | 0.66 | -4.12 | -3.47 | 0.03 |
| K02-24 | 64 | 34.8167 | 17 | 49.7080 | 1164.2 | 20240504 | 20241122 | 0.80 | -2.86 | -2.06 | 0.06 |
| K03-24 | 64 | 34.2393 | 17 | 46.4293 | 1289.2 | 20240504 | 20241122 | 0.79 | -1.79 | -1.00 | 0.03 |
| K04-24 | 64 | 33.2070 | 17 | 42.3638 | 1479.9 | 20240504 | 20241122 | 1.50 | -0.84 | 0.65 | 0.16 |
| K05-24 | 64 | 33.4449 | 17 | 35.4525 | 1677.9 | 20240504 | 20240926 | 1.49 | -0.11 | 1.37 | 0.02 |
| K06-24 | 64 | 38.3574 | 17 | 31.3104 | 1946.3 | 20240504 | 20240926 | 1.85 | 0.75 | 2.60 | 0.23 |
| K07-24 | 64 | 29.1116 | 17 | 42.0174 | 1530.5 | 20240504 | 20241122 | 1.55 | -0.36 | 1.19 | 0.21 |
| Kverk-24 | 64 | 38.6640 | 16 | 40.5191 | 1824.6 | 20240612 | 20240000 | 1.88 | | | 0.00 |
| S01-24 | 64 | 7.0173 | 17 | 49.9724 | 693.3 | 20240504 | | 0.35 | | | |
| S02-24 | 64 | 12.1659 | 17 | 48.9957 | 997.4 | 20240504 | 20241122 | 1.23 | -3.26 | -2.03 | 0.00 |
| S04-24 | 64 | 16.1761 | 17 | 48.1993 | 1153.9 | 20240504 | 20241122 | 1.47 | -2.43 | -0.96 | 0.03 |
| S05-24 | 64 | 20.5172 | 17 | 33.9922 | 1450.4 | 20240503 | 20241122 | 1.63 | -0.79 | 0.84 | 0.24 |
| Ske02-24 | 64 | 16.3571 | 16 | 59.2968 | 1196.9 | 20240502 | 20240000 | 1.27 | | | 0.00 |
| Ske03-24 | 64 | 18.0542 | 16 | 56.1678 | 1296.6 | 20240502 | 20241001 | 1.78 | -1.12 | 0.65 | 0.00 |
| Ske04-24 | 64 | 20.1442 | 16 | 51.8033 | 1397.7 | 20240502 | 20241121 | 2.19 | -0.81 | 1.38 | 0.15 |
| Ske05-24 | 64 | 22.2338 | 16 | 47.2258 | 1472.6 | 20240502 | 20241121 | 2.50 | -0.68 | 1.82 | 0.22 |
| Skf00-24 | 64 | 15.4813 | 15 | 54.0959 | 945.0 | 20240430 | 20240925 | 1.74 | -4.97 | -3.23 | 0.00 |
| Skf01-24 | 64 | 18.0173 | 16 | 5.0229 | 1283.4 | 20240430 | 20240925 | 2.76 | -0.97 | 1.79 | 0.00 |
| T01-24 | 64 | 19.1551 | 18 | 6.5258 | 753.1 | 20240505 | 20240129 | 0.22 | | | |
| T02-24 | 64 | 19.4775 | 18 | 4.5569 | 876.1 | 20240504 | 20241022 | 0.43 | -4.97 | -4.55 | 0.03 |
| T03-24 | 64 | 20.1986 | 17 | 58.6135 | 1058.9 | 20240504 | 20241001 | 0.85 | -3.41 | -2.56 | 0.00 |
| T04-24 | 64 | 21.3299 | 17 | 51.5161 | 1217.8 | 20240503 | 20241122 | 1.23 | -2.52 | -1.30 | 0.11 |
| T05-24 | 64 | 22.2627 | 17 | 42.9974 | 1343.9 | 20240503 | 20241122 | 1.28 | -1.44 | -0.17 | 0.17 |
| T06-24 | 64 | 24.2655 | 17 | 36.5159 | 1466.9 | 20240504 | 20241122 | 1.71 | -0.72 | 0.99 | 0.19 |
| T06-24 | 64 | 24.2655 | 17 | 36.5159 | 1466.9 | 20240504 | 20240930 | 1.71 | -0.75 | 0.96 | 0.03 |
| T07-24 | 64 | 25.2953 | 17 | 31.2118 | 1562.8 | 20240503 | 20241122 | 1.96 | -0.73 | 1.24 | 0.24 |
| T08-24 | 64 | 26.3007 | 17 | 27.7483 | 1635.9 | 20240503 | 20241122 | 1.96 | -0.70 | 1.27 | 0.27 |

Appendix B: Surface mass balance distribution by elevation in 2023_24.

ΔS : area in elevation range, $\sum \Delta S$: cumulative area above given elevation, b_w : specific winter balance, b_s : specific summer balance, b_n : specific winter balance, ΔB_w : winter balance at a given elevation range, $\sum \Delta B_w$: cumulative winter balance above given elevation, ΔB_s summer balance at a given elevation range, $\sum \Delta B_s$: cumulative summer balance above given elevation, ΔB_n : net annual balance in a given elevation range, $\sum B_n$: cumulative net annual balance above given elevation.

Vatnajökull

| Elevation (m a.s.l.) | ΔS (km ²) | $\sum \Delta S$ (km ²) | b_w (mm) | b_s (mm) | b_n (mm) | ΔB_w (10 ⁶ m ³) | $\sum \Delta B_w$ (10 ⁶ m ³) | ΔB_s (10 ⁶ m ³) | $\sum \Delta B_s$ (10 ⁶ m ³) | ΔB_n (10 ⁶ m ³) | $\sum B_n$ (10 ⁶ m ³) |
|-------------------------|----------------------------------|---------------------------------------|---------------|---------------|---------------|---|--|---|--|---|---|
|-------------------------|----------------------------------|---------------------------------------|---------------|---------------|---------------|---|--|---|--|---|---|

| | | | | | | | | | | | | | |
|------|------|------|-------|--------|-------|-------|--------|--------|---------|--------|----------|--------|---------|
| 2000 | 2050 | 2025 | 0.3 | 0.3 | 4851 | 2470 | 7322 | 1.7 | 1.7 | 0.9 | 0.9 | 2.6 | 2.6 |
| 1950 | 2000 | 1975 | 6.9 | 7.3 | 2549 | 967 | 3517 | 17.6 | 19.3 | 6.7 | 7.6 | 24.3 | 26.9 |
| 1900 | 1950 | 1925 | 41.3 | 48.6 | 2070 | 529 | 2599 | 85.6 | 104.9 | 21.9 | 29.4 | 107.4 | 134.3 |
| 1850 | 1900 | 1875 | 44.3 | 92.9 | 2288 | 526 | 2815 | 101.5 | 206.4 | 23.3 | 52.8 | 124.8 | 259.1 |
| 1800 | 1850 | 1825 | 45.6 | 138.6 | 2555 | 737 | 3292 | 116.6 | 323.0 | 33.7 | 86.4 | 150.3 | 409.4 |
| 1750 | 1800 | 1775 | 54.8 | 193.4 | 2266 | 417 | 2684 | 124.3 | 447.3 | 22.9 | 109.3 | 147.2 | 556.6 |
| 1700 | 1750 | 1725 | 114.4 | 307.8 | 2025 | 73 | 2099 | 231.7 | 679.0 | 8.5 | 117.8 | 240.2 | 796.8 |
| 1650 | 1700 | 1675 | 217.3 | 525.1 | 2016 | -185 | 1830 | 438.1 | 1117.2 | -40.3 | 77.4 | 397.8 | 1194.6 |
| 1600 | 1650 | 1625 | 373.6 | 898.7 | 2060 | -250 | 1809 | 770.0 | 1887.1 | -93.8 | -16.3 | 676.2 | 1870.8 |
| 1550 | 1600 | 1575 | 357.9 | 1256.6 | 2036 | -345 | 1691 | 728.8 | 2616.0 | -123.6 | -139.9 | 605.2 | 2476.0 |
| 1500 | 1550 | 1525 | 421.2 | 1677.8 | 1983 | -475 | 1507 | 835.7 | 3451.7 | -200.5 | -340.4 | 635.2 | 3111.2 |
| 1450 | 1500 | 1475 | 452.5 | 2130.4 | 1968 | -656 | 1311 | 890.8 | 4342.5 | -297.3 | -637.7 | 593.5 | 3704.8 |
| 1400 | 1450 | 1425 | 502.9 | 2633.3 | 1982 | -800 | 1182 | 996.8 | 5339.3 | -402.4 | -1040.1 | 594.4 | 4299.2 |
| 1350 | 1400 | 1375 | 540.3 | 3173.6 | 1958 | -961 | 997 | 1058.1 | 6397.4 | -519.3 | -1559.4 | 538.8 | 4838.0 |
| 1300 | 1350 | 1325 | 531.3 | 3704.8 | 1868 | -1140 | 728 | 992.9 | 7390.3 | -606.0 | -2165.4 | 386.9 | 5224.9 |
| 1250 | 1300 | 1275 | 496.7 | 4201.6 | 1758 | -1353 | 405 | 873.5 | 8263.8 | -672.1 | -2837.6 | 201.3 | 5426.2 |
| 1200 | 1250 | 1225 | 435.5 | 4637.1 | 1597 | -1680 | -83 | 695.8 | 8959.6 | -732.1 | -3569.6 | -36.2 | 5390.0 |
| 1150 | 1200 | 1175 | 387.9 | 5025.0 | 1448 | -2031 | -583 | 561.8 | 9521.4 | -788.0 | -4357.6 | -226.2 | 5163.8 |
| 1100 | 1150 | 1125 | 344.1 | 5369.1 | 1324 | -2349 | -1025 | 455.8 | 9977.2 | -808.5 | -5166.1 | -352.7 | 4811.1 |
| 1050 | 1100 | 1075 | 296.5 | 5665.6 | 1214 | -2670 | -1456 | 360.1 | 10337.3 | -791.8 | -5957.9 | -431.7 | 4379.4 |
| 1000 | 1050 | 1025 | 276.5 | 5942.1 | 1101 | -3023 | -1921 | 304.5 | 10641.8 | -835.9 | -6793.8 | -531.4 | 3848.0 |
| 950 | 1000 | 975 | 247.4 | 6189.5 | 1010 | -3311 | -2301 | 249.9 | 10891.8 | -819.4 | -7613.2 | -569.4 | 3278.6 |
| 900 | 950 | 925 | 214.0 | 6403.6 | 911 | -3575 | -2663 | 195.2 | 11086.9 | -765.2 | -8378.4 | -570.1 | 2708.5 |
| 850 | 900 | 875 | 184.3 | 6587.9 | 792 | -3854 | -3061 | 146.1 | 11233.0 | -710.4 | -9088.8 | -564.3 | 2144.2 |
| 800 | 850 | 825 | 166.7 | 6754.6 | 689 | -4153 | -3463 | 114.9 | 11347.9 | -692.2 | -9781.0 | -577.4 | 1566.9 |
| 750 | 800 | 775 | 145.4 | 6899.9 | 594 | -4388 | -3793 | 86.5 | 11434.4 | -637.9 | -10418.9 | -551.4 | 1015.4 |
| 700 | 750 | 725 | 114.8 | 7014.8 | 519 | -4550 | -4030 | 59.7 | 11494.1 | -522.5 | -10941.5 | -462.8 | 552.6 |
| 650 | 700 | 675 | 95.1 | 7109.9 | 516 | -4641 | -4125 | 49.1 | 11543.2 | -441.4 | -11382.9 | -392.3 | 160.3 |
| 600 | 650 | 625 | 64.3 | 7174.2 | 537 | -4770 | -4232 | 34.6 | 11577.8 | -306.9 | -11689.8 | -272.3 | -112.0 |
| 550 | 600 | 575 | 52.7 | 7226.9 | 455 | -5024 | -4568 | 24.0 | 11601.8 | -264.9 | -11954.7 | -240.9 | -352.9 |
| 500 | 550 | 525 | 53.6 | 7280.5 | 353 | -5296 | -4942 | 18.9 | 11620.7 | -283.8 | -12238.5 | -264.9 | -617.8 |
| 450 | 500 | 475 | 37.9 | 7318.4 | 253 | -5546 | -5292 | 9.6 | 11630.3 | -210.2 | -12448.7 | -200.5 | -818.4 |
| 400 | 450 | 425 | 34.7 | 7353.2 | 149 | -5776 | -5626 | 5.2 | 11635.5 | -200.7 | -12649.3 | -195.5 | -1013.8 |
| 350 | 400 | 375 | 38.9 | 7392.0 | 14 | -6034 | -6020 | 0.5 | 11636.1 | -234.6 | -12883.9 | -234.0 | -1247.8 |
| 300 | 350 | 325 | 35.2 | 7427.2 | -155 | -6373 | -6528 | -5.5 | 11630.6 | -224.1 | -13108.0 | -229.6 | -1477.4 |
| 250 | 300 | 275 | 31.9 | 7459.1 | -336 | -6721 | -7058 | -10.8 | 11619.9 | -214.5 | -13322.5 | -225.2 | -1702.6 |
| 200 | 250 | 225 | 30.7 | 7489.8 | -526 | -7082 | -7608 | -16.1 | 11603.7 | -217.2 | -13539.7 | -233.4 | -1936.0 |
| 150 | 200 | 175 | 29.6 | 7519.4 | -692 | -7449 | -8141 | -20.5 | 11583.2 | -220.7 | -13760.4 | -241.2 | -2177.2 |
| 100 | 150 | 125 | 28.2 | 7547.6 | -859 | -7885 | -8744 | -24.2 | 11559.0 | -222.3 | -13982.8 | -246.6 | -2423.8 |
| 50 | 100 | 75 | 22.2 | 7569.8 | -1035 | -8341 | -9376 | -23.0 | 11536.0 | -185.1 | -14167.9 | -208.1 | -2631.9 |
| 0 | 50 | 25 | 24.1 | 7593.9 | -1352 | -9124 | -10477 | -32.6 | 11503.4 | -219.7 | -14387.6 | -252.3 | -2884.1 |

Tungnaárjökull

| | Elevation (m a.s.l.) | ΔS (km ²) | $\sum \Delta S$ (km ²) | b_w (mm) | b_s (mm) | b_n (mm) | ΔB_w (10 ⁶ m ³) | $\sum \Delta B_w$ (10 ⁶ m ³) | ΔB_s (10 ⁶ m ³) | $\sum \Delta B_s$ (10 ⁶ m ³) | ΔB_n (10 ⁶ m ³) | $\sum B_n$ (10 ⁶ m ³) | |
|------|-------------------------|----------------------------------|---------------------------------------|---------------|---------------|---------------|---|--|---|--|---|---|--------|
| 1650 | 1700 | 1675 | 1.7 | 1.7 | 1899 | -525 | 1374 | 3.3 | 3.3 | -0.9 | -0.9 | 2.4 | 2.4 |
| 1600 | 1650 | 1625 | 12.3 | 14.0 | 1922 | -577 | 1345 | 23.7 | 27.0 | -7.1 | -8.0 | 16.6 | 18.9 |
| 1550 | 1600 | 1575 | 16.3 | 30.4 | 1863 | -558 | 1304 | 30.4 | 57.4 | -9.1 | -17.1 | 21.3 | 40.2 |
| 1500 | 1550 | 1525 | 16.1 | 46.4 | 1788 | -619 | 1169 | 28.7 | 86.1 | -9.9 | -27.1 | 18.8 | 59.0 |
| 1450 | 1500 | 1475 | 18.3 | 64.7 | 1670 | -711 | 958 | 30.6 | 116.7 | -13.0 | -40.1 | 17.5 | 76.6 |
| 1400 | 1450 | 1425 | 23.0 | 87.8 | 1540 | -932 | 608 | 35.5 | 152.1 | -21.5 | -61.6 | 14.0 | 90.6 |
| 1350 | 1400 | 1375 | 21.0 | 108.8 | 1401 | -1186 | 214 | 29.4 | 181.6 | -24.9 | -86.5 | 4.5 | 95.1 |
| 1300 | 1350 | 1325 | 27.1 | 135.9 | 1316 | -1499 | -183 | 35.7 | 217.3 | -40.6 | -127.1 | -5.0 | 90.1 |
| 1250 | 1300 | 1275 | 20.3 | 156.2 | 1283 | -1934 | -651 | 26.1 | 243.3 | -39.3 | -166.4 | -13.2 | 76.9 |
| 1200 | 1250 | 1225 | 22.2 | 178.4 | 1207 | -2418 | -1211 | 26.8 | 270.1 | -53.7 | -220.2 | -26.9 | 50.0 |
| 1150 | 1200 | 1175 | 21.0 | 199.4 | 1110 | -2759 | -1649 | 23.3 | 293.4 | -57.9 | -278.0 | -34.6 | 15.4 |
| 1100 | 1150 | 1125 | 17.6 | 217.0 | 977 | -3047 | -2069 | 17.3 | 310.7 | -53.8 | -331.8 | -36.5 | -21.1 |
| 1050 | 1100 | 1075 | 16.4 | 233.4 | 871 | -3364 | -2492 | 14.3 | 325.0 | -55.3 | -387.1 | -41.0 | -62.1 |
| 1000 | 1050 | 1025 | 16.7 | 250.2 | 770 | -3775 | -3005 | 12.9 | 337.9 | -63.1 | -450.3 | -50.3 | -112.4 |
| 950 | 1000 | 975 | 15.6 | 265.8 | 647 | -4209 | -3561 | 10.1 | 348.0 | -65.8 | -516.1 | -55.7 | -168.1 |
| 900 | 950 | 925 | 16.0 | 281.8 | 526 | -4615 | -4088 | 8.4 | 356.4 | -74.0 | -590.1 | -65.6 | -233.6 |
| 850 | 900 | 875 | 12.4 | 294.3 | 425 | -4984 | -4558 | 5.3 | 361.7 | -61.9 | -652.0 | -56.6 | -290.2 |
| 800 | 850 | 825 | 12.1 | 306.3 | 351 | -5303 | -4951 | 4.2 | 366.0 | -63.9 | -715.9 | -59.7 | -349.9 |
| 750 | 800 | 775 | 9.7 | 316.0 | 287 | -5689 | -5401 | 2.8 | 368.8 | -54.9 | -770.9 | -52.2 | -402.1 |
| 700 | 750 | 725 | 6.1 | 322.0 | 239 | -6032 | -5792 | 1.5 | 370.2 | -36.5 | -807.4 | -35.1 | -437.2 |
| 650 | 700 | 675 | 1.2 | 323.2 | 229 | -6116 | -5887 | 0.3 | 370.5 | -7.1 | -814.5 | -6.9 | -444.0 |

Sylgjujökull

| | Elevation (m a.s.l.) | ΔS (km ²) | $\sum \Delta S$ (km ²) | b_w (mm) | b_s (mm) | b_n (mm) | ΔB_w (10 ⁶ m ³) | $\sum \Delta B_w$ (10 ⁶ m ³) | ΔB_s (10 ⁶ m ³) | $\sum \Delta B_s$ (10 ⁶ m ³) | ΔB_n (10 ⁶ m ³) | $\sum B_n$ (10 ⁶ m ³) | |
|------|-------------------------|----------------------------------|---------------------------------------|---------------|---------------|---------------|---|--|---|--|---|---|--------|
| 1600 | 1650 | 1625 | 1.4 | 1.4 | 1790 | -320 | 1469 | 2.5 | 2.5 | -0.4 | -0.4 | 2.0 | 2.0 |
| 1550 | 1600 | 1575 | 5.1 | 6.5 | 1732 | -372 | 1359 | 8.9 | 11.3 | -1.9 | -2.3 | 7.0 | 9.0 |
| 1500 | 1550 | 1525 | 18.8 | 25.3 | 1612 | -436 | 1176 | 30.4 | 41.7 | -8.2 | -10.6 | 22.1 | 31.1 |
| 1450 | 1500 | 1475 | 13.4 | 38.7 | 1536 | -618 | 917 | 20.6 | 62.3 | -8.3 | -18.9 | 12.3 | 43.4 |
| 1400 | 1450 | 1425 | 8.3 | 47.1 | 1497 | -872 | 625 | 12.5 | 74.8 | -7.3 | -26.1 | 5.2 | 48.6 |
| 1350 | 1400 | 1375 | 5.6 | 52.6 | 1428 | -1094 | 334 | 8.0 | 82.7 | -6.1 | -32.2 | 1.9 | 50.5 |
| 1300 | 1350 | 1325 | 5.1 | 57.7 | 1362 | -1434 | -72 | 6.9 | 89.7 | -7.3 | -39.5 | -0.4 | 50.1 |
| 1250 | 1300 | 1275 | 9.6 | 67.3 | 1227 | -1991 | -763 | 11.8 | 101.5 | -19.1 | -58.7 | -7.3 | 42.8 |
| 1200 | 1250 | 1225 | 11.4 | 78.7 | 1048 | -2559 | -1511 | 11.9 | 113.4 | -29.2 | -87.9 | -17.2 | 25.6 |
| 1150 | 1200 | 1175 | 12.8 | 91.5 | 867 | -2907 | -2039 | 11.1 | 124.5 | -37.2 | -125.1 | -26.1 | -0.5 |
| 1100 | 1150 | 1125 | 12.1 | 103.6 | 726 | -3141 | -2415 | 8.8 | 133.3 | -38.0 | -163.1 | -29.2 | -29.7 |
| 1050 | 1100 | 1075 | 11.2 | 114.8 | 638 | -3379 | -2740 | 7.1 | 140.4 | -37.7 | -200.7 | -30.6 | -60.3 |
| 1000 | 1050 | 1025 | 9.9 | 124.7 | 576 | -3654 | -3077 | 5.7 | 146.2 | -36.3 | -237.1 | -30.6 | -90.9 |
| 950 | 1000 | 975 | 3.1 | 127.8 | 538 | -3825 | -3287 | 1.7 | 147.8 | -11.9 | -248.9 | -10.2 | -101.1 |
| 900 | 950 | 925 | 1.2 | 129.1 | 506 | -3998 | -3492 | 0.6 | 148.5 | -4.9 | -253.8 | -4.3 | -105.4 |

Köldukvíslarjökul

| Elevation (m a.s.l.) | ΔS (km ²) | $\sum \Delta S$ (km ²) | b _w (mm) | b _s (mm) | b _n (mm) | ΔB_w (10 ⁶ m ³) | $\sum \Delta B_w$ (10 ⁶ m ³) | ΔB_s (10 ⁶ m ³) | $\sum \Delta B_s$ (10 ⁶ m ³) | ΔB_n (10 ⁶ m ³) | $\sum B_n$ (10 ⁶ m ³) | | |
|--------------------------|----------------------------------|---------------------------------------|------------------------|------------------------|------------------------|---|--|---|--|---|---|-------|-------|
| 1950 | 2000 | 1975 | 0.6 | 0.6 | 1892 | 648 | 2540 | 1.2 | 1.2 | 0.4 | 0.4 | 1.6 | 1.6 |
| 1900 | 1950 | 1925 | 13.7 | 14.4 | 1869 | 461 | 2331 | 25.7 | 26.9 | 6.3 | 6.8 | 32.0 | 33.6 |
| 1850 | 1900 | 1875 | 6.6 | 20.9 | 1821 | 291 | 2113 | 12.0 | 38.9 | 1.9 | 8.7 | 13.9 | 47.5 |
| 1800 | 1850 | 1825 | 6.2 | 27.1 | 1810 | 213 | 2024 | 11.2 | 50.1 | 1.3 | 10.0 | 12.5 | 60.1 |
| 1750 | 1800 | 1775 | 10.1 | 37.3 | 1790 | 160 | 1950 | 18.2 | 68.2 | 1.6 | 11.6 | 19.8 | 79.9 |
| 1700 | 1750 | 1725 | 17.3 | 54.6 | 1715 | 48 | 1763 | 29.6 | 97.9 | 0.8 | 12.5 | 30.5 | 110.3 |
| 1650 | 1700 | 1675 | 16.0 | 70.5 | 1648 | -110 | 1538 | 26.3 | 124.2 | -1.8 | 10.7 | 24.6 | 134.9 |
| 1600 | 1650 | 1625 | 14.3 | 84.8 | 1615 | -261 | 1353 | 23.1 | 147.3 | -3.7 | 6.9 | 19.4 | 154.3 |
| 1550 | 1600 | 1575 | 18.4 | 103.3 | 1600 | -425 | 1175 | 29.5 | 176.8 | -7.8 | -0.9 | 21.7 | 176.0 |
| 1500 | 1550 | 1525 | 19.9 | 123.2 | 1530 | -582 | 947 | 30.5 | 207.3 | -11.6 | -12.5 | 18.9 | 194.8 |
| 1450 | 1500 | 1475 | 19.2 | 142.4 | 1460 | -791 | 668 | 28.1 | 235.4 | -15.2 | -27.7 | 12.9 | 207.7 |
| 1400 | 1450 | 1425 | 14.8 | 157.2 | 1361 | -1000 | 360 | 20.2 | 255.6 | -14.8 | -42.5 | 5.3 | 213.0 |
| 1350 | 1400 | 1375 | 14.7 | 172.0 | 1217 | -1265 | -48 | 18.0 | 273.5 | -18.7 | -61.2 | -0.7 | 212.3 |
| 1300 | 1350 | 1325 | 16.3 | 188.3 | 1064 | -1591 | -526 | 17.3 | 290.9 | -25.9 | -87.1 | -8.6 | 203.7 |
| 1250 | 1300 | 1275 | 17.3 | 205.6 | 948 | -2001 | -1053 | 16.4 | 307.3 | -34.7 | -121.8 | -18.2 | 185.5 |
| 1200 | 1250 | 1225 | 16.5 | 222.1 | 860 | -2447 | -1587 | 14.2 | 321.5 | -40.5 | -162.3 | -26.2 | 159.2 |
| 1150 | 1200 | 1175 | 15.9 | 238.0 | 784 | -2891 | -2107 | 12.5 | 334.0 | -46.0 | -208.3 | -33.5 | 125.7 |
| 1100 | 1150 | 1125 | 14.1 | 252.1 | 702 | -3324 | -2622 | 9.9 | 343.9 | -46.8 | -255.1 | -36.9 | 88.8 |
| 1050 | 1100 | 1075 | 12.7 | 264.8 | 616 | -3786 | -3170 | 7.8 | 351.7 | -47.9 | -303.0 | -40.1 | 48.7 |
| 1000 | 1050 | 1025 | 10.2 | 275.0 | 543 | -4226 | -3682 | 5.6 | 357.2 | -43.2 | -346.2 | -37.6 | 11.0 |
| 950 | 1000 | 975 | 7.2 | 282.2 | 494 | -4529 | -4034 | 3.6 | 360.8 | -32.8 | -379.0 | -29.2 | -18.2 |
| 900 | 950 | 925 | 1.2 | 283.5 | 460 | -4702 | -4242 | 0.6 | 361.4 | -5.7 | -384.7 | -5.1 | -23.4 |

Dyngjujökull

| Elevation (m a.s.l.) | ΔS (km ²) | $\sum \Delta S$ (km ²) | b _w (mm) | b _s (mm) | b _n (mm) | ΔB_w (10 ⁶ m ³) | $\sum \Delta B_w$ (10 ⁶ m ³) | ΔB_s (10 ⁶ m ³) | $\sum \Delta B_s$ (10 ⁶ m ³) | ΔB_n (10 ⁶ m ³) | $\sum B_n$ (10 ⁶ m ³) |
|--------------------------|----------------------------------|---------------------------------------|------------------------|------------------------|------------------------|---|--|---|--|---|---|
|--------------------------|----------------------------------|---------------------------------------|------------------------|------------------------|------------------------|---|--|---|--|---|---|

| | | | | | | | | | | | | | |
|------|------|------|-------|--------|------|-------|-------|-------|--------|--------|---------|--------|-------|
| 1950 | 2000 | 1975 | 2.4 | 2.4 | 1889 | 519 | 2409 | 4.5 | 4.5 | 1.2 | 1.2 | 5.7 | 5.7 |
| 1900 | 1950 | 1925 | 17.7 | 20.1 | 1899 | 385 | 2285 | 33.6 | 38.1 | 6.8 | 8.0 | 40.4 | 46.1 |
| 1850 | 1900 | 1875 | 21.7 | 41.8 | 1899 | 153 | 2053 | 41.3 | 79.4 | 3.3 | 11.4 | 44.6 | 90.8 |
| 1800 | 1850 | 1825 | 13.2 | 55.0 | 1897 | 126 | 2023 | 25.0 | 104.5 | 1.7 | 13.0 | 26.7 | 117.5 |
| 1750 | 1800 | 1775 | 15.6 | 70.7 | 1899 | 68 | 1967 | 29.7 | 134.2 | 1.1 | 14.1 | 30.8 | 148.3 |
| 1700 | 1750 | 1725 | 32.7 | 103.3 | 1907 | -54 | 1853 | 62.3 | 196.5 | -1.8 | 12.3 | 60.5 | 208.8 |
| 1650 | 1700 | 1675 | 74.5 | 177.8 | 1952 | -206 | 1746 | 145.5 | 342.0 | -15.4 | -3.1 | 130.1 | 338.9 |
| 1600 | 1650 | 1625 | 120.5 | 298.3 | 1955 | -255 | 1699 | 235.7 | 577.6 | -30.8 | -33.9 | 204.8 | 543.7 |
| 1550 | 1600 | 1575 | 96.3 | 394.6 | 1839 | -400 | 1438 | 177.2 | 754.8 | -38.6 | -72.5 | 138.6 | 682.3 |
| 1500 | 1550 | 1525 | 86.8 | 481.4 | 1740 | -570 | 1169 | 151.1 | 905.9 | -49.6 | -122.1 | 101.5 | 783.8 |
| 1450 | 1500 | 1475 | 72.6 | 554.0 | 1672 | -740 | 932 | 121.4 | 1027.3 | -53.7 | -175.8 | 67.7 | 851.5 |
| 1400 | 1450 | 1425 | 60.3 | 614.3 | 1599 | -896 | 703 | 96.4 | 1123.7 | -54.0 | -229.8 | 42.4 | 893.9 |
| 1350 | 1400 | 1375 | 47.7 | 661.9 | 1526 | -1172 | 353 | 72.7 | 1196.5 | -55.9 | -285.7 | 16.8 | 910.8 |
| 1300 | 1350 | 1325 | 36.1 | 698.0 | 1404 | -1551 | -147 | 50.7 | 1247.2 | -56.0 | -341.7 | -5.3 | 905.5 |
| 1250 | 1300 | 1275 | 39.2 | 737.2 | 1265 | -1910 | -645 | 49.6 | 1296.7 | -74.8 | -416.5 | -25.3 | 880.2 |
| 1200 | 1250 | 1225 | 43.5 | 780.7 | 1093 | -2273 | -1180 | 47.6 | 1344.3 | -98.9 | -515.4 | -51.3 | 828.9 |
| 1150 | 1200 | 1175 | 43.3 | 824.0 | 906 | -2726 | -1819 | 39.3 | 1383.5 | -118.0 | -633.5 | -78.8 | 750.1 |
| 1100 | 1150 | 1125 | 42.3 | 866.3 | 760 | -3198 | -2437 | 32.2 | 1415.8 | -135.4 | -768.9 | -103.2 | 646.9 |
| 1050 | 1100 | 1075 | 30.2 | 896.6 | 642 | -3709 | -3067 | 19.4 | 1435.2 | -112.2 | -881.1 | -92.8 | 554.1 |
| 1000 | 1050 | 1025 | 30.6 | 927.2 | 560 | -4239 | -3679 | 17.1 | 1452.3 | -129.7 | -1010.9 | -112.6 | 441.5 |
| 950 | 1000 | 975 | 28.4 | 955.6 | 477 | -4741 | -4263 | 13.6 | 1465.9 | -134.8 | -1145.7 | -121.3 | 320.2 |
| 900 | 950 | 925 | 24.3 | 979.9 | 405 | -5150 | -4744 | 9.9 | 1475.8 | -125.1 | -1270.8 | -115.3 | 204.9 |
| 850 | 900 | 875 | 20.4 | 1000.4 | 346 | -5560 | -5214 | 7.1 | 1482.9 | -113.6 | -1384.4 | -106.5 | 98.4 |
| 800 | 850 | 825 | 16.5 | 1016.9 | 305 | -5976 | -5671 | 5.0 | 1487.9 | -98.7 | -1483.1 | -93.7 | 4.8 |
| 750 | 800 | 775 | 8.5 | 1025.4 | 270 | -6287 | -6016 | 2.3 | 1490.2 | -53.5 | -1536.6 | -51.2 | -46.4 |
| 700 | 750 | 725 | 0.3 | 1025.7 | 245 | -6402 | -6156 | 0.1 | 1490.3 | -2.2 | -1538.8 | -2.1 | -48.5 |

Brúarjökull

| | Elevation (m a.s.l.) | ΔS (km ²) | $\sum \Delta S$ (km ²) | b _w (mm) | b _s (mm) | b _n (mm) | ΔB_w (10 ⁶ m ³) | $\sum \Delta B_w$ (10 ⁶ m ³) | ΔB_s (10 ⁶ m ³) | $\sum \Delta B_s$ (10 ⁶ m ³) | ΔB_n (10 ⁶ m ³) | $\sum B_n$ (10 ⁶ m ³) | |
|------|-------------------------|----------------------------------|---------------------------------------|------------------------|------------------------|------------------------|---|--|---|--|---|---|--------|
| 1900 | 1950 | 1925 | 0.0 | 0.0 | 1899 | 259 | 2159 | 0.1 | 0.1 | 0.0 | 0.0 | 0.1 | 0.1 |
| 1850 | 1900 | 1875 | 1.2 | 1.3 | 1890 | 316 | 2207 | 2.3 | 2.4 | 0.4 | 0.4 | 2.7 | 2.8 |
| 1800 | 1850 | 1825 | 4.4 | 5.6 | 1878 | 318 | 2197 | 8.2 | 10.6 | 1.4 | 1.8 | 9.6 | 12.4 |
| 1750 | 1800 | 1775 | 2.8 | 8.5 | 1923 | 173 | 2097 | 5.5 | 16.1 | 0.5 | 2.3 | 5.9 | 18.4 |
| 1700 | 1750 | 1725 | 4.0 | 12.5 | 1973 | 47 | 2021 | 7.9 | 23.9 | 0.2 | 2.5 | 8.1 | 26.4 |
| 1650 | 1700 | 1675 | 5.6 | 18.1 | 1993 | -40 | 1953 | 11.2 | 35.1 | -0.2 | 2.3 | 11.0 | 37.4 |
| 1600 | 1650 | 1625 | 51.6 | 69.6 | 2056 | -182 | 1873 | 106.0 | 141.1 | -9.4 | -7.1 | 96.6 | 134.0 |
| 1550 | 1600 | 1575 | 47.7 | 117.3 | 2039 | -229 | 1810 | 97.2 | 238.4 | -10.9 | -18.1 | 86.3 | 220.3 |
| 1500 | 1550 | 1525 | 73.6 | 190.9 | 1972 | -308 | 1663 | 145.1 | 383.5 | -22.7 | -40.8 | 122.4 | 342.7 |
| 1450 | 1500 | 1475 | 80.1 | 271.0 | 1956 | -519 | 1436 | 156.7 | 540.2 | -41.6 | -82.4 | 115.1 | 457.7 |
| 1400 | 1450 | 1425 | 114.0 | 385.0 | 2071 | -706 | 1364 | 236.1 | 776.2 | -80.5 | -162.9 | 155.6 | 613.3 |
| 1350 | 1400 | 1375 | 157.5 | 542.4 | 2060 | -934 | 1126 | 324.5 | 1100.8 | -147.1 | -310.1 | 177.4 | 790.7 |
| 1300 | 1350 | 1325 | 147.2 | 689.7 | 1963 | -1125 | 837 | 289.0 | 1389.8 | -165.7 | -475.7 | 123.4 | 914.1 |
| 1250 | 1300 | 1275 | 137.9 | 827.6 | 1869 | -1304 | 564 | 257.8 | 1647.6 | -180.0 | -655.7 | 77.9 | 991.9 |
| 1200 | 1250 | 1225 | 115.8 | 943.4 | 1739 | -1603 | 135 | 201.4 | 1849.0 | -185.6 | -841.3 | 15.7 | 1007.7 |
| 1150 | 1200 | 1175 | 99.5 | 1042.9 | 1572 | -1970 | -397 | 156.5 | 2005.5 | -196.0 | -1037.3 | -39.5 | 968.2 |
| 1100 | 1150 | 1125 | 80.2 | 1123.1 | 1386 | -2295 | -908 | 111.2 | 2116.7 | -184.1 | -1221.4 | -72.9 | 895.3 |
| 1050 | 1100 | 1075 | 64.9 | 1188.0 | 1200 | -2557 | -1356 | 77.9 | 2194.6 | -166.0 | -1387.4 | -88.1 | 807.2 |
| 1000 | 1050 | 1025 | 57.2 | 1245.2 | 1053 | -2842 | -1788 | 60.2 | 2254.8 | -162.5 | -1549.9 | -102.3 | 704.9 |
| 950 | 1000 | 975 | 51.6 | 1296.8 | 932 | -3181 | -2249 | 48.1 | 2303.0 | -164.3 | -1714.2 | -116.2 | 588.7 |
| 900 | 950 | 925 | 44.6 | 1341.4 | 802 | -3548 | -2745 | 35.8 | 2338.8 | -158.2 | -1872.5 | -122.4 | 466.3 |
| 850 | 900 | 875 | 38.4 | 1379.8 | 636 | -3889 | -3252 | 24.4 | 2363.2 | -149.2 | -2021.7 | -124.8 | 341.5 |
| 800 | 850 | 825 | 34.2 | 1414.0 | 464 | -4233 | -3769 | 15.9 | 2379.1 | -145.0 | -2166.7 | -129.1 | 212.4 |
| 750 | 800 | 775 | 30.9 | 1444.9 | 304 | -4613 | -4308 | 9.4 | 2388.5 | -142.7 | -2309.4 | -133.3 | 79.1 |
| 700 | 750 | 725 | 26.1 | 1471.0 | 205 | -4951 | -4745 | 5.4 | 2393.9 | -129.2 | -2438.6 | -123.8 | -44.7 |
| 650 | 700 | 675 | 9.5 | 1480.6 | 132 | -5188 | -5056 | 1.3 | 2395.1 | -49.5 | -2488.1 | -48.3 | -93.0 |
| 600 | 650 | 625 | 0.5 | 1481.1 | 96 | -5311 | -5215 | 0.0 | 2395.2 | -2.6 | -2490.7 | -2.5 | -95.5 |

Eyjabakkajökull

| | Elevation (m a.s.l.) | ΔS (km ²) | $\sum \Delta S$ (km ²) | b _w (mm) | b _s (mm) | b _n (mm) | ΔB_w (10 ⁶ m ³) | $\sum \Delta B_w$ (10 ⁶ m ³) | ΔB_s (10 ⁶ m ³) | $\sum \Delta B_s$ (10 ⁶ m ³) | ΔB_n (10 ⁶ m ³) | $\sum B_n$ (10 ⁶ m ³) | |
|------|-------------------------|----------------------------------|---------------------------------------|------------------------|------------------------|------------------------|---|--|---|--|---|---|-------|
| 1550 | 1600 | 1575 | 0.0 | 0.0 | 2299 | -31 | 2268 | 0.0 | 0.0 | 0.0 | 0.0 | 0.0 | 0.0 |
| 1500 | 1550 | 1525 | 0.1 | 0.1 | 2299 | 11 | 2311 | 0.2 | 0.2 | 0.0 | 0.0 | 0.2 | 0.2 |
| 1450 | 1500 | 1475 | 1.1 | 1.2 | 2299 | 13 | 2313 | 2.6 | 2.8 | 0.0 | 0.0 | 2.6 | 2.8 |
| 1400 | 1450 | 1425 | 2.0 | 3.3 | 2299 | -30 | 2269 | 4.7 | 7.5 | -0.1 | 0.0 | 4.6 | 7.5 |
| 1350 | 1400 | 1375 | 2.6 | 5.9 | 2289 | -182 | 2107 | 6.0 | 13.5 | -0.5 | -0.5 | 5.5 | 13.0 |
| 1300 | 1350 | 1325 | 4.2 | 10.1 | 2262 | -452 | 1809 | 9.5 | 23.0 | -1.9 | -2.4 | 7.6 | 20.6 |
| 1250 | 1300 | 1275 | 13.4 | 23.5 | 2083 | -980 | 1102 | 27.9 | 50.9 | -13.1 | -15.5 | 14.7 | 35.3 |
| 1200 | 1250 | 1225 | 12.4 | 35.9 | 2018 | -1302 | 715 | 25.1 | 76.0 | -16.2 | -31.8 | 8.9 | 44.2 |
| 1150 | 1200 | 1175 | 13.9 | 49.8 | 1889 | -1626 | 263 | 26.2 | 102.2 | -22.6 | -54.3 | 3.7 | 47.9 |
| 1100 | 1150 | 1125 | 11.4 | 61.2 | 1720 | -1980 | -260 | 19.7 | 121.9 | -22.7 | -77.0 | -3.0 | 44.9 |
| 1050 | 1100 | 1075 | 9.8 | 71.1 | 1518 | -2425 | -907 | 14.9 | 136.8 | -23.8 | -100.8 | -8.9 | 36.0 |
| 1000 | 1050 | 1025 | 9.1 | 80.2 | 1310 | -2809 | -1498 | 12.0 | 148.8 | -25.7 | -126.5 | -13.7 | 22.3 |
| 950 | 1000 | 975 | 7.6 | 87.8 | 1117 | -3285 | -2168 | 8.5 | 157.3 | -25.0 | -151.5 | -16.5 | 5.8 |
| 900 | 950 | 925 | 5.0 | 92.8 | 919 | -3839 | -2920 | 4.6 | 161.9 | -19.4 | -170.8 | -14.7 | -8.9 |
| 850 | 900 | 875 | 3.9 | 96.7 | 774 | -4226 | -3452 | 3.0 | 165.0 | -16.5 | -187.4 | -13.5 | -22.4 |
| 800 | 850 | 825 | 2.9 | 99.6 | 641 | -4577 | -3935 | 1.8 | 166.8 | -13.1 | -200.4 | -11.2 | -33.6 |
| 750 | 800 | 775 | 1.8 | 101.4 | 465 | -4988 | -4523 | 0.8 | 167.6 | -8.7 | -209.2 | -7.9 | -41.6 |
| 700 | 750 | 725 | 1.6 | 103.0 | 317 | -5356 | -5038 | 0.5 | 168.1 | -8.8 | -218.0 | -8.3 | -49.8 |
| 650 | 700 | 675 | 0.6 | 103.6 | 200 | -5660 | -5459 | 0.1 | 168.3 | -3.6 | -221.6 | -3.5 | -53.3 |

Hoffellsjökull

| Elevation (m a.s.l.) | ΔS (km ²) | $\Sigma \Delta S$ (km ²) | b _w (mm) | b _s (mm) | b _n (mm) | ΔB_w (10 ⁶ m ³) | $\Sigma \Delta B_w$ (10 ⁶ m ³) | ΔB_s (10 ⁶ m ³) | $\Sigma \Delta B_s$ (10 ⁶ m ³) | ΔB_n (10 ⁶ m ³) | ΣB_n (10 ⁶ m ³) | | |
|-------------------------|----------------------------------|---|------------------------|------------------------|------------------------|---|--|---|--|---|---|-------|-------|
| 1450 | 1500 | 1475 | 1.2 | 1.2 | 2299 | 45 | 2345 | 2.7 | 2.7 | 0.1 | 0.1 | 2.7 | 2.7 |
| 1400 | 1450 | 1425 | 7.3 | 8.4 | 2235 | -368 | 1867 | 16.3 | 18.9 | -2.7 | -2.6 | 13.6 | 16.3 |
| 1350 | 1400 | 1375 | 9.8 | 18.3 | 2227 | -509 | 1717 | 21.9 | 40.9 | -5.0 | -7.6 | 16.9 | 33.2 |
| 1300 | 1350 | 1325 | 16.1 | 34.4 | 2207 | -704 | 1502 | 35.5 | 76.4 | -11.3 | -19.0 | 24.2 | 57.4 |
| 1250 | 1300 | 1275 | 34.4 | 68.7 | 2151 | -952 | 1198 | 73.9 | 150.3 | -32.7 | -51.7 | 41.2 | 98.6 |
| 1200 | 1250 | 1225 | 25.5 | 94.3 | 2190 | -1081 | 1109 | 55.9 | 206.2 | -27.6 | -79.3 | 28.3 | 126.9 |
| 1150 | 1200 | 1175 | 17.6 | 111.9 | 2184 | -1336 | 847 | 38.4 | 244.7 | -23.5 | -102.8 | 14.9 | 141.8 |
| 1100 | 1150 | 1125 | 16.6 | 128.4 | 2148 | -1653 | 494 | 35.6 | 280.2 | -27.4 | -130.2 | 8.2 | 150.0 |
| 1050 | 1100 | 1075 | 12.4 | 140.8 | 2042 | -2008 | 34 | 25.4 | 305.6 | -25.0 | -155.2 | 0.4 | 150.5 |
| 1000 | 1050 | 1025 | 9.4 | 150.3 | 1937 | -2286 | -348 | 18.3 | 323.9 | -21.6 | -176.7 | -3.3 | 147.2 |
| 950 | 1000 | 975 | 8.6 | 158.9 | 1821 | -2558 | -736 | 15.7 | 339.6 | -22.1 | -198.8 | -6.4 | 140.8 |
| 900 | 950 | 925 | 6.7 | 165.6 | 1668 | -2811 | -1143 | 11.1 | 350.7 | -18.7 | -217.5 | -7.6 | 133.2 |
| 850 | 900 | 875 | 4.2 | 169.7 | 1522 | -3089 | -1567 | 6.4 | 357.1 | -12.9 | -230.4 | -6.5 | 126.6 |
| 800 | 850 | 825 | 3.4 | 173.2 | 1408 | -3327 | -1919 | 4.8 | 361.9 | -11.4 | -241.8 | -6.6 | 120.1 |
| 750 | 800 | 775 | 2.9 | 176.1 | 1316 | -3454 | -2138 | 3.8 | 365.7 | -10.1 | -251.9 | -6.2 | 113.8 |
| 700 | 750 | 725 | 2.9 | 179.0 | 1111 | -3849 | -2737 | 3.3 | 369.0 | -11.3 | -263.2 | -8.0 | 105.8 |
| 650 | 700 | 675 | 3.2 | 182.2 | 914 | -4327 | -3412 | 2.9 | 371.9 | -13.7 | -276.9 | -10.8 | 95.0 |
| 600 | 650 | 625 | 2.5 | 184.7 | 800 | -4625 | -3824 | 2.0 | 373.9 | -11.6 | -288.5 | -9.6 | 85.4 |
| 550 | 600 | 575 | 1.8 | 186.5 | 698 | -4861 | -4163 | 1.3 | 375.2 | -8.7 | -297.2 | -7.5 | 78.0 |
| 500 | 550 | 525 | 1.5 | 188.0 | 596 | -5125 | -4529 | 0.9 | 376.1 | -7.7 | -304.9 | -6.8 | 71.1 |
| 450 | 500 | 475 | 1.1 | 189.0 | 429 | -5478 | -5049 | 0.5 | 376.5 | -5.8 | -310.7 | -5.4 | 65.8 |
| 400 | 450 | 425 | 0.7 | 189.8 | 258 | -5720 | -5462 | 0.2 | 376.7 | -4.1 | -314.9 | -3.9 | 61.8 |
| 350 | 400 | 375 | 0.7 | 190.5 | -1 | -6003 | -6004 | 0.0 | 376.7 | -4.3 | -319.1 | -4.3 | 57.5 |
| 300 | 350 | 325 | 0.5 | 191.0 | -245 | -6346 | -6591 | -0.1 | 376.6 | -3.2 | -322.3 | -3.3 | 54.2 |
| 250 | 300 | 275 | 0.6 | 191.6 | -442 | -6684 | -7126 | -0.3 | 376.3 | -4.0 | -326.4 | -4.3 | 49.9 |
| 200 | 250 | 225 | 0.9 | 192.4 | -596 | -7050 | -7647 | -0.5 | 375.8 | -6.0 | -332.4 | -6.5 | 43.4 |
| 150 | 200 | 175 | 1.8 | 194.2 | -751 | -7469 | -8221 | -1.3 | 374.5 | -13.4 | -345.8 | -14.7 | 28.7 |
| 100 | 150 | 125 | 2.4 | 196.6 | -916 | -7950 | -8866 | -2.2 | 372.3 | -18.8 | -364.6 | -21.0 | 7.7 |
| 50 | 100 | 75 | 2.2 | 198.8 | -1231 | -8453 | -9684 | -2.7 | 369.6 | -18.5 | -383.1 | -21.2 | -13.5 |
| 0 | 50 | 25 | 2.9 | 201.7 | -1720 | -9302 | -11022 | -5.0 | 364.6 | -26.9 | -409.9 | -31.8 | -45.3 |

Breiðamerkurjökull

| Elevation (m a.s.l.) | ΔS (km ²) | $\Sigma \Delta S$ (km ²) | b _w (mm) | b _s (mm) | b _n (mm) | ΔB_w (10 ⁶ m ³) | $\Sigma \Delta B_w$ (10 ⁶ m ³) | ΔB_s (10 ⁶ m ³) | $\Sigma \Delta B_s$ (10 ⁶ m ³) | ΔB_n (10 ⁶ m ³) | ΣB_n (10 ⁶ m ³) | | |
|-------------------------|----------------------------------|---|------------------------|------------------------|------------------------|---|--|---|--|---|---|--------|--------|
| 1900 | 1950 | 1925 | 0.0 | 0.0 | 4715 | 2299 | 7015 | 0.2 | 0.2 | 0.1 | 0.1 | 0.3 | 0.3 |
| 1850 | 1900 | 1875 | 0.4 | 0.4 | 4692 | 2338 | 7030 | 1.7 | 2.0 | 0.9 | 1.0 | 2.6 | 3.0 |
| 1800 | 1850 | 1825 | 0.5 | 0.9 | 4565 | 2266 | 6831 | 2.2 | 4.2 | 1.1 | 2.1 | 3.3 | 6.2 |
| 1750 | 1800 | 1775 | 0.9 | 1.8 | 4392 | 1974 | 6367 | 4.0 | 8.2 | 1.8 | 3.9 | 5.8 | 12.0 |
| 1700 | 1750 | 1725 | 2.6 | 4.4 | 3423 | 917 | 4340 | 8.8 | 17.0 | 2.4 | 6.2 | 11.2 | 23.2 |
| 1650 | 1700 | 1675 | 6.0 | 10.4 | 2726 | 333 | 3060 | 16.3 | 33.3 | 2.0 | 8.2 | 18.3 | 41.6 |
| 1600 | 1650 | 1625 | 18.0 | 28.3 | 2515 | 98 | 2613 | 45.2 | 78.5 | 1.8 | 10.0 | 46.9 | 88.5 |
| 1550 | 1600 | 1575 | 26.4 | 54.7 | 2397 | -96 | 2300 | 63.2 | 141.7 | -2.5 | 7.5 | 60.6 | 149.1 |
| 1500 | 1550 | 1525 | 31.8 | 86.5 | 2321 | -316 | 2005 | 73.9 | 215.5 | -10.1 | -2.6 | 63.8 | 212.9 |
| 1450 | 1500 | 1475 | 46.6 | 133.1 | 2261 | -523 | 1737 | 105.3 | 320.8 | -24.4 | -27.0 | 80.9 | 293.8 |
| 1400 | 1450 | 1425 | 57.5 | 190.6 | 2234 | -695 | 1539 | 128.5 | 449.3 | -40.0 | -67.0 | 88.5 | 382.3 |
| 1350 | 1400 | 1375 | 88.2 | 278.8 | 2200 | -868 | 1332 | 194.1 | 643.5 | -76.6 | -143.6 | 117.5 | 499.9 |
| 1300 | 1350 | 1325 | 94.3 | 373.1 | 2128 | -917 | 1210 | 200.6 | 844.1 | -86.5 | -230.1 | 114.1 | 614.0 |
| 1250 | 1300 | 1275 | 56.9 | 430.0 | 1991 | -978 | 1012 | 113.3 | 957.3 | -55.7 | -285.7 | 57.6 | 671.6 |
| 1200 | 1250 | 1225 | 38.2 | 468.2 | 1852 | -1154 | 698 | 70.9 | 1028.2 | -44.2 | -329.9 | 26.7 | 698.3 |
| 1150 | 1200 | 1175 | 30.7 | 498.9 | 1736 | -1414 | 322 | 53.3 | 1081.5 | -43.4 | -373.4 | 9.9 | 708.2 |
| 1100 | 1150 | 1125 | 25.1 | 524.1 | 1625 | -1690 | -64 | 40.8 | 1122.4 | -42.5 | -415.8 | -1.6 | 706.6 |
| 1050 | 1100 | 1075 | 21.6 | 545.7 | 1527 | -1953 | -426 | 33.1 | 1155.4 | -42.3 | -458.1 | -9.2 | 697.3 |
| 1000 | 1050 | 1025 | 18.7 | 564.4 | 1438 | -2201 | -762 | 26.9 | 1182.4 | -41.2 | -499.3 | -14.3 | 683.0 |
| 950 | 1000 | 975 | 20.3 | 584.7 | 1320 | -2549 | -1229 | 26.8 | 1209.1 | -51.7 | -551.0 | -24.9 | 658.1 |
| 900 | 950 | 925 | 21.9 | 606.6 | 1244 | -2817 | -1572 | 27.3 | 1236.4 | -61.7 | -612.7 | -34.4 | 623.7 |
| 850 | 900 | 875 | 17.9 | 624.5 | 1155 | -3104 | -1949 | 20.7 | 1257.1 | -55.7 | -668.4 | -35.0 | 588.7 |
| 800 | 850 | 825 | 20.8 | 645.4 | 1030 | -3414 | -2384 | 21.5 | 1278.6 | -71.2 | -739.6 | -49.7 | 539.0 |
| 750 | 800 | 775 | 21.8 | 667.2 | 896 | -3752 | -2855 | 19.5 | 1298.1 | -81.8 | -821.3 | -62.2 | 476.8 |
| 700 | 750 | 725 | 16.7 | 683.8 | 798 | -4042 | -3244 | 13.3 | 1311.4 | -67.3 | -888.6 | -54.0 | 422.8 |
| 650 | 700 | 675 | 22.4 | 706.3 | 714 | -4326 | -3611 | 16.0 | 1327.5 | -97.1 | -985.7 | -81.0 | 341.8 |
| 600 | 650 | 625 | 25.4 | 731.6 | 614 | -4618 | -4004 | 15.6 | 1343.1 | -117.2 | -1102.9 | -101.6 | 240.1 |
| 550 | 600 | 575 | 22.5 | 754.2 | 508 | -4917 | -4409 | 11.5 | 1354.5 | -110.9 | -1213.8 | -99.4 | 140.7 |
| 500 | 550 | 525 | 21.2 | 775.4 | 405 | -5125 | -4719 | 8.6 | 1363.1 | -108.7 | -1322.5 | -100.1 | 40.7 |
| 450 | 500 | 475 | 12.1 | 787.5 | 297 | -5352 | -5054 | 3.6 | 1366.7 | -64.9 | -1387.4 | -61.3 | -20.6 |
| 400 | 450 | 425 | 13.3 | 800.8 | 182 | -5632 | -5449 | 2.4 | 1369.2 | -74.8 | -1462.2 | -72.4 | -93.0 |
| 350 | 400 | 375 | 14.7 | 815.5 | 46 | -5982 | -5936 | 0.7 | 1369.8 | -87.8 | -1550.0 | -87.2 | -180.2 |
| 300 | 350 | 325 | 11.6 | 827.1 | -128 | -6380 | -6508 | -1.5 | 1368.4 | -74.2 | -1624.2 | -75.6 | -255.8 |
| 250 | 300 | 275 | 9.8 | 836.9 | -379 | -6723 | -7103 | -3.7 | 1364.6 | -66.1 | -1690.2 | -69.8 | -325.6 |
| 200 | 250 | 225 | 9.9 | 846.8 | -631 | -7020 | -7651 | -6.3 | 1358.4 | -69.7 | -1759.9 | -75.9 | -401.6 |
| 150 | 200 | 175 | 8.9 | 855.7 | -823 | -7340 | -8164 | -7.3 | 1351.0 | -65.1 | -1825.0 | -72.4 | -474.0 |
| 100 | 150 | 125 | 9.1 | 864.8 | -952 | -7811 | -8764 | -8.7 | 1342.4 | -71.0 | -1896.0 | -79.6 | -553.6 |
| 50 | 100 | 75 | 7.0 | 871.8 | -1078 | -8384 | -9462 | -7.6 | 1334.8 | -58.9 | -1954.9 | -66.5 | -620.1 |
| 0 | 50 | 25 | 3.0 | 874.8 | -1187 | -9067 | -10255 | -3.5 | 1331.3 | -26.9 | -1981.8 | -30.4 | -650.5 |

Síðujökull

| Elevation (m a.s.l.) | ΔS (km ²) | $\Sigma \Delta S$ (km ²) | b _w (mm) | b _s (mm) | b _n (mm) | ΔB_w (10 ⁶ m ³) | $\Sigma \Delta B_w$ (10 ⁶ m ³) | ΔB_s (10 ⁶ m ³) | $\Sigma \Delta B_s$ (10 ⁶ m ³) | ΔB_n (10 ⁶ m ³) | ΣB_n (10 ⁶ m ³) | | |
|-------------------------|----------------------------------|---|------------------------|------------------------|------------------------|---|--|---|--|---|---|-------|--------|
| 1700 | 1750 | 1725 | 0.9 | 0.9 | 2386 | 248 | 2635 | 2.2 | 2.2 | 0.2 | 0.2 | 2.4 | |
| 1650 | 1700 | 1675 | 5.9 | 6.9 | 2281 | -290 | 1991 | 13.6 | 15.8 | -1.7 | -1.5 | 11.8 | 14.3 |
| 1600 | 1650 | 1625 | 11.3 | 18.1 | 2136 | -549 | 1586 | 24.0 | 39.8 | -6.2 | -7.7 | 17.9 | 32.1 |
| 1550 | 1600 | 1575 | 11.7 | 29.8 | 2101 | -615 | 1485 | 24.5 | 64.3 | -7.2 | -14.9 | 17.3 | 49.5 |
| 1500 | 1550 | 1525 | 21.4 | 51.2 | 1998 | -722 | 1276 | 42.8 | 107.1 | -15.5 | -30.3 | 27.4 | 76.8 |
| 1450 | 1500 | 1475 | 38.0 | 89.2 | 1786 | -837 | 948 | 67.9 | 175.0 | -31.8 | -62.2 | 36.1 | 112.9 |
| 1400 | 1450 | 1425 | 24.8 | 114.0 | 1671 | -956 | 715 | 41.4 | 216.4 | -23.7 | -85.9 | 17.7 | 130.6 |
| 1350 | 1400 | 1375 | 21.0 | 135.0 | 1631 | -1240 | 391 | 34.2 | 250.7 | -26.0 | -111.9 | 8.2 | 138.8 |
| 1300 | 1350 | 1325 | 17.1 | 152.0 | 1574 | -1542 | 31 | 26.9 | 277.6 | -26.3 | -138.2 | 0.5 | 139.3 |
| 1250 | 1300 | 1275 | 15.1 | 167.2 | 1540 | -1800 | -259 | 23.3 | 300.9 | -27.2 | -165.5 | -3.9 | 135.4 |
| 1200 | 1250 | 1225 | 21.1 | 188.3 | 1521 | -2005 | -483 | 32.1 | 333.0 | -42.3 | -207.8 | -10.2 | 125.2 |
| 1150 | 1200 | 1175 | 17.5 | 205.8 | 1472 | -2293 | -820 | 25.8 | 358.9 | -40.3 | -248.1 | -14.4 | 110.8 |
| 1100 | 1150 | 1125 | 16.6 | 222.5 | 1405 | -2583 | -1177 | 23.4 | 382.2 | -43.0 | -291.1 | -19.6 | 91.2 |
| 1050 | 1100 | 1075 | 15.0 | 237.5 | 1338 | -2900 | -1561 | 20.1 | 402.4 | -43.6 | -334.7 | -23.5 | 67.7 |
| 1000 | 1050 | 1025 | 18.5 | 256.0 | 1252 | -3158 | -1906 | 23.1 | 425.5 | -58.3 | -393.0 | -35.2 | 32.5 |
| 950 | 1000 | 975 | 19.4 | 275.4 | 1121 | -3379 | -2258 | 21.7 | 447.2 | -65.4 | -458.5 | -43.7 | -11.2 |
| 900 | 950 | 925 | 19.6 | 294.9 | 960 | -3605 | -2645 | 18.8 | 466.0 | -70.5 | -529.0 | -51.7 | -63.0 |
| 850 | 900 | 875 | 18.8 | 313.7 | 829 | -3848 | -3019 | 15.6 | 481.6 | -72.3 | -601.2 | -56.7 | -119.7 |
| 800 | 850 | 825 | 17.7 | 331.4 | 697 | -4097 | -3399 | 12.3 | 493.9 | -72.4 | -673.6 | -60.1 | -179.7 |
| 750 | 800 | 775 | 20.1 | 351.5 | 558 | -4399 | -3841 | 11.2 | 505.1 | -88.5 | -762.1 | -77.3 | -257.0 |
| 700 | 750 | 725 | 20.0 | 371.5 | 428 | -4702 | -4273 | 8.6 | 513.7 | -94.3 | -856.4 | -85.7 | -342.7 |
| 650 | 700 | 675 | 19.9 | 391.4 | 305 | -5018 | -4713 | 6.1 | 519.8 | -99.9 | -956.3 | -93.8 | -436.5 |
| 600 | 650 | 625 | 8.9 | 400.3 | 231 | -5281 | -5050 | 2.1 | 521.8 | -47.0 | -1003.3 | -45.0 | -481.5 |
| 550 | 600 | 575 | 0.0 | 400.4 | 201 | -5400 | -5198 | 0.0 | 521.8 | -0.2 | -1003.6 | -0.2 | -481.7 |

Skaftárjökull

| Elevation (m a.s.l.) | ΔS (km ²) | $\Sigma \Delta S$ (km ²) | b _w (mm) | b _s (mm) | b _n (mm) | ΔB_w (10 ⁶ m ³) | $\Sigma \Delta B_w$ (10 ⁶ m ³) | ΔB_s (10 ⁶ m ³) | $\Sigma \Delta B_s$ (10 ⁶ m ³) | ΔB_n (10 ⁶ m ³) | ΣB_n (10 ⁶ m ³) | | |
|-------------------------|----------------------------------|---|------------------------|------------------------|------------------------|---|--|---|--|---|---|-------|--------|
| 1400 | 1450 | 1425 | 0.0 | 0.0 | 1500 | -1100 | 399 | 0.0 | 0.0 | 0.0 | 0.0 | 0.0 | |
| 1350 | 1400 | 1375 | 2.5 | 2.5 | 1471 | -1260 | 211 | 3.6 | 3.6 | -3.1 | -3.1 | 0.5 | 0.5 |
| 1300 | 1350 | 1325 | 5.2 | 7.7 | 1421 | -1526 | -105 | 7.4 | 11.1 | -8.0 | -11.1 | -0.6 | 0.0 |
| 1250 | 1300 | 1275 | 4.0 | 11.7 | 1400 | -1868 | -468 | 5.5 | 16.6 | -7.4 | -18.5 | -1.9 | -1.9 |
| 1200 | 1250 | 1225 | 6.3 | 17.9 | 1393 | -2253 | -860 | 8.7 | 25.4 | -14.1 | -32.6 | -5.4 | -7.3 |
| 1150 | 1200 | 1175 | 7.4 | 25.3 | 1356 | -2550 | -1194 | 10.0 | 35.3 | -18.8 | -51.4 | -8.8 | -16.1 |
| 1100 | 1150 | 1125 | 10.6 | 35.9 | 1275 | -2832 | -1557 | 13.5 | 48.9 | -30.1 | -81.5 | -16.5 | -32.6 |
| 1050 | 1100 | 1075 | 11.7 | 47.6 | 1174 | -3130 | -1955 | 13.7 | 62.6 | -36.6 | -118.1 | -22.9 | -55.5 |
| 1000 | 1050 | 1025 | 12.7 | 60.4 | 1048 | -3425 | -2376 | 13.4 | 76.0 | -43.6 | -161.8 | -30.3 | -85.8 |
| 950 | 1000 | 975 | 8.8 | 69.2 | 895 | -3698 | -2802 | 7.9 | 83.9 | -32.6 | -194.4 | -24.7 | -110.5 |
| 900 | 950 | 925 | 5.8 | 75.0 | 781 | -3926 | -3144 | 4.5 | 88.4 | -22.7 | -217.2 | -18.2 | -128.7 |
| 850 | 900 | 875 | 4.7 | 79.7 | 668 | -4173 | -3505 | 3.2 | 91.6 | -19.7 | -236.8 | -16.5 | -145.2 |
| 800 | 850 | 825 | 4.8 | 84.5 | 561 | -4426 | -3864 | 2.7 | 94.3 | -21.2 | -258.0 | -18.5 | -163.7 |
| 750 | 800 | 775 | 4.5 | 88.9 | 461 | -4656 | -4194 | 2.1 | 96.3 | -20.8 | -278.8 | -18.8 | -182.5 |
| 700 | 750 | 725 | 3.9 | 92.9 | 365 | -4886 | -4521 | 1.4 | 97.8 | -19.1 | -297.9 | -17.7 | -200.2 |
| 650 | 700 | 675 | 2.8 | 95.7 | 280 | -5088 | -4807 | 0.8 | 98.5 | -14.2 | -312.2 | -13.5 | -213.6 |
| 600 | 650 | 625 | 0.5 | 96.2 | 236 | -5187 | -4951 | 0.1 | 98.7 | -2.7 | -314.8 | -2.5 | -216.2 |

Vestari Skaftárketill

| Elevation (m a.s.l.) | ΔS (km ²) | $\sum \Delta S$ (km ²) | b _w (mm) | b _s (mm) | b _n (mm) | ΔB_w (10 ⁶ m ³) | $\sum \Delta B_w$ (10 ⁶ m ³) | ΔB_s (10 ⁶ m ³) | $\sum \Delta B_s$ (10 ⁶ m ³) | ΔB_n (10 ⁶ m ³) | $\sum B_n$ (10 ⁶ m ³) |
|-------------------------|----------------------------------|---------------------------------------|------------------------|------------------------|------------------------|---|--|---|--|---|---|
| 1900 | 1950 | 1925 | 0.5 | 0.5 | 1899 | 258 | 2158 | 1.0 | 1.0 | 0.1 | 0.1 |
| 1850 | 1900 | 1875 | 0.7 | 1.2 | 1899 | 227 | 2127 | 1.2 | 2.3 | 0.1 | 0.3 |
| 1800 | 1850 | 1825 | 0.8 | 2.0 | 1899 | 208 | 2108 | 1.5 | 3.7 | 0.2 | 0.4 |
| 1750 | 1800 | 1775 | 2.5 | 4.4 | 1887 | 144 | 2031 | 4.7 | 8.4 | 0.4 | 0.8 |
| 1700 | 1750 | 1725 | 5.4 | 9.9 | 1772 | 20 | 1793 | 9.6 | 18.0 | 0.1 | 0.9 |
| 1650 | 1700 | 1675 | 6.5 | 16.3 | 1705 | -116 | 1588 | 11.0 | 29.0 | -0.8 | 0.2 |
| 1600 | 1650 | 1625 | 7.3 | 23.6 | 1711 | -221 | 1489 | 12.4 | 41.5 | -1.6 | -1.4 |
| 1550 | 1600 | 1575 | 5.0 | 28.6 | 1688 | -289 | 1399 | 8.4 | 49.9 | -1.4 | -2.9 |
| 1500 | 1550 | 1525 | 2.7 | 31.2 | 1685 | -317 | 1367 | 4.5 | 54.4 | -0.8 | -3.7 |
| | | | | | | | | | | 3.6 | 50.7 |

Eystrí Skaftárketill

| Elevation (m a.s.l.) | ΔS (km ²) | $\sum \Delta S$ (km ²) | b _w (mm) | b _s (mm) | b _n (mm) | ΔB_w (10 ⁶ m ³) | $\sum \Delta B_w$ (10 ⁶ m ³) | ΔB_s (10 ⁶ m ³) | $\sum \Delta B_s$ (10 ⁶ m ³) | ΔB_n (10 ⁶ m ³) | $\sum B_n$ (10 ⁶ m ³) |
|-------------------------|----------------------------------|---------------------------------------|------------------------|------------------------|------------------------|---|--|---|--|---|---|
| 1750 | 1800 | 1775 | 1.1 | 1.1 | 1899 | 109 | 2009 | 2.1 | 2.1 | 0.1 | 0.1 |
| 1700 | 1750 | 1725 | 10.0 | 11.1 | 1818 | -59 | 1759 | 18.2 | 20.3 | -0.6 | -0.5 |
| 1650 | 1700 | 1675 | 15.5 | 26.6 | 1837 | -247 | 1589 | 28.5 | 48.7 | -3.8 | -4.3 |
| 1600 | 1650 | 1625 | 9.2 | 35.8 | 1821 | -306 | 1515 | 16.8 | 65.5 | -2.8 | -7.1 |
| 1550 | 1600 | 1575 | 4.2 | 39.9 | 1799 | -327 | 1472 | 7.5 | 73.0 | -1.4 | -8.5 |
| | | | | | | | | | | 6.1 | 64.5 |

Gjálp

| Elevation (m a.s.l.) | ΔS (km ²) | $\sum \Delta S$ (km ²) | b _w (mm) | b _s (mm) | b _n (mm) | ΔB_w (10 ⁶ m ³) | $\sum \Delta B_w$ (10 ⁶ m ³) | ΔB_s (10 ⁶ m ³) | $\sum \Delta B_s$ (10 ⁶ m ³) | ΔB_n (10 ⁶ m ³) | $\sum B_n$ (10 ⁶ m ³) |
|-------------------------|----------------------------------|---------------------------------------|------------------------|------------------------|------------------------|---|--|---|--|---|---|
| 1900 | 1950 | 1925 | 0.4 | 0.4 | 1899 | 251 | 2151 | 0.7 | 0.7 | 0.1 | 0.1 |
| 1850 | 1900 | 1875 | 0.8 | 1.1 | 1899 | 206 | 2106 | 1.4 | 2.1 | 0.2 | 0.2 |
| 1800 | 1850 | 1825 | 1.2 | 2.3 | 1899 | 177 | 2077 | 2.3 | 4.4 | 0.2 | 0.5 |
| 1750 | 1800 | 1775 | 5.5 | 7.8 | 1899 | 105 | 2005 | 10.5 | 14.9 | 0.6 | 1.0 |
| 1700 | 1750 | 1725 | 23.7 | 31.5 | 1899 | -125 | 1774 | 45.1 | 59.9 | -3.0 | -1.9 |
| 1650 | 1700 | 1675 | 7.8 | 39.4 | 1899 | -263 | 1636 | 14.9 | 74.8 | -2.1 | -4.0 |
| | | | | | | | | | | 12.8 | 70.8 |

Grímsvötn

| Elevation (m a.s.l.) | ΔS (km ²) | $\sum \Delta S$ (km ²) | b _w (mm) | b _s (mm) | b _n (mm) | ΔB_w (10 ⁶ m ³) | $\sum \Delta B_w$ (10 ⁶ m ³) | ΔB_s (10 ⁶ m ³) | $\sum \Delta B_s$ (10 ⁶ m ³) | ΔB_n (10 ⁶ m ³) | $\sum B_n$ (10 ⁶ m ³) |
|-------------------------|----------------------------------|---------------------------------------|------------------------|------------------------|------------------------|---|--|---|--|---|---|
| 1700 | 1750 | 1725 | 1.3 | 1.3 | 1900 | -281 | 1618 | 2.6 | 2.6 | -0.4 | -0.4 |
| 1650 | 1700 | 1675 | 40.7 | 42.1 | 1947 | -401 | 1546 | 79.3 | 81.9 | -16.3 | -16.7 |
| 1600 | 1650 | 1625 | 30.7 | 72.8 | 1935 | -628 | 1307 | 59.4 | 141.3 | -19.3 | -36.0 |
| 1550 | 1600 | 1575 | 19.6 | 92.4 | 1920 | -805 | 1115 | 37.7 | 178.9 | -15.8 | -51.8 |
| 1500 | 1550 | 1525 | 16.3 | 108.7 | 1903 | -1176 | 726 | 31.0 | 210.0 | -19.2 | -71.0 |
| 1450 | 1500 | 1475 | 9.5 | 118.2 | 1840 | -1662 | 177 | 17.5 | 227.4 | -15.8 | -86.7 |
| 1400 | 1450 | 1425 | 13.7 | 131.9 | 1850 | -2050 | -200 | 25.4 | 252.8 | -28.1 | -114.9 |
| 1350 | 1400 | 1375 | 1.2 | 133.1 | 1818 | -2059 | -241 | 2.3 | 255.1 | -2.6 | -117.4 |
| | | | | | | | | | | -0.3 | 137.6 |

Appendix C: Coordinates of the velocity measurement stakes in 2024.

Position of the velocity measurement stakes determined by GPS sub-metre differential (I), fast static (FS) and kinematic (K). (Accuracy of horizontal position 0.5 – 1.0 m, and vertical accuracy 1-2 m for DGPS, about 1cm for fast static, and 3 cm for kinematic).

The station Hofn in Höfn í Hornafirði is used as a stationary reference for all measurements, ÍSN93 datum, h_l is elevation above ellipsoid, dL antenna height, N estimated difference between ellipsoid and sea-level, H elevation in metres above sea level ($H = h_l + N + dL$). X and Y are ÍSN93 Lambert conformal conic projected coordinates. M is a quality marker.

| Site | Calender | | | | | | | | | | | | | Y | M |
|----------|----------|------|----|------|----------|-------------|----------------|----------|---------|--------------|--------|---------|-----------|-----------|---|
| | time | Date | # | Year | Latitude | Longitude | h _l | dL | N | H | | | | | |
| | | | | | | | (m a. e.) | (m) | (m) | (m a. s. l.) | X | | | | |
| B07-23 | 11.72 | 4 | 5 | 124 | 2023 | 64 25.79652 | 16 | 17.48091 | 1425.86 | 0.00 | -67.05 | 1358.81 | 630454.15 | 439244.78 | K |
| B07-24 | 16.856 | 25 | 9 | 269 | 2024 | 64 25.79490 | 16 | 17.48586 | 1424.18 | -2.15 | -67.05 | 1354.98 | 630450.30 | 439241.60 | K |
| B07-24 | 13.926 | 21 | 11 | 326 | 2024 | 64 25.79450 | 16 | 17.48241 | 1424.10 | -2.10 | -67.05 | 1354.95 | 630453.10 | 439240.99 | K |
| B09-24 | 15.421 | 2 | 5 | 123 | 2024 | 64 44.48405 | 16 | 6.18781 | 786.85 | 0.00 | -66.68 | 720.17 | 637922.46 | 474331.61 | K |
| B10-24 | 14.651 | 2 | 5 | 123 | 2024 | 64 43.68419 | 16 | 6.70273 | 818.93 | 0.00 | -66.71 | 752.22 | 637582.03 | 472828.32 | K |
| B11-24 | 18.871 | 1 | 5 | 122 | 2024 | 64 40.93900 | 16 | 10.48002 | 1008.78 | 0.00 | -66.81 | 941.97 | 634813.11 | 467597.34 | K |
| B12-24 | 17.885 | 1 | 5 | 122 | 2024 | 64 38.26292 | 16 | 14.15062 | 1144.05 | 0.00 | -66.90 | 1077.15 | 632113.23 | 462500.89 | K |
| B12-24 | 16.665 | 23 | 11 | 328 | 2024 | 64 38.27489 | 16 | 14.14049 | 1140.73 | 0.00 | -66.90 | 1073.83 | 632120.32 | 462523.46 | K |
| B13-24 | 17.897 | 2 | 5 | 123 | 2024 | 64 34.65838 | 16 | 19.56103 | 1286.24 | 0.00 | -67.01 | 1219.23 | 628089.19 | 455624.28 | K |
| B13-24 | 14.758 | 21 | 11 | 326 | 2024 | 64 34.66970 | 16 | 19.54725 | 1283.46 | 0.00 | -67.01 | 1216.45 | 628099.29 | 455645.75 | K |
| B13ror15 | 11.3 | 10 | 6 | 162 | 2024 | 64 34.66375 | 16 | 19.56016 | 1285.52 | 0.00 | -67.01 | 1218.51 | 628089.46 | 455634.27 | K |
| B13ror15 | 14.611 | 21 | 11 | 326 | 2024 | 64 34.67479 | 16 | 19.54760 | 1285.73 | 0.00 | -67.01 | 1218.72 | 628098.61 | 455655.19 | K |
| B14-24 | 15.161 | 1 | 5 | 122 | 2024 | 64 31.64983 | 16 | 24.77075 | 1391.92 | 0.00 | -67.11 | 1324.82 | 624160.98 | 449866.02 | K |
| B14-24 | 16.372 | 21 | 11 | 326 | 2024 | 64 31.65792 | 16 | 24.75669 | 1388.92 | 0.00 | -67.11 | 1321.81 | 624171.60 | 449881.49 | K |
| B15-24 | 14.334 | 1 | 5 | 122 | 2024 | 64 28.51275 | 16 | 30.03235 | 1472.92 | 0.00 | -67.21 | 1405.71 | 620185.09 | 443872.57 | K |
| B15-24 | 14.754 | 21 | 11 | 326 | 2024 | 64 28.51800 | 16 | 30.01885 | 1471.87 | -1.84 | -67.21 | 1402.82 | 620195.51 | 443882.74 | K |
| B16-24 | 12.993 | 1 | 5 | 122 | 2024 | 64 24.12385 | 16 | 40.91390 | 1596.25 | 0.00 | -67.33 | 1528.92 | 611767.56 | 435391.19 | K |
| B16-24 | 15.699 | 21 | 11 | 326 | 2024 | 64 24.12424 | 16 | 40.91212 | 1595.91 | -1.70 | -67.33 | 1526.87 | 611768.95 | 435391.97 | K |
| B17-24 | 16.261 | 1 | 5 | 122 | 2024 | 64 36.73258 | 16 | 28.79586 | 1283.68 | 0.00 | -67.12 | 1216.56 | 620566.84 | 459172.19 | K |
| B17-24 | 15.789 | 21 | 11 | 326 | 2024 | 64 36.74379 | 16 | 28.78844 | 1279.65 | 0.00 | -67.12 | 1212.53 | 620571.93 | 459193.24 | K |
| B18-24 | 18.625 | 1 | 5 | 122 | 2024 | 64 31.58165 | 16 | 0.11955 | 1383.15 | 0.00 | -66.92 | 1316.22 | 643870.62 | 450610.43 | K |
| B18-24 | 13.282 | 21 | 11 | 326 | 2024 | 64 31.58882 | 16 | 0.12351 | 1379.28 | 0.00 | -66.92 | 1312.36 | 643866.82 | 450623.60 | K |
| B19-24 | 11.796 | 1 | 5 | 122 | 2024 | 64 28.00978 | 15 | 55.98620 | 1505.53 | 0.00 | -66.89 | 1438.64 | 647495.79 | 444140.30 | K |
| B19-24 | 12.659 | 21 | 11 | 326 | 2024 | 64 28.01009 | 15 | 55.98630 | 1502.00 | 0.00 | -66.89 | 1435.11 | 647495.69 | 444140.88 | K |
| Bb0-24 | 10.401 | 1 | 5 | 122 | 2024 | 64 22.70650 | 16 | 5.05749 | 1583.38 | 0.00 | -66.85 | 1515.51 | 640684.32 | 433953.23 | K |
| Bb0-24 | 11.575 | 21 | 11 | 326 | 2024 | 64 22.70632 | 16 | 5.05832 | 1579.97 | 0.00 | -66.85 | 1513.12 | 640683.67 | 433952.86 | K |
| Barc-24 | 15.627 | 9 | 6 | 161 | 2024 | 64 38.42065 | 17 | 26.76110 | 1974.48 | 0.00 | -67.87 | 1906.61 | 574281.75 | 460818.20 | K |
| Barc-24 | 11.462 | 27 | 9 | 271 | 2024 | 64 38.42037 | 17 | 26.75646 | 1973.85 | -1.25 | -67.87 | 1904.73 | 574285.46 | 460817.77 | K |
| BARS-24 | 19.631 | 10 | 5 | 131 | 2024 | 64 33.96845 | 17 | 24.94570 | 1831.66 | -1.15 | -67.84 | 1762.66 | 575935.03 | 452584.53 | K |
| BB01-24 | 13.15 | 10 | 5 | 131 | 2024 | 64 37.82246 | 17 | 23.14747 | 1922.82 | -1.15 | -67.85 | 1853.82 | 577188.43 | 459779.27 | K |
| BB01-24 | 9.762 | 27 | 9 | 271 | 2024 | 64 37.82112 | 17 | 23.13418 | 1921.55 | -1.50 | -67.85 | 1852.21 | 577199.08 | 459777.05 | K |
| BB02-24 | 11.683 | 10 | 5 | 131 | 2024 | 64 38.42285 | 17 | 26.76238 | 1975.35 | -1.15 | -67.87 | 1906.33 | 574280.63 | 460822.26 | K |
| BB02-24 | 18.831 | 26 | 9 | 270 | 2024 | 64 38.42255 | 17 | 26.75643 | 1974.66 | -1.40 | -67.87 | 1905.39 | 574285.39 | 460821.83 | K |
| BB05-24 | 15.642 | 10 | 5 | 131 | 2024 | 64 36.58709 | 17 | 30.79372 | 1981.33 | -1.15 | -67.87 | 1912.31 | 571149.76 | 457335.13 | K |
| BB05-24 | 14.235 | 27 | 9 | 271 | 2024 | 64 36.58519 | 17 | 30.79528 | 1979.96 | -1.30 | -67.87 | 1910.79 | 571148.60 | 457331.56 | K |
| BB07-24 | 19.912 | 9 | 5 | 130 | 2024 | 64 36.56393 | 17 | 25.04691 | 1951.21 | -1.15 | -67.86 | 1882.21 | 575733.49 | 457403.38 | K |
| BB07-24 | 16.218 | 26 | 9 | 270 | 2024 | 64 36.56332 | 17 | 25.04123 | 1950.37 | -1.10 | -67.86 | 1881.42 | 575738.04 | 457402.36 | K |
| BB08-24 | 12.457 | 10 | 5 | 131 | 2024 | 64 39.00630 | 17 | 23.29569 | 1940.50 | -1.15 | -67.84 | 1871.50 | 577014.26 | 461975.11 | K |
| BB08-24 | 10.737 | 27 | 9 | 271 | 2024 | 64 39.00682 | 17 | 23.28887 | 1939.37 | -1.60 | -67.84 | 1869.93 | 577019.66 | 461976.22 | K |
| BB09-24 | 17.146 | 10 | 5 | 131 | 2024 | 64 39.66720 | 17 | 28.02056 | 1983.77 | -1.15 | -67.87 | 1914.75 | 573222.41 | 463109.11 | K |
| BB09-24 | 11.758 | 27 | 9 | 271 | 2024 | 64 39.66697 | 17 | 28.01804 | 1982.85 | -1.40 | -67.87 | 1913.58 | 573224.42 | 463108.72 | K |
| BB10-24 | 16.421 | 10 | 5 | 131 | 2024 | 64 38.63950 | 17 | 32.51580 | 2029.03 | -1.15 | -67.87 | 1960.01 | 569688.55 | 461115.50 | K |
| BB10-24 | 13.179 | 27 | 9 | 271 | 2024 | 64 38.63911 | 17 | 32.51501 | 2028.09 | -1.70 | -67.87 | 1958.52 | 569689.19 | 461114.78 | K |
| BB11-24 | 11.166 | 10 | 5 | 131 | 2024 | 64 37.49393 | 17 | 27.96813 | 1982.18 | -1.15 | -67.87 | 1913.16 | 573362.10 | 459073.38 | K |
| BB11-24 | 17.64 | 26 | 9 | 270 | 2024 | 64 37.49361 | 17 | 27.96396 | 1981.47 | -1.40 | -67.87 | 1912.20 | 573365.43 | 459072.86 | K |
| BB12-24 | 20.751 | 10 | 5 | 131 | 2024 | 64 36.48235 | 17 | 16.52334 | 1698.50 | -1.15 | -67.74 | 1629.61 | 582534.30 | 457429.68 | K |
| BB12-24 | 14.63 | 26 | 9 | 270 | 2024 | 64 36.48282 | 17 | 16.51204 | 1695.74 | -0.35 | -67.74 | 1627.65 | 582543.29 | 457430.80 | K |

| | | | | | | | | | | | | | | | | | |
|----------|--------|----|----|-----|------|------|----------|----------|----------|----------|--------|--------|---------|-----------|-----------|-----------|---|
| BB13-24 | 21.72 | 10 | 5 | 131 | 2024 | 64 | 39.57969 | 17 | 16.97270 | 1620.64 | -1.15 | -67.71 | 1551.78 | 582019.68 | 463172.66 | K | |
| BB13-24 | 12.453 | 26 | 9 | 270 | 2024 | 64 | 39.58301 | 17 | 16.96094 | 1617.45 | -0.30 | -67.71 | 1549.44 | 582028.87 | 463179.08 | K | |
| BB14-24 | 22.625 | 10 | 5 | 131 | 2024 | 64 | 41.74082 | 17 | 21.22675 | 1627.88 | -1.15 | -67.76 | 1558.97 | 578529.28 | 467096.58 | K | |
| BB14-24 | 11.391 | 26 | 9 | 270 | 2024 | 64 | 41.74331 | 17 | 21.21862 | 1624.67 | -0.25 | -67.76 | 1556.66 | 578535.62 | 467101.38 | K | |
| Bor-24 | 13.362 | 9 | 6 | 161 | 2024 | 64 | 24.93529 | 17 | 20.15227 | 1475.72 | 0.00 | -67.70 | 1408.02 | 580205.20 | 435905.13 | K | |
| Bor-24 | 16.859 | 23 | 11 | 328 | 2024 | 64 | 24.93166 | 17 | 20.15528 | 1492.15 | -1.80 | -67.70 | 1422.65 | 580202.96 | 435898.34 | K | |
| Br1-23 | 16.216 | 12 | 6 | 164 | 2024 | 64 | 5.96323 | 16 | 19.82099 | 126.98 | -1.95 | -65.90 | 59.13 | 630132.63 | 402347.09 | K | |
| Br1-24 | 16.269 | 12 | 6 | 164 | 2024 | 64 | 5.95725 | 16 | 19.82470 | 126.58 | -1.95 | -65.90 | 58.73 | 630130.08 | 402335.86 | K | |
| Br1n-24 | 14.581 | 28 | 9 | 272 | 2024 | 64 | 6.31510 | 16 | 20.10596 | 183.14 | -0.20 | -65.95 | 117.00 | 629873.70 | 402990.52 | K | |
| Br2-23 | 13.82 | 12 | 6 | 164 | 2024 | 64 | 6.35333 | 16 | 22.52293 | 208.21 | -1.95 | -66.03 | 140.23 | 627908.71 | 402979.36 | K | |
| Br2-24 | 14.75 | 12 | 6 | 164 | 2024 | 64 | 6.35384 | 16 | 22.52342 | 207.38 | -1.03 | -66.03 | 140.32 | 627908.27 | 402980.29 | K | |
| Br2-24 | 14.959 | 28 | 9 | 272 | 2024 | 64 | 6.35332 | 16 | 22.52402 | 200.51 | -0.20 | -66.03 | 134.28 | 627907.82 | 402979.31 | K | |
| Br3-23 | 12.111 | 12 | 6 | 164 | 2024 | 64 | 8.40616 | 16 | 23.96131 | 410.93 | -1.95 | -66.26 | 342.72 | 626584.20 | 406742.11 | K | |
| Br3-24 | 12.159 | 12 | 6 | 164 | 2024 | 64 | 8.40686 | 16 | 23.96260 | 411.08 | -1.95 | -66.26 | 342.87 | 626583.09 | 406743.36 | K | |
| Br7-24 | 19.314 | 1 | 5 | 122 | 2024 | 64 | 22.14129 | 16 | 16.93093 | 1310.12 | 0.00 | -67.01 | 1243.11 | 631187.23 | 432478.58 | K | |
| Br7-24 | 12.101 | 21 | 11 | 326 | 2024 | 64 | 22.10726 | 16 | 16.92040 | 1307.69 | -2.00 | -67.01 | 1238.68 | 631198.42 | 432415.78 | K | |
| Bru-24 | 17.322 | 1 | 5 | 122 | 2024 | 64 | 39.75607 | 15 | 56.53328 | 956.12 | 0.00 | -66.78 | 889.34 | 646002.39 | 465918.10 | K | |
| Bru-24 | 15.311 | 23 | 11 | 328 | 2024 | 64 | 39.76875 | 15 | 56.52821 | 952.88 | 0.00 | -66.78 | 886.09 | 646005.29 | 465941.83 | K | |
| Bud-24 | 17.846 | 1 | 5 | 122 | 2024 | 64 | 35.99204 | 15 | 59.88686 | 1204.24 | 0.00 | -66.88 | 1137.36 | 643667.61 | 458804.51 | K | |
| Bud-24 | 13.887 | 21 | 11 | 326 | 2024 | 64 | 36.00788 | 15 | 59.88352 | 1200.22 | 0.00 | -66.88 | 1133.34 | 643668.88 | 458834.05 | K | |
| D01-23 | | 13 | 3 | 5 | 124 | 2024 | 64 | 47.86880 | 16 | 49.97568 | 900.14 | 0.00 | -67.05 | 833.09 | 602976.52 | 479225.05 | K |
| D01-24 | 13.177 | 3 | 5 | 124 | 2024 | 64 | 47.86803 | 16 | 49.97378 | 900.72 | 0.00 | -67.05 | 833.67 | 602978.08 | 479223.67 | K | |
| D05-24 | 12.186 | 3 | 5 | 124 | 2024 | 64 | 42.22978 | 16 | 54.68273 | 1274.01 | 0.00 | -67.35 | 1206.66 | 599596.12 | 468627.96 | K | |
| D05-24 | 14.064 | 23 | 11 | 328 | 2024 | 64 | 42.24995 | 16 | 54.65293 | 1272.60 | -1.40 | -67.35 | 1203.85 | 599618.56 | 468666.18 | K | |
| D07-24 | 11.108 | 3 | 5 | 124 | 2024 | 64 | 38.29462 | 16 | 59.25557 | 1445.86 | 0.00 | -67.50 | 1378.36 | 596195.81 | 461202.26 | K | |
| D07-24 | 12.829 | 23 | 11 | 328 | 2024 | 64 | 38.31895 | 16 | 59.23063 | 1443.90 | -1.60 | -67.50 | 1374.80 | 596214.23 | 461248.07 | K | |
| D08-24 | 10.425 | 3 | 5 | 124 | 2024 | 64 | 34.68584 | 17 | 1.52077 | 1556.37 | 0.00 | -67.56 | 1488.81 | 594601.15 | 454443.50 | K | |
| D08-24 | 12.179 | 23 | 11 | 328 | 2024 | 64 | 34.69727 | 17 | 1.51699 | 1555.64 | -1.80 | -67.56 | 1486.28 | 594603.50 | 454464.83 | K | |
| D12-24 | 21.55 | 23 | 11 | 328 | 2024 | 64 | 28.97199 | 17 | 0.18388 | 1717.73 | -1.13 | -67.55 | 1649.05 | 596003.55 | 443866.04 | K | |
| E01-24 | 16.575 | 1 | 5 | 122 | 2024 | 64 | 40.66327 | 15 | 34.83165 | 814.48 | 0.00 | -66.72 | 747.77 | 663165.41 | 468485.92 | K | |
| E02-24 | 16.029 | 1 | 5 | 122 | 2024 | 64 | 39.11108 | 15 | 36.00208 | 1015.27 | 0.00 | -66.79 | 948.48 | 662390.53 | 465555.92 | K | |
| E02-24 | 13.53 | 23 | 11 | 328 | 2024 | 64 | 39.13490 | 15 | 35.99671 | 1011.36 | 0.00 | -66.79 | 944.58 | 662392.43 | 465600.34 | K | |
| E03-24 | 13.991 | 1 | 5 | 122 | 2024 | 64 | 36.66427 | 15 | 36.92615 | 1252.01 | 0.00 | -66.85 | 1185.16 | 661898.92 | 460976.78 | K | |
| E03-24 | 13.127 | 23 | 11 | 328 | 2024 | 64 | 36.67112 | 15 | 36.93034 | 1246.69 | 0.00 | -66.85 | 1179.84 | 661894.90 | 460989.32 | K | |
| E04-24 | 13.429 | 1 | 5 | 122 | 2024 | 64 | 34.95301 | 15 | 37.14648 | 1353.49 | 0.00 | -66.83 | 1286.66 | 661893.40 | 457792.42 | K | |
| E04-24 | 12.272 | 23 | 11 | 328 | 2024 | 64 | 34.95402 | 15 | 37.14575 | 1349.44 | 0.00 | -66.83 | 1282.61 | 661893.87 | 457794.32 | K | |
| E07-24 | 14.725 | 1 | 5 | 122 | 2024 | 64 | 38.41275 | 15 | 24.69953 | 1134.54 | 0.00 | -66.62 | 1067.93 | 671452.01 | 464757.80 | K | |
| E08-24 | 15.261 | 1 | 5 | 122 | 2024 | 64 | 39.72195 | 15 | 23.84883 | 1012.11 | 0.00 | -66.55 | 945.56 | 671990.19 | 467224.88 | K | |
| FI01-24 | 11.186 | 1 | 5 | 122 | 2024 | 64 | 26.15781 | 15 | 55.62463 | 1412.82 | 0.00 | -66.82 | 1345.99 | 647952.58 | 440717.48 | K | |
| FI01-24 | 12.259 | 21 | 11 | 326 | 2024 | 64 | 26.14973 | 15 | 55.60586 | 1408.31 | 0.00 | -66.82 | 1341.49 | 647968.36 | 440703.22 | K | |
| G02-24 | 12.544 | 3 | 5 | 124 | 2024 | 64 | 26.84949 | 17 | 17.71085 | 1635.25 | 0.00 | -67.73 | 1567.53 | 582069.96 | 439512.68 | K | |
| G02-24 | 19.355 | 22 | 11 | 327 | 2024 | 64 | 26.84429 | 17 | 17.71470 | 1632.71 | 0.00 | -67.73 | 1564.98 | 582067.14 | 439502.95 | K | |
| G03-24 | 11.722 | 3 | 5 | 124 | 2024 | 64 | 28.44321 | 17 | 16.33172 | 1728.67 | 0.00 | -67.74 | 1660.94 | 583095.29 | 442502.75 | K | |
| G03-24 | 19.03 | 22 | 11 | 327 | 2024 | 64 | 28.44088 | 17 | 16.33252 | 1726.48 | 0.00 | -67.74 | 1658.74 | 583094.77 | 442498.40 | K | |
| G04-24 | 10.901 | 3 | 5 | 124 | 2024 | 64 | 30.02181 | 17 | 15.03839 | 1758.40 | 0.00 | -67.73 | 1690.67 | 584050.54 | 445463.17 | K | |
| G04-24 | 17.844 | 27 | 9 | 271 | 2024 | 64 | 30.02206 | 17 | 15.03789 | 1757.62 | -1.00 | -67.73 | 1688.89 | 584050.94 | 445463.65 | K | |
| Go1-24 | 11.947 | 4 | 5 | 125 | 2024 | 64 | 33.97403 | 17 | 24.92539 | 1829.16 | 0.00 | -67.84 | 1761.32 | 575951.00 | 452595.29 | K | |
| Go1-24 | 9.567 | 26 | 9 | 270 | 2024 | 64 | 33.97275 | 17 | 24.92451 | 1827.94 | -0.40 | -67.84 | 1759.70 | 575951.76 | 452592.93 | K | |
| GWi-24 | 16.829 | 11 | 6 | 163 | 2024 | 64 | 24.39652 | 17 | 20.42740 | 1446.05 | 0.00 | -67.68 | 1378.36 | 580010.53 | 434898.64 | K | |
| Haab-24 | 21.857 | 4 | 5 | 125 | 2024 | 64 | 20.99610 | 17 | 24.11026 | 1797.09 | 0.00 | -67.54 | 1729.56 | 577212.96 | 428450.69 | K | |
| Haab-24 | 18.017 | 22 | 11 | 327 | 2024 | 64 | 20.99654 | 17 | 24.10883 | 1795.86 | -0.43 | -67.54 | 1727.89 | 577214.10 | 428451.54 | K | |
| Hof01-24 | 12.771 | 1 | 5 | 122 | 2024 | 64 | 32.34335 | 15 | 35.85454 | 1207.25 | 0.00 | -66.67 | 1140.57 | 663184.31 | 453006.02 | K | |
| Hof01-24 | 12.75 | 23 | 11 | 328 | 2024 | 64 | 32.33510 | 15 | 35.85387 | 1203.26 | 0.00 | -66.67 | 1136.59 | 663185.68 | 452990.75 | K | |
| K01-24 | 19.119 | 4 | 5 | 125 | 2024 | 64 | 35.16968 | 17 | 51.85664 | 1104.07 | 0.00 | -67.58 | 1036.49 | 554399.65 | 454353.54 | K | |
| K01-24 | 17.179 | 22 | 11 | 327 | 2024 | 64 | 35.17103 | 17 | 51.86375 | 1099.66 | 0.00 | -67.58 | 1032.08 | 554393.92 | 454355.96 | K | |
| K02-24 | 18.733 | 4 | 5 | 125 | 2024 | 64 | 34.81674 | 17 | 49.70803 | 1231.85 | 0.00 | -67.61 | 1164.24 | 556126.86 | 453729.20 | K | |
| K02-24 | 16.901 | 22 | 11 | 327 | 2024 | 64 | 34.81965 | 17 | 49.72358 | 1228.47 | 0.00 | -67.61 | 1160.86 | 556114.35 | 453734.39 | K | |
| K03-24 | 17.894 | 4 | 5 | 125 | 2024 | 64 | 34.23933 | 17 | 46.42930 | 1356.88 | 0.00 | -67.67 | 1289.21 | 558765.36 | 452706.23 | K | |
| K03-24 | 15.805 | 22 | 11 | 327 | 2024 | 64 | 34.24218 | 17 | 46.44956 | 1354.60 | 0.00 | -67.67 | 1286.93 | 558749.07 | 452711.20 | K | |
| K04-24 | 16.976 | 4 | 5 | 125 | 2024 | 64 | 33.20699 | 17 | 42.36377 | 1547.61 | 0.00 | -67.73 | 1479.88 | 562051.56 | 450853.27 | K | |
| K04-24 | 16.357 | 22 | 11 | 327 | 2024 | 64 | 33.21133 | 17 | 42.39233 | 1544.49 | 0.00 | -67.73 | 1476.76 | 562028.57 | 450860.86 | K | |
| K05-24 | 15.282 | 4 | 5 | 125 | 2024 | 64 | 33.44493 | 17 | 35.45251 | 1745.73 | 0.00 | -67.82 | 1677.91 | 567564.72 | 451413.35 | K | |
| K05-24 | 15.196 | 26 | 9 | 270 | 2024 | 64 | 33.44270 | 17 | 35.46428 | 1744.64 | -0.45 | -67.82 | 1676.37 | 567555.41 | 451408.99 | K | |
| K06-24 | 13.854 | 4 | 5 | 125 | 2024 | 64 | 38.3573 | | | | | | | | | | |

| | | | | | | | | | | | | | | | | |
|----------|--------|----|----|-----|------|----|----------|----|----------|---------|-------|--------|---------|-----------|-----------|---|
| Kverk-24 | 13.204 | 12 | 6 | 164 | 2024 | 64 | 38.66399 | 16 | 40.51911 | 1891.95 | 0.00 | -67.38 | 1824.57 | 611091.44 | 462400.10 | K |
| S01-24 | 20.403 | 4 | 5 | 125 | 2024 | 64 | 7.01727 | 17 | 49.97243 | 760.11 | 0.00 | -66.84 | 693.28 | 556869.32 | 402082.38 | K |
| S02-24 | 19.496 | 4 | 5 | 125 | 2024 | 64 | 12.16594 | 17 | 48.99572 | 1064.44 | 0.00 | -67.05 | 997.40 | 557483.34 | 411661.87 | K |
| S02-24 | 13.14 | 22 | 11 | 327 | 2024 | 64 | 12.15008 | 17 | 49.00411 | 1060.04 | 0.00 | -67.04 | 992.99 | 557477.10 | 411632.27 | K |
| S04-24 | 12.75 | 4 | 5 | 124 | 2024 | 64 | 16.17608 | 17 | 48.19933 | 1221.12 | 0.00 | -67.21 | 1153.91 | 557986.97 | 419123.59 | K |
| S04-24 | 12.75 | 22 | 11 | 327 | 2024 | 64 | 16.15596 | 17 | 48.22035 | 1216.87 | 0.00 | -67.21 | 1149.66 | 557970.70 | 419085.89 | K |
| S045-auk | 12.568 | 22 | 11 | 327 | 2024 | 64 | 16.44727 | 17 | 46.50468 | 1245.45 | 0.00 | -67.23 | 1178.22 | 559345.65 | 419653.59 | K |
| S05-24 | 17.693 | 3 | 5 | 124 | 2024 | 64 | 20.51715 | 17 | 33.99216 | 1517.93 | 0.00 | -67.51 | 1450.41 | 569276.14 | 427425.96 | K |
| S05-24 | 11.887 | 22 | 11 | 327 | 2024 | 64 | 20.51440 | 17 | 34.01438 | 1514.65 | 0.00 | -67.51 | 1447.14 | 569258.37 | 427420.45 | K |
| Ske02-24 | 14.666 | 2 | 5 | 123 | 2024 | 64 | 16.35713 | 16 | 59.29677 | 1263.97 | 0.00 | -67.09 | 1196.88 | 597459.85 | 420461.97 | K |
| Ske03-24 | 13.919 | 2 | 5 | 123 | 2024 | 64 | 18.05421 | 16 | 56.16782 | 1363.84 | 0.00 | -67.20 | 1296.64 | 599882.46 | 423694.93 | K |
| Ske03-24 | 18.157 | 21 | 11 | 326 | 2024 | 64 | 18.02240 | 16 | 56.24667 | 1357.65 | 0.00 | -67.20 | 1290.45 | 599820.82 | 423633.78 | K |
| Ske04-24 | 12.105 | 2 | 5 | 123 | 2024 | 64 | 20.14421 | 16 | 51.80334 | 1464.99 | 0.00 | -67.30 | 1397.70 | 603270.29 | 427692.90 | K |
| Ske04-24 | 17.759 | 21 | 11 | 326 | 2024 | 64 | 20.13141 | 16 | 51.83679 | 1461.13 | 0.00 | -67.30 | 1393.83 | 603244.16 | 427668.21 | K |
| Ske05-24 | 11.459 | 2 | 5 | 123 | 2024 | 64 | 22.23379 | 16 | 47.22575 | 1539.90 | 0.00 | -67.35 | 1472.55 | 606820.47 | 431699.83 | K |
| Ske05-24 | 17.309 | 21 | 11 | 326 | 2024 | 64 | 22.22828 | 16 | 47.23753 | 1536.76 | 0.00 | -67.35 | 1469.42 | 606811.35 | 431689.26 | K |
| Skf00-24 | 15.862 | 25 | 9 | 269 | 2024 | 64 | 15.46669 | 15 | 54.05167 | 1004.44 | -0.20 | -66.03 | 938.21 | 650187.22 | 420938.79 | K |
| Skf01-24 | 16.342 | 25 | 9 | 269 | 2024 | 64 | 18.01655 | 16 | 5.00634 | 1345.98 | -2.15 | -66.64 | 1277.19 | 641127.31 | 425250.43 | K |
| Skf01-24 | 11.032 | 21 | 11 | 326 | 2024 | 64 | 18.01510 | 16 | 5.00011 | 1343.27 | 0.00 | -66.64 | 1276.64 | 641132.45 | 425247.98 | K |
| T01-24 | 11.832 | 5 | 5 | 126 | 2024 | 64 | 19.15510 | 18 | 6.52581 | 820.32 | 0.00 | -67.25 | 753.07 | 543109.43 | 424413.69 | K |
| T02-24 | 15.914 | 4 | 5 | 125 | 2024 | 64 | 19.47747 | 18 | 4.55689 | 943.41 | 0.00 | -67.27 | 876.14 | 544687.86 | 425035.36 | K |
| T02-24 | 15.857 | 22 | 11 | 327 | 2024 | 64 | 19.47772 | 18 | 4.56198 | 939.84 | -1.25 | -67.27 | 871.33 | 544683.75 | 425035.77 | K |
| T03-24 | 13.751 | 4 | 5 | 125 | 2024 | 64 | 20.19863 | 17 | 58.61349 | 1126.17 | 0.00 | -67.30 | 1058.87 | 549456.23 | 426448.89 | K |
| T03-24 | 15.034 | 22 | 11 | 327 | 2024 | 64 | 20.19630 | 17 | 58.62903 | 1124.07 | -1.35 | -67.30 | 1055.42 | 549443.78 | 426444.36 | K |
| T04-24 | 16.657 | 3 | 5 | 124 | 2024 | 64 | 21.32992 | 17 | 51.51609 | 1285.15 | 0.00 | -67.36 | 1217.79 | 555135.73 | 428648.38 | K |
| T04-24 | 14.291 | 22 | 11 | 327 | 2024 | 64 | 21.32518 | 17 | 51.53348 | 1283.49 | -1.45 | -67.36 | 1214.67 | 555121.89 | 428639.34 | K |
| T05-24 | 15.751 | 3 | 5 | 124 | 2024 | 64 | 22.26272 | 17 | 42.99740 | 1411.35 | 0.00 | -67.47 | 1343.88 | 561957.97 | 430512.70 | K |
| T05-24 | 12.953 | 22 | 11 | 327 | 2024 | 64 | 22.25821 | 17 | 43.01495 | 1409.90 | -1.78 | -67.47 | 1340.65 | 561944.03 | 430504.03 | K |
| T05rorh | 13.083 | 22 | 11 | 327 | 2024 | 64 | 22.21754 | 17 | 43.27393 | 1405.11 | -2.10 | -67.46 | 1335.55 | 561737.20 | 430424.28 | K |
| T06-24 | 11.387 | 4 | 5 | 125 | 2024 | 64 | 24.26551 | 17 | 36.51589 | 1534.48 | 0.00 | -67.61 | 1466.87 | 567090.43 | 434343.32 | K |
| T06-24 | 11.599 | 22 | 11 | 327 | 2024 | 64 | 24.26071 | 17 | 36.53036 | 1534.22 | -2.17 | -67.61 | 1464.44 | 567079.00 | 434334.15 | K |
| T07-24 | 14.397 | 3 | 5 | 124 | 2024 | 64 | 25.29527 | 17 | 31.21182 | 1630.47 | 0.00 | -67.70 | 1562.77 | 571307.41 | 436352.89 | K |
| T07-24 | 11.023 | 22 | 11 | 327 | 2024 | 64 | 25.29292 | 17 | 31.22112 | 1630.09 | -1.98 | -67.70 | 1560.41 | 571300.05 | 436348.35 | K |
| T08-24 | 13.643 | 3 | 5 | 124 | 2024 | 64 | 26.30065 | 17 | 27.74827 | 1703.66 | 0.00 | -67.75 | 1635.91 | 574043.09 | 438286.72 | K |
| T08-24 | 10.633 | 22 | 11 | 327 | 2024 | 64 | 26.30050 | 17 | 27.74920 | 1703.92 | -2.20 | -67.75 | 1633.97 | 574042.35 | 438286.43 | K |

Appendix D: Measured surface velocity at marked sites on Vatnajökull in 2024.

| Site | Calendar | | Calendar | | # of days | translation (m) | velocity | | |
|----------|----------|-----|----------|-----|-----------|-----------------|----------|----------|-----------|
| | day date | # | day date | # | | | (°) | (cm/day) | (m/annum) |
| B07-24 | 240925 | 269 | 241121 | 326 | 57 | 2.87 | 105 | 5.03 | 18.35 |
| B12-24 | 240501 | 122 | 241123 | 328 | 206 | 23.59 | 20 | 11.45 | 41.80 |
| B13-24 | 240502 | 123 | 241121 | 326 | 203 | 23.68 | 28 | 11.66 | 42.57 |
| B13ror15 | 231026 | 299 | 240610 | 162 | 228 | 5.97 | 41 | 2.62 | 9.57 |
| B13ror15 | 240610 | 162 | 241121 | 326 | 164 | 22.77 | 26 | 13.89 | 50.68 |
| B14-24 | 240501 | 122 | 241121 | 326 | 204 | 18.73 | 37 | 9.18 | 33.52 |
| B15-24 | 240501 | 122 | 241121 | 326 | 204 | 14.54 | 48 | 7.13 | 26.02 |
| B16-24 | 240501 | 122 | 241121 | 326 | 204 | 1.60 | 63 | 0.79 | 2.87 |
| B17-24 | 240501 | 122 | 241121 | 326 | 204 | 21.59 | 16 | 10.58 | 38.62 |
| B18-24 | 240501 | 122 | 241121 | 326 | 204 | 13.65 | 347 | 6.69 | 24.43 |
| B19-24 | 240501 | 122 | 241121 | 326 | 204 | 0.58 | 352 | 0.28 | 1.04 |
| Bb0-24 | 240501 | 122 | 241121 | 326 | 204 | 0.75 | 243 | 0.37 | 1.33 |
| Barc-24 | 240609 | 161 | 240927 | 271 | 110 | 3.73 | 98 | 3.39 | 12.38 |
| BB01-24 | 240510 | 131 | 240927 | 271 | 140 | 10.88 | 103 | 7.77 | 28.35 |
| BB02-24 | 240510 | 131 | 240926 | 270 | 139 | 4.77 | 97 | 3.43 | 12.53 |
| BB05-24 | 240510 | 131 | 240927 | 271 | 140 | 3.73 | 199 | 2.67 | 9.73 |
| BB07-24 | 240509 | 130 | 240926 | 270 | 140 | 4.67 | 104 | 3.33 | 12.17 |
| BB08-24 | 240510 | 131 | 240927 | 271 | 140 | 5.51 | 80 | 3.94 | 14.38 |
| BB09-24 | 240510 | 131 | 240927 | 271 | 140 | 2.05 | 102 | 1.46 | 5.34 |
| BB10-24 | 240510 | 131 | 240927 | 271 | 140 | 0.96 | 139 | 0.68 | 2.50 |
| BB11-24 | 240510 | 131 | 240926 | 270 | 139 | 3.38 | 100 | 2.43 | 8.86 |
| BB12-24 | 240510 | 131 | 240926 | 270 | 139 | 9.05 | 84 | 6.51 | 23.77 |
| BB13-24 | 240510 | 131 | 240926 | 270 | 139 | 11.20 | 57 | 8.06 | 29.40 |
| BB14-24 | 240510 | 131 | 240926 | 270 | 139 | 7.94 | 54 | 5.71 | 20.85 |
| Bor-24 | 240609 | 161 | 241123 | 328 | 167 | 7.14 | 200 | 4.28 | 15.61 |
| Br1-23 | 231022 | 295 | 240612 | 164 | 234 | 0.08 | 198 | 0.03 | 0.12 |
| Br2-23 | 231022 | 295 | 240612 | 164 | 234 | 0.46 | 178 | 0.20 | 0.72 |
| Br2-24 | 240612 | 164 | 240928 | 272 | 108 | 1.08 | 207 | 1.00 | 3.65 |
| Br3-23 | 231022 | 295 | 240612 | 164 | 234 | 8.45 | 151 | 3.61 | 13.18 |
| Br7-24 | 240501 | 122 | 241121 | 326 | 204 | 63.59 | 172 | 31.17 | 113.78 |
| Bru-24 | 240501 | 122 | 241123 | 328 | 206 | 23.83 | 10 | 11.57 | 42.22 |
| Bud-24 | 240501 | 122 | 241121 | 326 | 204 | 29.46 | 5 | 14.44 | 52.70 |
| D01-23 | 230505 | 125 | 240503 | 124 | 364 | 1.68 | 339 | 0.46 | 1.69 |
| D05-24 | 240503 | 124 | 241123 | 328 | 204 | 44.23 | 32 | 21.68 | 79.13 |
| D07-24 | 240503 | 124 | 241123 | 328 | 204 | 49.24 | 24 | 24.14 | 88.11 |
| D08-24 | 240503 | 124 | 241123 | 328 | 204 | 21.38 | 8 | 10.48 | 38.26 |
| E02-24 | 240501 | 122 | 241123 | 328 | 206 | 44.32 | 6 | 21.52 | 78.53 |
| E03-24 | 240501 | 122 | 241123 | 328 | 206 | 13.12 | 345 | 6.37 | 23.24 |
| E04-24 | 240501 | 122 | 241123 | 328 | 206 | 1.96 | 17 | 0.95 | 3.47 |
| Fl01-24 | 240501 | 122 | 241121 | 326 | 204 | 21.23 | 135 | 10.41 | 37.99 |
| G02-24 | 240503 | 124 | 241122 | 327 | 203 | 10.11 | 198 | 4.98 | 18.18 |
| G03-24 | 240503 | 124 | 241122 | 327 | 203 | 4.36 | 188 | 2.15 | 7.84 |
| G04-24 | 240503 | 124 | 240927 | 271 | 147 | 0.61 | 41 | 0.42 | 1.52 |
| Go1-24 | 240504 | 125 | 240926 | 270 | 145 | 2.47 | 163 | 1.71 | 6.22 |
| Haab-24 | 240504 | 125 | 241122 | 327 | 202 | 1.41 | 55 | 0.70 | 2.55 |
| Hof01-24 | 240501 | 122 | 241123 | 328 | 206 | 15.29 | 178 | 7.42 | 27.09 |

| | | | | | | | | | |
|----------|--------|-----|--------|-----|-----|-------|-----|-------|--------|
| K01-24 | 240504 | 125 | 241122 | 327 | 202 | 6.20 | 294 | 3.07 | 11.20 |
| K02-24 | 240504 | 125 | 241122 | 327 | 202 | 13.53 | 293 | 6.70 | 24.45 |
| K03-24 | 240504 | 125 | 241122 | 327 | 202 | 17.02 | 288 | 8.42 | 30.75 |
| K04-24 | 240504 | 125 | 241122 | 327 | 202 | 24.19 | 289 | 11.98 | 43.71 |
| K05-24 | 240504 | 125 | 240926 | 270 | 145 | 10.27 | 246 | 7.08 | 25.85 |
| K06-24 | 240504 | 125 | 240927 | 271 | 146 | 1.93 | 113 | 1.32 | 4.83 |
| K07-24 | 240504 | 125 | 241122 | 327 | 202 | 1.83 | 282 | 0.90 | 3.30 |
| S01-24 | 240504 | 125 | 250129 | 0 | 240 | 0.15 | 12 | 0.06 | 0.23 |
| S02-24 | 240504 | 125 | 241122 | 327 | 202 | 30.15 | 193 | 14.92 | 54.47 |
| S04-24 | 240504 | 124 | 241122 | 327 | 203 | 40.94 | 204 | 20.17 | 73.62 |
| S05-24 | 240503 | 124 | 241122 | 327 | 203 | 18.60 | 254 | 9.16 | 33.45 |
| Ske03-24 | 240502 | 123 | 241121 | 326 | 203 | 86.68 | 227 | 42.70 | 155.86 |
| Ske04-24 | 240502 | 123 | 241121 | 326 | 203 | 35.88 | 229 | 17.68 | 64.52 |
| Ske05-24 | 240502 | 123 | 241121 | 326 | 203 | 13.93 | 223 | 6.86 | 25.04 |
| Skf01-24 | 240925 | 269 | 241121 | 326 | 57 | 5.70 | 118 | 9.99 | 36.48 |
| T02-24 | 240504 | 125 | 241122 | 327 | 202 | 4.13 | 276 | 2.04 | 7.46 |
| T03-24 | 240504 | 125 | 241122 | 327 | 202 | 13.24 | 251 | 6.55 | 23.92 |
| T04-24 | 240503 | 124 | 241122 | 327 | 203 | 16.52 | 238 | 8.14 | 29.70 |
| T05-24 | 240503 | 124 | 241122 | 327 | 203 | 16.40 | 239 | 8.08 | 29.49 |
| T05rorh | 221018 | 291 | 241122 | 327 | 766 | 53.52 | 239 | 6.99 | 25.50 |
| T06-24 | 240504 | 125 | 241122 | 327 | 202 | 14.63 | 233 | 7.24 | 26.44 |
| T07-24 | 240503 | 124 | 241122 | 327 | 203 | 8.64 | 240 | 4.26 | 15.54 |
| T08-24 | 240503 | 124 | 241122 | 327 | 203 | 0.80 | 250 | 0.39 | 1.43 |

Appendix E: Melt water runoff to selected rivers in summer 2024, derived from summer surface balance.

ΔS : area in each elevation range where summer balance is negative, $\Sigma \Delta S$: cumulative area above a given elevation, ΔQ_s : melt water runoff from a given elevation range, $\Sigma \Delta Q_s$: cumulative melt water runoff from an area above given elevation.

Tungnaá water drainage basin

| Elevation (m a. s. l.) | ΔS km^2 | $\Sigma \Delta S$ km^2 | ΔQ_s (10^6m^3) | $\Sigma \Delta Q_s$ (10^6m^3) |
|---------------------------|-----------------------------|------------------------------------|-------------------------------------|--|
|---------------------------|-----------------------------|------------------------------------|-------------------------------------|--|

| | | | | | |
|------|------|------|-------|------|-------|
| 1350 | 1400 | 0.3 | 0.3 | 0.4 | 0.4 |
| 1300 | 1350 | 6.0 | 6.3 | 9.0 | 9.4 |
| 1250 | 1300 | 9.8 | 16.1 | 20.2 | 29.6 |
| 1200 | 1250 | 10.7 | 26.8 | 27.3 | 56.9 |
| 1150 | 1200 | 9.5 | 36.4 | 27.6 | 84.5 |
| 1100 | 1150 | 11.0 | 47.4 | 34.4 | 118.9 |
| 1050 | 1100 | 10.3 | 57.7 | 35.3 | 154.2 |
| 1000 | 1050 | 9.5 | 67.2 | 36.5 | 190.7 |
| 950 | 1000 | 8.8 | 76.1 | 37.3 | 228.0 |
| 900 | 950 | 8.5 | 84.6 | 39.8 | 267.8 |
| 850 | 900 | 6.3 | 90.9 | 32.6 | 300.3 |
| 800 | 850 | 6.3 | 97.1 | 34.7 | 335.0 |
| 750 | 800 | 4.6 | 101.8 | 27.2 | 362.3 |
| 700 | 750 | 2.5 | 104.2 | 15.3 | 377.6 |
| 650 | 700 | 0.1 | 104.4 | 0.9 | 378.5 |

Sylgja water drainage basin

| Elevation (m a. s. l.) | ΔS km^2 | $\Sigma \Delta S$ km^2 | ΔQ_s (10^6m^3) | $\Sigma \Delta Q_s$ (10^6m^3) |
|---------------------------|-----------------------------|------------------------------------|-------------------------------------|--|
|---------------------------|-----------------------------|------------------------------------|-------------------------------------|--|

| | | | | | |
|------|------|-----|------|------|-------|
| 1300 | 1350 | 1.1 | 1.1 | 1.8 | 1.8 |
| 1250 | 1300 | 3.4 | 4.5 | 6.9 | 8.7 |
| 1200 | 1250 | 5.3 | 9.7 | 13.7 | 22.4 |
| 1150 | 1200 | 8.0 | 17.8 | 23.2 | 45.6 |
| 1100 | 1150 | 5.8 | 23.5 | 18.2 | 63.8 |
| 1050 | 1100 | 6.0 | 29.5 | 20.3 | 84.1 |
| 1000 | 1050 | 5.7 | 35.3 | 21.1 | 105.3 |
| 950 | 1000 | 1.8 | 37.1 | 7.1 | 112.3 |
| 900 | 950 | 0.7 | 37.8 | 2.7 | 115.0 |

Western Skaftá cauldron water drainage basin

| Elevation (m a. s. l.) | ΔS km^2 | $\Sigma \Delta S$ km^2 | ΔQ_s (10^6m^3) | $\Sigma \Delta Q_s$ (10^6m^3) |
|---------------------------|-----------------------------|------------------------------------|-------------------------------------|--|
|---------------------------|-----------------------------|------------------------------------|-------------------------------------|--|

| | | | | | |
|------|------|-----|------|-----|-----|
| 1700 | 1750 | 2.2 | 2.2 | 0.1 | 0.1 |
| 1650 | 1700 | 7.1 | 9.3 | 0.8 | 0.9 |
| 1600 | 1650 | 7.9 | 17.3 | 1.9 | 2.8 |
| 1550 | 1600 | 5.0 | 22.3 | 1.4 | 4.2 |
| 1500 | 1550 | 2.6 | 24.9 | 0.8 | 5.1 |

Eastern Skaftár cauldron water drainage basin

| Elevation (m a. s. l.) | ΔS km^2 | $\sum \Delta S$ km^2 | ΔQ_s (10^6m^3) | $\sum \Delta Q_s$ (10^6m^3) |
|---------------------------|-----------------------------|----------------------------------|-------------------------------------|--|
|---------------------------|-----------------------------|----------------------------------|-------------------------------------|--|

| | | | | | |
|------|------|------|------|-----|-----|
| 1700 | 1750 | 6.9 | 6.9 | 0.6 | 0.6 |
| 1650 | 1700 | 13.7 | 20.6 | 3.6 | 4.1 |
| 1600 | 1650 | 9.4 | 30.0 | 2.8 | 7.0 |
| 1550 | 1600 | 4.0 | 34.0 | 1.3 | 8.3 |

Grímsvötn water drainage basin

| Elevation (m a. s. l.) | ΔS km^2 | $\sum \Delta S$ km^2 | ΔQ_s (10^6m^3) | $\sum \Delta Q_s$ (10^6m^3) |
|---------------------------|-----------------------------|----------------------------------|-------------------------------------|--|
|---------------------------|-----------------------------|----------------------------------|-------------------------------------|--|

| | | | | | |
|------|------|------|-------|------|-------|
| 1700 | 1750 | 21.8 | 21.8 | 3.3 | 3.3 |
| 1650 | 1700 | 48.0 | 69.8 | 18.2 | 21.5 |
| 1600 | 1650 | 30.7 | 100.5 | 19.3 | 40.8 |
| 1550 | 1600 | 19.6 | 120.1 | 15.8 | 56.5 |
| 1500 | 1550 | 16.2 | 136.3 | 19.1 | 75.6 |
| 1450 | 1500 | 9.5 | 145.8 | 15.8 | 91.4 |
| 1400 | 1450 | 13.7 | 159.5 | 28.1 | 119.5 |
| 1350 | 1400 | 1.2 | 160.7 | 2.6 | 122.1 |

Kaldakvísl water drainage basin

| Elevation (m a. s. l.) | ΔS km^2 | $\sum \Delta S$ km^2 | ΔQ_s (10^6m^3) | $\sum \Delta Q_s$ (10^6m^3) |
|---------------------------|-----------------------------|----------------------------------|-------------------------------------|--|
|---------------------------|-----------------------------|----------------------------------|-------------------------------------|--|

| | | | | | |
|------|------|------|-------|------|-------|
| 1700 | 1750 | 3.8 | 3.8 | 0.1 | 0.1 |
| 1650 | 1700 | 16.7 | 20.5 | 1.8 | 1.9 |
| 1600 | 1650 | 14.5 | 35.0 | 3.8 | 5.7 |
| 1550 | 1600 | 18.4 | 53.4 | 7.8 | 13.5 |
| 1500 | 1550 | 24.1 | 77.6 | 13.7 | 27.2 |
| 1450 | 1500 | 27.8 | 105.3 | 20.7 | 47.9 |
| 1400 | 1450 | 22.3 | 127.7 | 21.4 | 69.3 |
| 1350 | 1400 | 20.5 | 148.2 | 25.0 | 94.3 |
| 1300 | 1350 | 19.2 | 167.4 | 29.8 | 124.1 |
| 1250 | 1300 | 20.5 | 187.9 | 40.4 | 164.5 |
| 1200 | 1250 | 20.0 | 207.9 | 48.9 | 213.4 |
| 1150 | 1200 | 19.0 | 226.9 | 55.0 | 268.5 |
| 1100 | 1150 | 17.0 | 243.9 | 55.9 | 324.4 |
| 1050 | 1100 | 15.7 | 259.6 | 58.3 | 382.7 |
| 1000 | 1050 | 12.9 | 272.5 | 52.9 | 435.6 |
| 950 | 1000 | 7.2 | 279.7 | 32.8 | 468.4 |
| 900 | 950 | 1.2 | 281.0 | 5.7 | 474.1 |

Jökulsá á Fjöllum water drainage basin

| Elevation (m a. s. l.) | | ΔS km^2 | $\sum \Delta S$ km^2 | ΔQ_s (10^6m^3) | $\sum \Delta Q_s$ (10^6m^3) |
|---------------------------|------|-----------------------------|----------------------------------|---------------------------------------|--|
| 1800 | 1850 | 0.0 | 0.0 | 0.0 | 0.0 |
| 1750 | 1800 | 1.9 | 1.9 | 0.0 | 0.0 |
| 1700 | 1750 | 26.5 | 28.5 | 2.4 | 2.4 |
| 1650 | 1700 | 79.5 | 108.0 | 16.5 | 18.9 |
| 1600 | 1650 | 121.1 | 229.2 | 31.3 | 50.2 |
| 1550 | 1600 | 100.2 | 329.3 | 40.3 | 90.6 |
| 1500 | 1550 | 92.1 | 421.5 | 52.7 | 143.2 |
| 1450 | 1500 | 79.3 | 500.8 | 58.2 | 201.5 |
| 1400 | 1450 | 68.7 | 569.5 | 61.2 | 262.7 |
| 1350 | 1400 | 54.2 | 623.7 | 63.4 | 326.1 |
| 1300 | 1350 | 42.7 | 666.4 | 66.1 | 392.2 |
| 1250 | 1300 | 46.3 | 712.6 | 88.7 | 480.9 |
| 1200 | 1250 | 49.3 | 761.9 | 112.4 | 593.2 |
| 1150 | 1200 | 48.7 | 810.6 | 133.3 | 726.5 |
| 1100 | 1150 | 44.1 | 854.7 | 141.1 | 867.6 |
| 1050 | 1100 | 31.0 | 885.6 | 114.9 | 982.6 |
| 1000 | 1050 | 31.1 | 916.7 | 131.8 | 1114.4 |
| 950 | 1000 | 28.9 | 945.6 | 136.8 | 1251.3 |
| 900 | 950 | 24.7 | 970.3 | 127.0 | 1378.3 |
| 850 | 900 | 20.5 | 990.8 | 114.1 | 1492.4 |
| 800 | 850 | 16.5 | 1007.3 | 98.7 | 1591.1 |
| 750 | 800 | 8.5 | 1015.8 | 53.5 | 1644.6 |
| 700 | 750 | 0.3 | 1016.2 | 2.2 | 1646.8 |

Kreppa and Kverká water drainage basin

| Elevation (m a. s. l.) | ΔS km^2 | $\Sigma \Delta S$ km^2 | ΔQ_s (10^6m^3) | $\Sigma \Delta Q_s$ (10^6m^3) |
|---------------------------|-----------------------------|------------------------------------|-------------------------------------|--|
|---------------------------|-----------------------------|------------------------------------|-------------------------------------|--|

| | | | | | |
|------|------|------|-------|------|-------|
| 1900 | 1950 | 0.0 | 0.0 | 0.0 | 0.0 |
| 1750 | 1800 | 0.0 | 0.0 | 0.0 | 0.0 |
| 1700 | 1750 | 1.2 | 1.2 | 0.0 | 0.0 |
| 1650 | 1700 | 4.5 | 5.8 | 0.2 | 0.2 |
| 1600 | 1650 | 41.6 | 47.3 | 7.2 | 7.5 |
| 1550 | 1600 | 20.4 | 67.7 | 4.6 | 12.0 |
| 1500 | 1550 | 13.4 | 81.2 | 4.7 | 16.7 |
| 1450 | 1500 | 16.3 | 97.4 | 8.5 | 25.3 |
| 1400 | 1450 | 20.1 | 117.5 | 15.5 | 40.8 |
| 1350 | 1400 | 25.9 | 143.4 | 26.7 | 67.5 |
| 1300 | 1350 | 20.3 | 163.7 | 26.3 | 93.8 |
| 1250 | 1300 | 15.3 | 179.0 | 27.7 | 121.5 |
| 1200 | 1250 | 17.7 | 196.7 | 41.3 | 162.8 |
| 1150 | 1200 | 17.2 | 213.9 | 44.5 | 207.3 |
| 1100 | 1150 | 16.1 | 230.0 | 43.9 | 251.2 |
| 1050 | 1100 | 10.4 | 240.4 | 29.3 | 280.5 |
| 1000 | 1050 | 11.6 | 252.0 | 33.7 | 314.2 |
| 950 | 1000 | 12.7 | 264.7 | 40.8 | 355.0 |
| 900 | 950 | 12.8 | 277.5 | 45.9 | 400.9 |
| 850 | 900 | 11.9 | 289.4 | 46.2 | 447.1 |
| 800 | 850 | 9.8 | 299.2 | 41.5 | 488.6 |
| 750 | 800 | 6.7 | 305.9 | 31.0 | 519.6 |
| 700 | 750 | 3.4 | 309.3 | 16.8 | 536.4 |
| 650 | 700 | 0.2 | 309.5 | 0.8 | 537.2 |

Hálslón water drainage basin

| Elevation (m a. s. l.) | ΔS km^2 | $\Sigma \Delta S$ km^2 | ΔQ_s (10^6m^3) | $\Sigma \Delta Q_s$ (10^6m^3) |
|---------------------------|-----------------------------|------------------------------------|-------------------------------------|--|
|---------------------------|-----------------------------|------------------------------------|-------------------------------------|--|

| | | | | | |
|------|------|-------|--------|-------|--------|
| 1600 | 1650 | 11.2 | 11.2 | 2.3 | 2.3 |
| 1550 | 1600 | 33.6 | 44.8 | 8.1 | 10.5 |
| 1500 | 1550 | 65.2 | 110.0 | 20.0 | 30.5 |
| 1450 | 1500 | 70.0 | 180.0 | 36.4 | 66.9 |
| 1400 | 1450 | 98.9 | 278.9 | 68.3 | 135.2 |
| 1350 | 1400 | 132.9 | 411.8 | 121.6 | 256.8 |
| 1300 | 1350 | 129.1 | 540.9 | 141.3 | 398.0 |
| 1250 | 1300 | 122.4 | 663.3 | 151.8 | 549.9 |
| 1200 | 1250 | 97.2 | 760.5 | 142.9 | 692.8 |
| 1150 | 1200 | 81.9 | 842.5 | 150.7 | 843.5 |
| 1100 | 1150 | 64.0 | 906.5 | 140.0 | 983.5 |
| 1050 | 1100 | 54.6 | 961.0 | 136.9 | 1120.4 |
| 1000 | 1050 | 45.8 | 1006.9 | 129.3 | 1249.7 |
| 950 | 1000 | 39.1 | 1046.0 | 123.9 | 1373.6 |
| 900 | 950 | 31.9 | 1077.9 | 112.4 | 1486.1 |
| 850 | 900 | 26.6 | 1104.5 | 103.2 | 1589.3 |
| 800 | 850 | 24.4 | 1128.9 | 103.7 | 1693.0 |
| 750 | 800 | 24.2 | 1153.1 | 111.7 | 1804.6 |
| 700 | 750 | 22.7 | 1175.8 | 112.3 | 1916.9 |
| 650 | 700 | 9.4 | 1185.2 | 48.7 | 1965.7 |
| 600 | 650 | 0.5 | 1185.7 | 2.6 | 1968.2 |

Jökulsá á Fljótsdal water drainage basin

| Elevation (m a. s. l.) | ΔS km^2 | $\Sigma \Delta S$ km^2 | ΔQ_s (10^6m^3) | $\Sigma \Delta Q_s$ (10^6m^3) |
|---------------------------|-----------------------------|------------------------------------|-------------------------------------|--|
|---------------------------|-----------------------------|------------------------------------|-------------------------------------|--|

| | | | | | |
|------|------|------|-------|------|-------|
| 1550 | 1600 | 0.0 | 0.0 | 0.0 | 0.0 |
| 1500 | 1550 | 0.0 | 0.0 | 0.0 | 0.0 |
| 1450 | 1500 | 0.3 | 0.4 | 0.0 | 0.0 |
| 1400 | 1450 | 1.2 | 1.6 | 0.1 | 0.1 |
| 1350 | 1400 | 2.8 | 4.4 | 0.6 | 0.7 |
| 1300 | 1350 | 5.4 | 9.8 | 2.8 | 3.6 |
| 1250 | 1300 | 15.8 | 25.6 | 15.5 | 19.1 |
| 1200 | 1250 | 14.8 | 40.4 | 19.2 | 38.3 |
| 1150 | 1200 | 16.4 | 56.9 | 26.2 | 64.5 |
| 1100 | 1150 | 14.0 | 70.9 | 27.2 | 91.7 |
| 1050 | 1100 | 11.7 | 82.6 | 27.7 | 119.4 |
| 1000 | 1050 | 10.8 | 93.4 | 29.4 | 148.7 |
| 950 | 1000 | 8.7 | 102.1 | 27.8 | 176.6 |
| 900 | 950 | 5.5 | 107.6 | 20.6 | 197.2 |
| 850 | 900 | 4.2 | 111.8 | 17.3 | 214.5 |
| 800 | 850 | 2.9 | 114.8 | 13.3 | 227.8 |
| 750 | 800 | 1.8 | 116.5 | 8.7 | 236.6 |
| 700 | 750 | 1.6 | 118.2 | 8.8 | 245.3 |
| 650 | 700 | 0.6 | 118.8 | 3.6 | 249.0 |

Hornafjarðarfljót water drainage basin

| Elevation (m a. s. l.) | ΔS km^2 | $\sum \Delta S$ km^2 | ΔQ_s (10^6m^3) | $\sum \Delta Q_s$ (10^6m^3) |
|---------------------------|-----------------------------|----------------------------------|-------------------------------------|--|
|---------------------------|-----------------------------|----------------------------------|-------------------------------------|--|

| | | | | | |
|------|------|------|-------|------|-------|
| 1450 | 1500 | 0.1 | 0.1 | 0.0 | 0.0 |
| 1400 | 1450 | 6.5 | 6.6 | 3.7 | 3.7 |
| 1350 | 1400 | 11.6 | 18.3 | 7.3 | 11.1 |
| 1300 | 1350 | 18.9 | 37.2 | 15.0 | 26.0 |
| 1250 | 1300 | 37.3 | 74.6 | 36.8 | 62.8 |
| 1200 | 1250 | 28.7 | 103.2 | 32.2 | 95.1 |
| 1150 | 1200 | 19.9 | 123.1 | 27.6 | 122.7 |
| 1100 | 1150 | 18.3 | 141.4 | 30.7 | 153.4 |
| 1050 | 1100 | 13.8 | 155.2 | 27.9 | 181.2 |
| 1000 | 1050 | 10.6 | 165.8 | 24.2 | 205.4 |
| 950 | 1000 | 10.1 | 175.9 | 25.8 | 231.2 |
| 900 | 950 | 8.1 | 184.0 | 22.7 | 254.0 |
| 850 | 900 | 5.1 | 189.0 | 15.8 | 269.8 |
| 800 | 850 | 4.2 | 193.2 | 14.2 | 284.0 |
| 750 | 800 | 3.3 | 196.5 | 11.5 | 295.5 |
| 700 | 750 | 3.1 | 199.6 | 11.8 | 307.3 |
| 650 | 700 | 3.3 | 202.9 | 14.2 | 321.5 |
| 600 | 650 | 2.6 | 205.4 | 11.9 | 333.4 |
| 550 | 600 | 1.9 | 207.4 | 9.3 | 342.7 |
| 500 | 550 | 1.7 | 209.1 | 8.8 | 351.5 |
| 450 | 500 | 1.3 | 210.4 | 7.3 | 358.8 |
| 400 | 450 | 1.0 | 211.4 | 5.9 | 364.6 |
| 350 | 400 | 1.0 | 212.4 | 5.8 | 370.4 |
| 300 | 350 | 0.6 | 213.0 | 3.7 | 374.1 |
| 250 | 300 | 0.7 | 213.7 | 4.5 | 378.7 |
| 200 | 250 | 0.9 | 214.5 | 6.3 | 384.9 |
| 150 | 200 | 1.8 | 216.3 | 13.4 | 398.3 |
| 100 | 150 | 2.4 | 218.7 | 18.8 | 417.1 |
| 50 | 100 | 2.2 | 220.9 | 18.5 | 435.6 |
| 0 | 50 | 2.9 | 223.8 | 26.9 | 462.5 |

Jökulsá á Breiðamerkursandi water drainage basin

| Elevation (m a. s. l.) | ΔS km ² | $\sum \Delta S$ km ² | ΔQ_s (10 ⁶ m ³) | $\sum \Delta Q_s$ (10 ⁶ m ³) |
|---------------------------|-------------------------------|------------------------------------|---|--|
|---------------------------|-------------------------------|------------------------------------|---|--|

| | | | | | |
|------|------|------|-------|------|--------|
| 1650 | 1700 | 0.5 | 0.5 | 0.1 | 0.1 |
| 1600 | 1650 | 2.6 | 3.1 | 0.2 | 0.3 |
| 1550 | 1600 | 15.3 | 18.5 | 1.8 | 2.1 |
| 1500 | 1550 | 22.7 | 41.2 | 7.4 | 9.5 |
| 1450 | 1500 | 36.2 | 77.4 | 19.2 | 28.7 |
| 1400 | 1450 | 50.9 | 128.3 | 35.4 | 64.2 |
| 1350 | 1400 | 83.0 | 211.4 | 71.9 | 136.1 |
| 1300 | 1350 | 82.6 | 294.0 | 74.4 | 210.5 |
| 1250 | 1300 | 51.0 | 344.9 | 48.9 | 259.4 |
| 1200 | 1250 | 33.6 | 378.5 | 38.2 | 297.7 |
| 1150 | 1200 | 27.2 | 405.7 | 38.4 | 336.1 |
| 1100 | 1150 | 22.1 | 427.8 | 37.5 | 373.6 |
| 1050 | 1100 | 18.4 | 446.2 | 36.1 | 409.6 |
| 1000 | 1050 | 14.5 | 460.7 | 32.4 | 442.1 |
| 950 | 1000 | 15.2 | 476.0 | 38.9 | 481.0 |
| 900 | 950 | 15.5 | 491.5 | 43.9 | 524.9 |
| 850 | 900 | 13.1 | 504.6 | 40.7 | 565.6 |
| 800 | 850 | 15.2 | 519.8 | 51.8 | 617.4 |
| 750 | 800 | 16.9 | 536.7 | 63.5 | 680.9 |
| 700 | 750 | 12.9 | 549.7 | 52.4 | 733.3 |
| 650 | 700 | 20.3 | 569.9 | 87.8 | 821.1 |
| 600 | 650 | 20.9 | 590.8 | 96.3 | 917.5 |
| 550 | 600 | 15.9 | 606.8 | 78.3 | 995.8 |
| 500 | 550 | 14.1 | 620.8 | 72.2 | 1068.0 |
| 450 | 500 | 4.8 | 625.6 | 25.8 | 1093.8 |
| 400 | 450 | 6.1 | 631.8 | 34.8 | 1128.6 |
| 350 | 400 | 5.7 | 637.5 | 34.3 | 1162.9 |
| 300 | 350 | 4.5 | 641.9 | 28.6 | 1191.5 |
| 250 | 300 | 4.6 | 646.5 | 31.3 | 1222.7 |
| 200 | 250 | 4.9 | 651.5 | 34.6 | 1257.3 |
| 150 | 200 | 4.4 | 655.8 | 32.2 | 1289.5 |
| 100 | 150 | 4.7 | 660.5 | 36.7 | 1326.2 |
| 50 | 100 | 4.1 | 664.6 | 34.3 | 1360.5 |
| 0 | 50 | 1.2 | 665.8 | 10.7 | 1371.3 |

Breiðárlón/Fjallsárlón water drainage basin

| Elevation (m a. s. l.) | | ΔS km ² | $\Sigma \Delta S$ km ² | ΔQ_s (10 ⁶ m ³) | $\Sigma \Delta Q_s$ (10 ⁶ m ³) |
|---------------------------|------|-------------------------------|--------------------------------------|---|--|
| 1700 | 1750 | 0.0 | 0.0 | 0.0 | 0.0 |
| 1650 | 1700 | 0.0 | 0.0 | 0.0 | 0.0 |
| 1600 | 1650 | 0.0 | 0.0 | 0.0 | 0.0 |
| 1550 | 1600 | 1.2 | 1.2 | 0.1 | 0.1 |
| 1500 | 1550 | 2.5 | 3.8 | 0.7 | 0.9 |
| 1450 | 1500 | 3.8 | 7.5 | 1.2 | 2.1 |
| 1400 | 1450 | 4.8 | 12.3 | 2.3 | 4.4 |
| 1350 | 1400 | 6.3 | 18.7 | 5.1 | 9.5 |
| 1300 | 1350 | 12.5 | 31.2 | 12.8 | 22.3 |
| 1250 | 1300 | 6.4 | 37.6 | 7.3 | 29.7 |
| 1200 | 1250 | 5.5 | 43.1 | 7.1 | 36.7 |
| 1150 | 1200 | 4.7 | 47.8 | 6.8 | 43.5 |
| 1100 | 1150 | 4.2 | 52.0 | 7.2 | 50.6 |
| 1050 | 1100 | 4.6 | 56.7 | 8.9 | 59.5 |
| 1000 | 1050 | 5.6 | 62.2 | 11.8 | 71.3 |
| 950 | 1000 | 6.2 | 68.5 | 15.9 | 87.2 |
| 900 | 950 | 7.2 | 75.7 | 20.2 | 107.3 |
| 850 | 900 | 5.7 | 81.4 | 17.4 | 124.8 |
| 800 | 850 | 6.8 | 88.2 | 23.3 | 148.0 |
| 750 | 800 | 7.9 | 96.1 | 29.5 | 177.5 |
| 700 | 750 | 6.2 | 102.4 | 25.1 | 202.6 |
| 650 | 700 | 5.1 | 107.4 | 21.9 | 224.5 |
| 600 | 650 | 6.2 | 113.6 | 28.6 | 253.1 |
| 550 | 600 | 7.0 | 120.7 | 34.7 | 287.8 |
| 500 | 550 | 7.6 | 128.2 | 38.8 | 326.6 |
| 450 | 500 | 7.9 | 136.2 | 42.5 | 369.1 |
| 400 | 450 | 8.0 | 144.2 | 44.8 | 413.9 |
| 350 | 400 | 9.9 | 154.1 | 58.7 | 472.6 |
| 300 | 350 | 8.0 | 162.0 | 50.8 | 523.4 |
| 250 | 300 | 6.0 | 168.1 | 40.3 | 563.6 |
| 200 | 250 | 6.0 | 174.1 | 41.9 | 605.5 |
| 150 | 200 | 5.6 | 179.6 | 40.9 | 646.4 |
| 100 | 150 | 5.6 | 185.2 | 43.9 | 690.3 |
| 50 | 100 | 3.9 | 189.1 | 33.3 | 723.6 |
| 0 | 50 | 5.0 | 194.2 | 46.1 | 769.7 |

Skeiðarársandur (Gígja) water drainage basin

| Elevation (m a. s. l.) | ΔS km^2 | $\Sigma \Delta S$ km^2 | ΔQ_s (10^6m^3) | $\Sigma \Delta Q_s$ (10^6m^3) |
|---------------------------|-----------------------------|------------------------------------|-------------------------------------|--|
|---------------------------|-----------------------------|------------------------------------|-------------------------------------|--|

| | | | | | |
|------|------|-------|--------|-------|--------|
| 1700 | 1750 | 0.0 | 0.0 | 0.0 | 0.0 |
| 1650 | 1700 | 15.9 | 15.9 | 6.5 | 6.5 |
| 1600 | 1650 | 65.3 | 81.2 | 19.8 | 26.3 |
| 1550 | 1600 | 82.4 | 163.6 | 26.4 | 52.7 |
| 1500 | 1550 | 110.7 | 274.3 | 47.8 | 100.5 |
| 1450 | 1500 | 106.4 | 380.7 | 69.7 | 170.2 |
| 1400 | 1450 | 103.6 | 484.3 | 82.6 | 252.8 |
| 1350 | 1400 | 90.7 | 575.0 | 84.5 | 337.3 |
| 1300 | 1350 | 77.4 | 652.4 | 83.1 | 420.4 |
| 1250 | 1300 | 68.7 | 721.1 | 85.9 | 506.3 |
| 1200 | 1250 | 59.7 | 780.8 | 86.8 | 593.1 |
| 1150 | 1200 | 54.1 | 834.9 | 91.7 | 684.8 |
| 1100 | 1150 | 50.3 | 885.2 | 97.4 | 782.2 |
| 1050 | 1100 | 45.4 | 930.6 | 104.0 | 886.2 |
| 1000 | 1050 | 40.0 | 970.6 | 104.4 | 990.6 |
| 950 | 1000 | 39.4 | 1010.0 | 112.4 | 1103.0 |
| 900 | 950 | 35.8 | 1045.8 | 109.5 | 1212.5 |
| 850 | 900 | 37.6 | 1083.4 | 123.2 | 1335.7 |
| 800 | 850 | 32.1 | 1115.5 | 114.8 | 1450.5 |
| 750 | 800 | 28.3 | 1143.8 | 110.2 | 1560.7 |
| 700 | 750 | 23.6 | 1167.4 | 98.0 | 1658.7 |
| 650 | 700 | 21.9 | 1189.3 | 97.3 | 1756.0 |
| 600 | 650 | 14.5 | 1203.8 | 70.5 | 1826.5 |
| 550 | 600 | 20.0 | 1223.8 | 103.7 | 1930.2 |
| 500 | 550 | 21.9 | 1245.7 | 120.8 | 2051.0 |
| 450 | 500 | 16.5 | 1262.2 | 93.8 | 2144.8 |
| 400 | 450 | 11.4 | 1273.6 | 68.3 | 2213.1 |
| 350 | 400 | 11.5 | 1285.1 | 70.7 | 2283.8 |
| 300 | 350 | 12.9 | 1298.0 | 82.2 | 2366.0 |
| 250 | 300 | 13.1 | 1311.1 | 88.1 | 2454.1 |
| 200 | 250 | 11.6 | 1322.7 | 83.0 | 2537.1 |
| 150 | 200 | 11.6 | 1334.3 | 86.9 | 2624.0 |
| 100 | 150 | 9.6 | 1343.9 | 75.8 | 2699.8 |
| 50 | 100 | 6.8 | 1350.7 | 55.6 | 2755.4 |
| 0 | 50 | 3.5 | 1354.2 | 29.9 | 2785.3 |

Djúpá water drainage basin

| Elevation (m a. s. l.) | ΔS km^2 | $\Sigma \Delta S$ km^2 | ΔQ_s (10^6m^3) | $\Sigma \Delta Q_s$ (10^6m^3) |
|---------------------------|-----------------------------|------------------------------------|-------------------------------------|--|
|---------------------------|-----------------------------|------------------------------------|-------------------------------------|--|

| | | | | | |
|------|------|-----|------|------|-------|
| 1450 | 1500 | 0.1 | 0.1 | 0.1 | 0.1 |
| 1400 | 1450 | 0.3 | 0.4 | 0.4 | 0.5 |
| 1350 | 1400 | 0.6 | 1.0 | 0.9 | 1.4 |
| 1300 | 1350 | 3.4 | 4.4 | 5.1 | 6.5 |
| 1250 | 1300 | 3.2 | 7.5 | 5.2 | 11.8 |
| 1200 | 1250 | 2.9 | 10.4 | 5.4 | 17.2 |
| 1150 | 1200 | 3.2 | 13.6 | 7.0 | 24.2 |
| 1100 | 1150 | 5.0 | 18.7 | 12.5 | 36.7 |
| 1050 | 1100 | 5.0 | 23.6 | 14.4 | 51.1 |
| 1000 | 1050 | 8.4 | 32.1 | 26.3 | 77.4 |
| 950 | 1000 | 7.3 | 39.3 | 24.5 | 101.9 |
| 900 | 950 | 7.4 | 46.7 | 26.6 | 128.5 |
| 850 | 900 | 6.0 | 52.7 | 23.4 | 151.9 |
| 800 | 850 | 5.8 | 58.5 | 23.8 | 175.7 |
| 750 | 800 | 5.9 | 64.4 | 26.3 | 202.0 |
| 700 | 750 | 3.6 | 68.1 | 17.4 | 219.3 |
| 650 | 700 | 2.0 | 70.1 | 10.0 | 229.3 |
| 600 | 650 | 0.1 | 70.1 | 0.5 | 229.8 |

Brunná water drainage basin

| Elevation (m a. s. l.) | ΔS km^2 | $\Sigma \Delta S$ km^2 | ΔQ_s (10^6m^3) | $\Sigma \Delta Q_s$ (10^6m^3) |
|---------------------------|-----------------------------|------------------------------------|-------------------------------------|--|
|---------------------------|-----------------------------|------------------------------------|-------------------------------------|--|

| | | | | | |
|------|------|-----|------|------|-------|
| 1000 | 1050 | 0.7 | 0.7 | 2.1 | 2.1 |
| 950 | 1000 | 1.8 | 2.4 | 6.0 | 8.1 |
| 900 | 950 | 3.8 | 6.2 | 13.7 | 21.8 |
| 850 | 900 | 3.9 | 10.1 | 15.0 | 36.8 |
| 800 | 850 | 3.6 | 13.7 | 15.0 | 51.8 |
| 750 | 800 | 3.9 | 17.7 | 17.2 | 69.1 |
| 700 | 750 | 4.4 | 22.1 | 20.6 | 89.7 |
| 650 | 700 | 5.2 | 27.2 | 25.9 | 115.6 |
| 600 | 650 | 2.5 | 29.8 | 13.2 | 128.9 |
| 550 | 600 | 0.0 | 29.8 | 0.0 | 128.9 |

Hverfisfljót water drainage basin

| Elevation (m a. s. l.) | ΔS km ² | $\Sigma \Delta S$ km ² | ΔQ_s (10 ⁶ m ³) | $\Sigma \Delta Q_s$ (10 ⁶ m ³) |
|---------------------------|-------------------------------|--------------------------------------|---|--|
|---------------------------|-------------------------------|--------------------------------------|---|--|

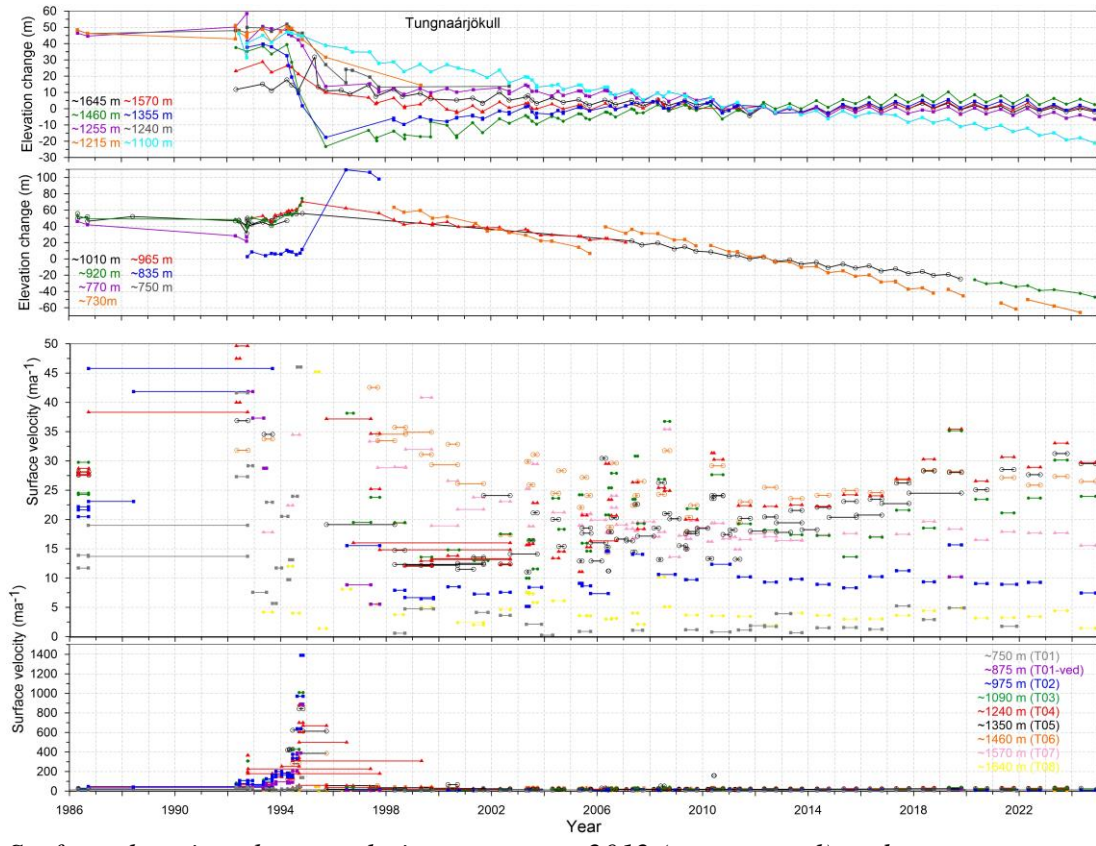
| | | | | | |
|------|------|------|-------|------|-------|
| 1700 | 1750 | 0.0 | 0.0 | 0.0 | 0.0 |
| 1650 | 1700 | 4.6 | 4.6 | 1.9 | 1.9 |
| 1600 | 1650 | 9.1 | 13.7 | 4.7 | 6.6 |
| 1550 | 1600 | 10.6 | 24.3 | 6.4 | 13.0 |
| 1500 | 1550 | 20.8 | 45.1 | 15.1 | 28.1 |
| 1450 | 1500 | 40.1 | 85.3 | 33.8 | 61.9 |
| 1400 | 1450 | 26.5 | 111.8 | 25.4 | 87.4 |
| 1350 | 1400 | 24.0 | 135.8 | 29.7 | 117.1 |
| 1300 | 1350 | 22.5 | 158.3 | 34.5 | 151.6 |
| 1250 | 1300 | 17.2 | 175.5 | 31.0 | 182.7 |
| 1200 | 1250 | 20.3 | 195.8 | 40.8 | 223.4 |
| 1150 | 1200 | 14.2 | 210.1 | 32.5 | 255.9 |
| 1100 | 1150 | 10.6 | 220.7 | 27.4 | 283.3 |
| 1050 | 1100 | 9.4 | 230.1 | 27.3 | 310.6 |
| 1000 | 1050 | 8.4 | 238.5 | 26.6 | 337.2 |
| 950 | 1000 | 8.5 | 247.0 | 28.9 | 366.0 |
| 900 | 950 | 7.5 | 254.5 | 26.9 | 392.9 |
| 850 | 900 | 7.9 | 262.4 | 30.2 | 423.2 |
| 800 | 850 | 6.7 | 269.0 | 27.4 | 450.5 |
| 750 | 800 | 7.5 | 276.6 | 32.9 | 483.5 |
| 700 | 750 | 9.5 | 286.0 | 44.3 | 527.7 |
| 650 | 700 | 11.1 | 297.2 | 55.9 | 583.6 |
| 600 | 650 | 6.3 | 303.4 | 33.1 | 616.8 |
| 550 | 600 | 0.0 | 303.5 | 0.2 | 617.0 |

Skaftá water drainage basin

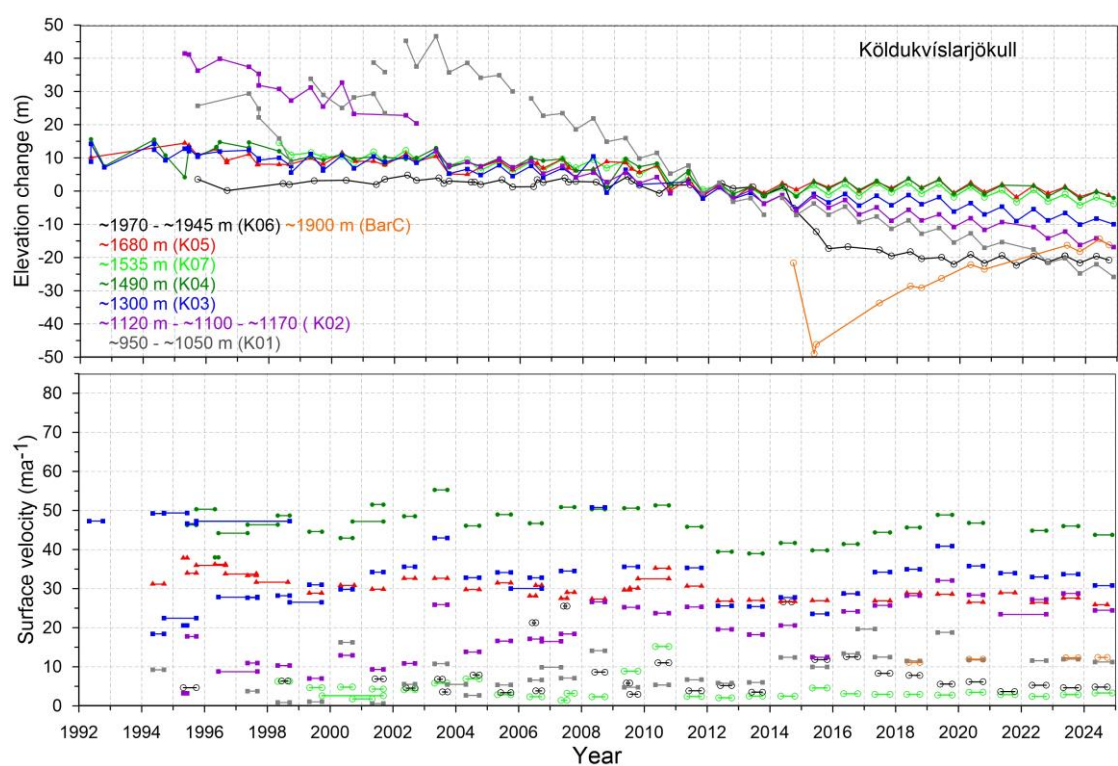
| Elevation (m a. s. l.) | ΔS km ² | $\Sigma \Delta S$ km ² | ΔQ_s (10 ⁶ m ³) | $\Sigma \Delta Q_s$ (10 ⁶ m ³) |
|---------------------------|-------------------------------|--------------------------------------|---|--|
|---------------------------|-------------------------------|--------------------------------------|---|--|

| | | | | | |
|------|------|------|-------|------|--------|
| 1650 | 1700 | 2.0 | 2.0 | 1.2 | 1.2 |
| 1600 | 1650 | 14.9 | 16.9 | 9.0 | 10.2 |
| 1550 | 1600 | 22.9 | 39.8 | 15.7 | 25.9 |
| 1500 | 1550 | 31.9 | 71.7 | 25.7 | 51.6 |
| 1450 | 1500 | 24.6 | 96.3 | 21.6 | 73.3 |
| 1400 | 1450 | 22.4 | 118.6 | 25.1 | 98.3 |
| 1350 | 1400 | 20.4 | 139.0 | 30.2 | 128.6 |
| 1300 | 1350 | 22.1 | 161.1 | 40.6 | 169.2 |
| 1250 | 1300 | 14.8 | 175.9 | 32.5 | 201.7 |
| 1200 | 1250 | 20.2 | 196.1 | 52.1 | 253.8 |
| 1150 | 1200 | 22.0 | 218.0 | 64.8 | 318.7 |
| 1100 | 1150 | 23.1 | 241.1 | 75.7 | 394.4 |
| 1050 | 1100 | 21.8 | 262.9 | 79.1 | 473.5 |
| 1000 | 1050 | 24.8 | 287.8 | 99.5 | 573.0 |
| 950 | 1000 | 20.0 | 307.8 | 88.2 | 661.1 |
| 900 | 950 | 16.6 | 324.5 | 78.5 | 739.6 |
| 850 | 900 | 13.6 | 338.0 | 68.0 | 807.6 |
| 800 | 850 | 13.5 | 351.5 | 71.8 | 879.4 |
| 750 | 800 | 12.5 | 364.0 | 70.3 | 949.7 |
| 700 | 750 | 10.1 | 374.1 | 59.7 | 1009.4 |
| 650 | 700 | 5.5 | 379.5 | 33.9 | 1043.3 |
| 600 | 650 | 0.6 | 380.1 | 3.5 | 1046.8 |

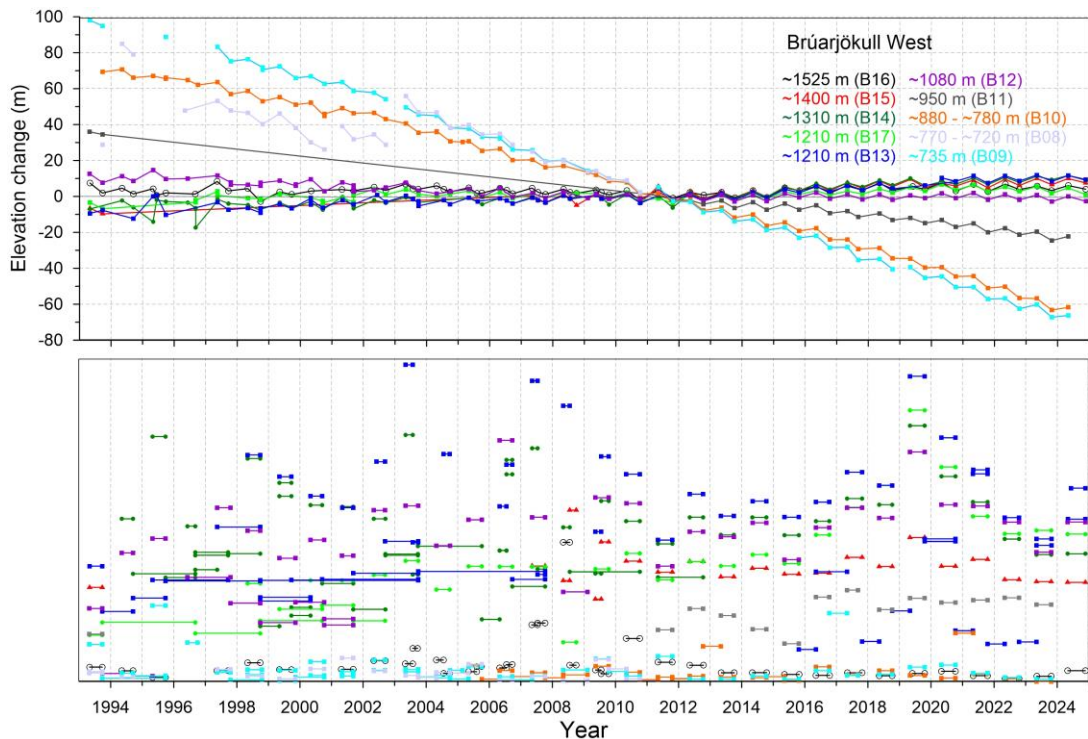
Appendix F: Records of surface elevation change a surface velocity at mass balance survey sites on Vatnajökull.



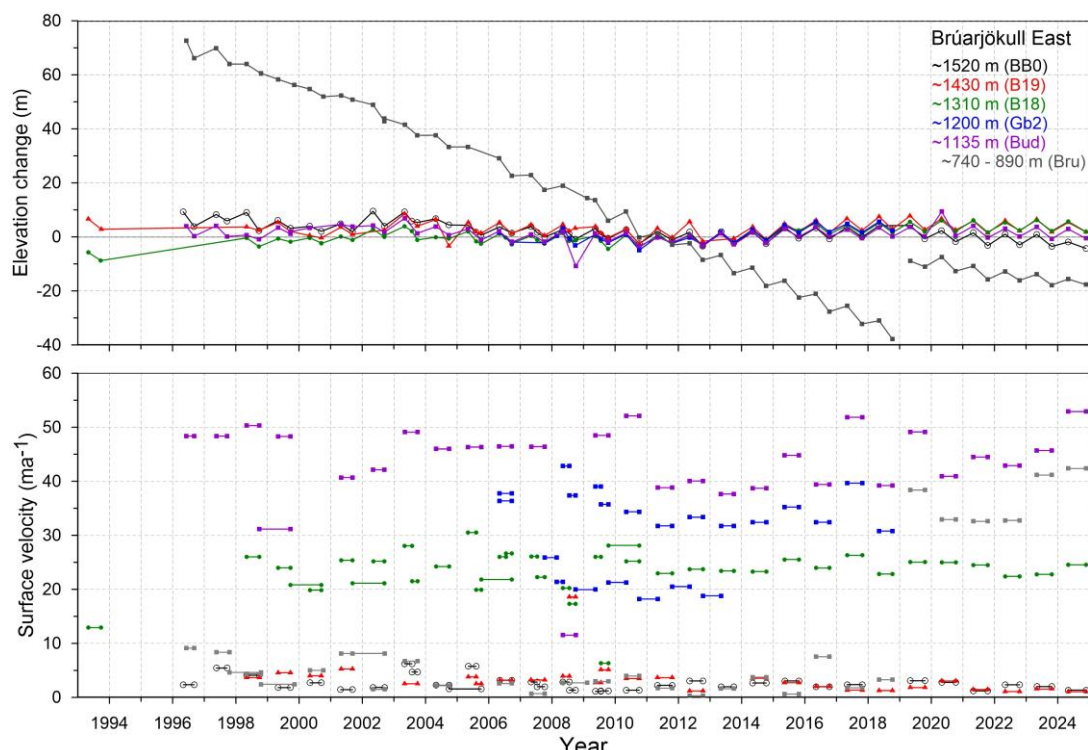
Surface elevation change relative to summer 2012 (upper panel) and average surface velocity (lower panel) at mb sites on Tungnaárljökull in 1986 to 2024.



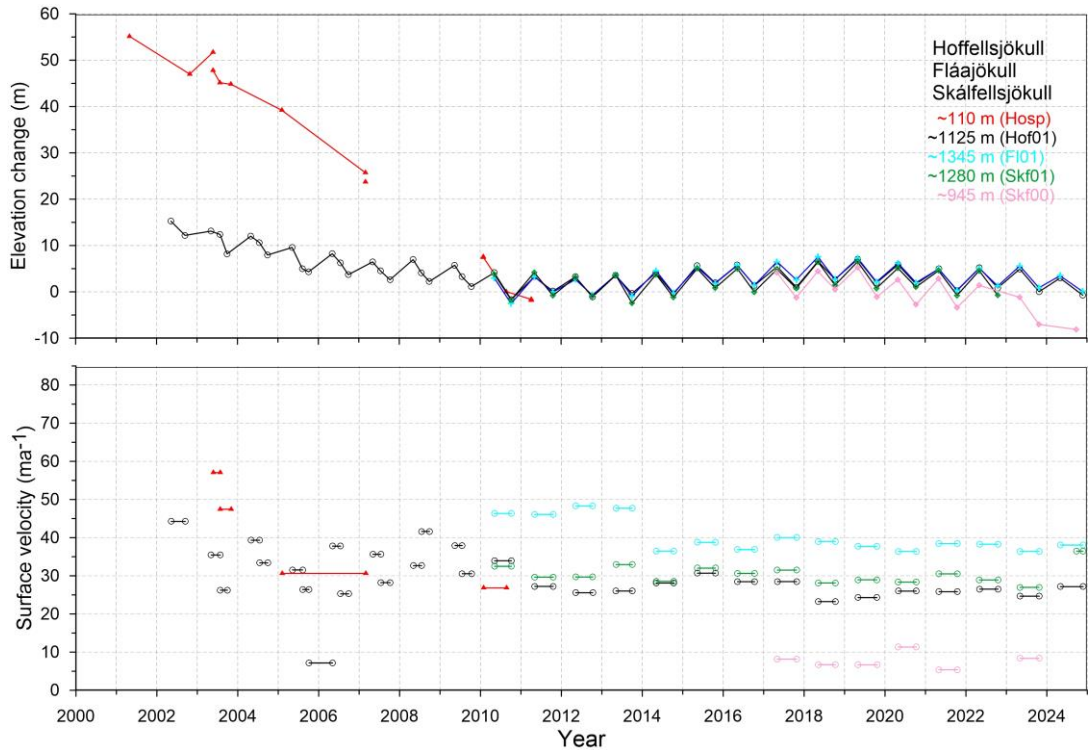
Surface elevation change relative to summer 2011-12 (upper panel) and average surface velocity (lower panel) at mb sites on Köldukvíslarjökull in 1992 to 2024.



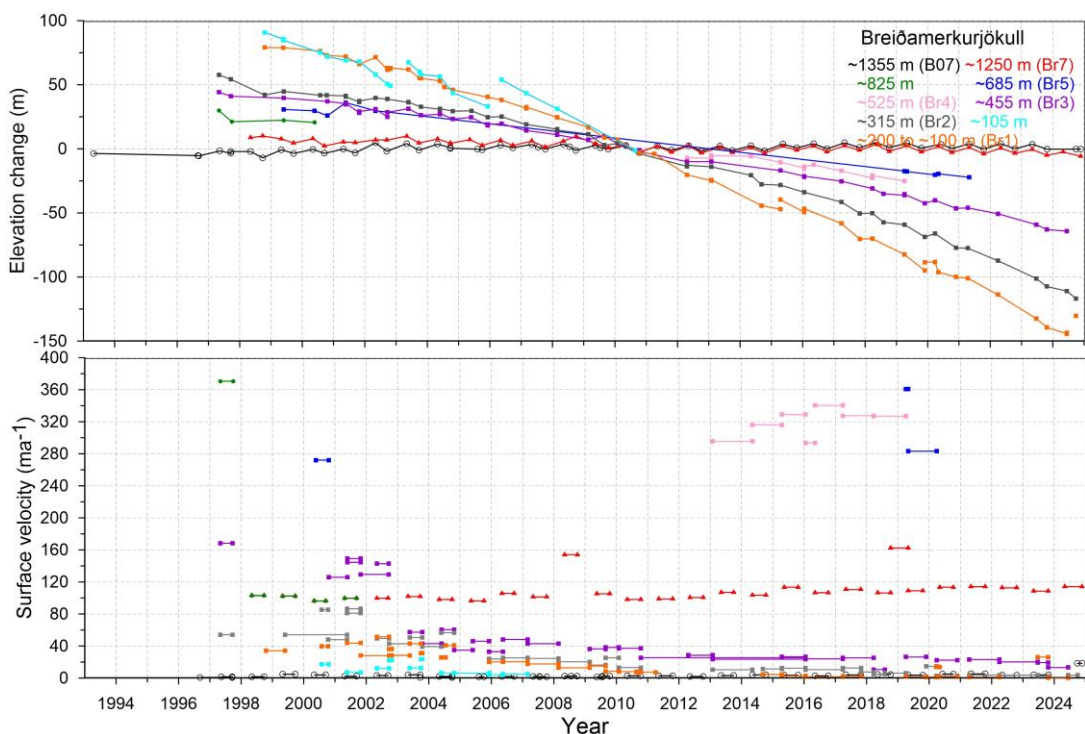
Surface elevation change relative to summer 2011 (upper panel) and average surface velocity at mb sites (lower panel) on W-Brúarjökull in 1993 to 2024.



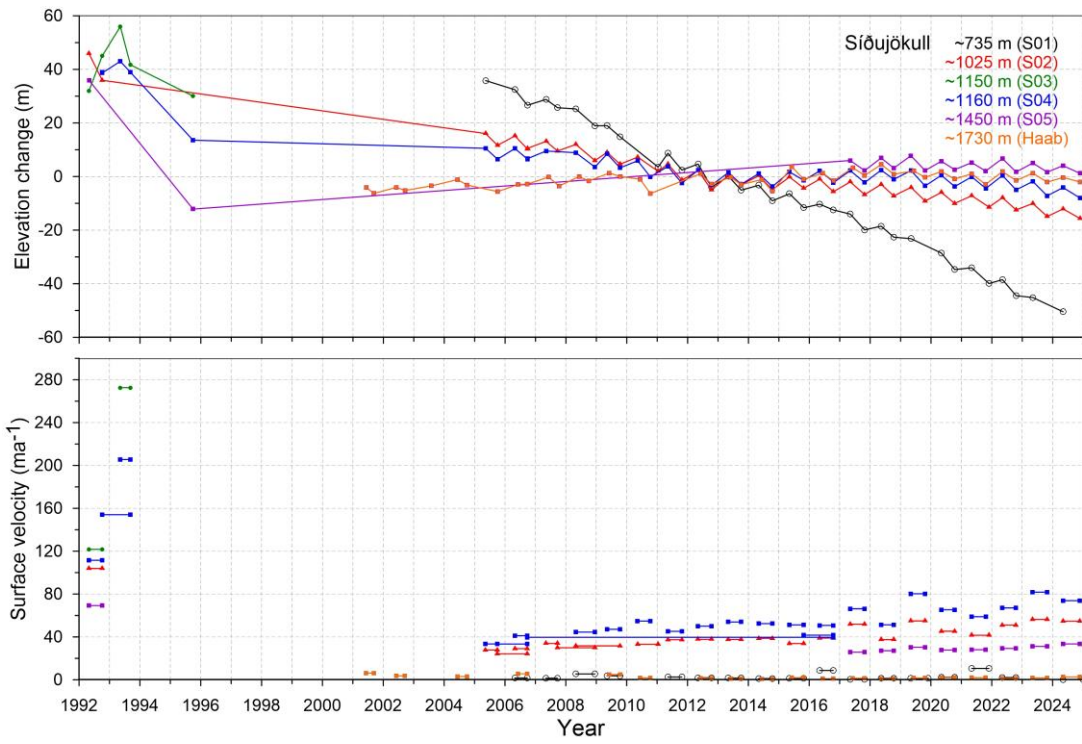
Surface elevation change relative to summer 2010 (upper panel) and average surface velocity at mb sites (lower panel) on E-Brúarjökull in 1993 to 2024.



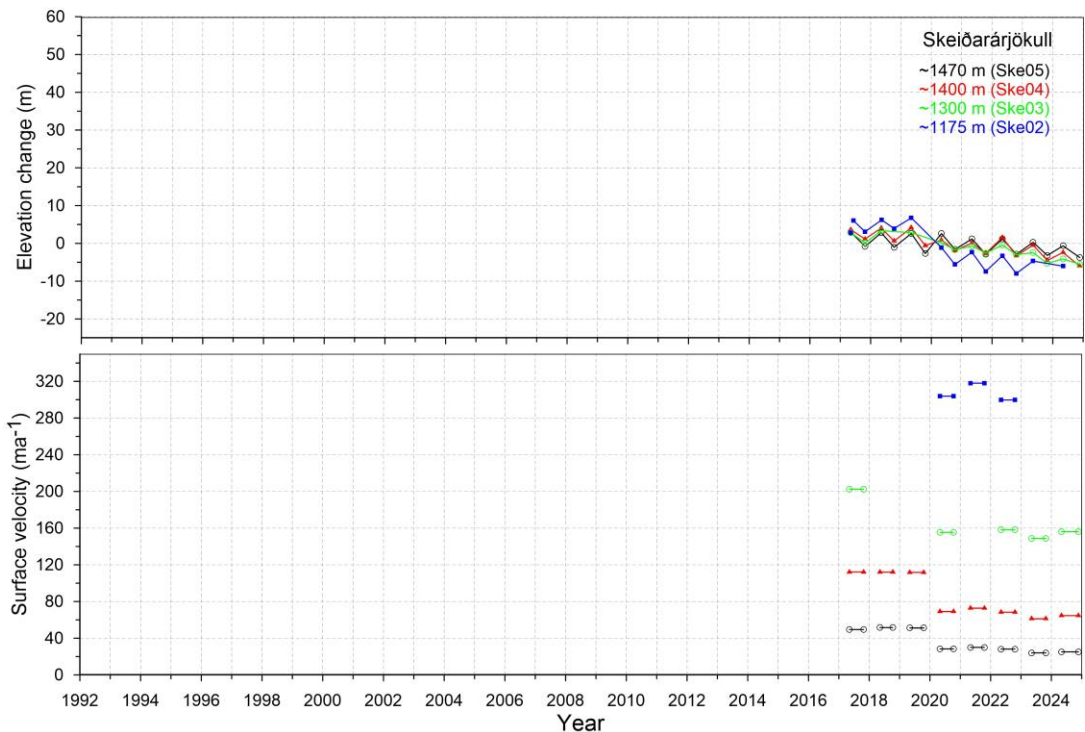
Surface elevation change relative to summer 2010 (upper panel) and average surface velocity) at mb sites (lower panel) on SE-Vatnajökull outlets in 2000 to 2024.



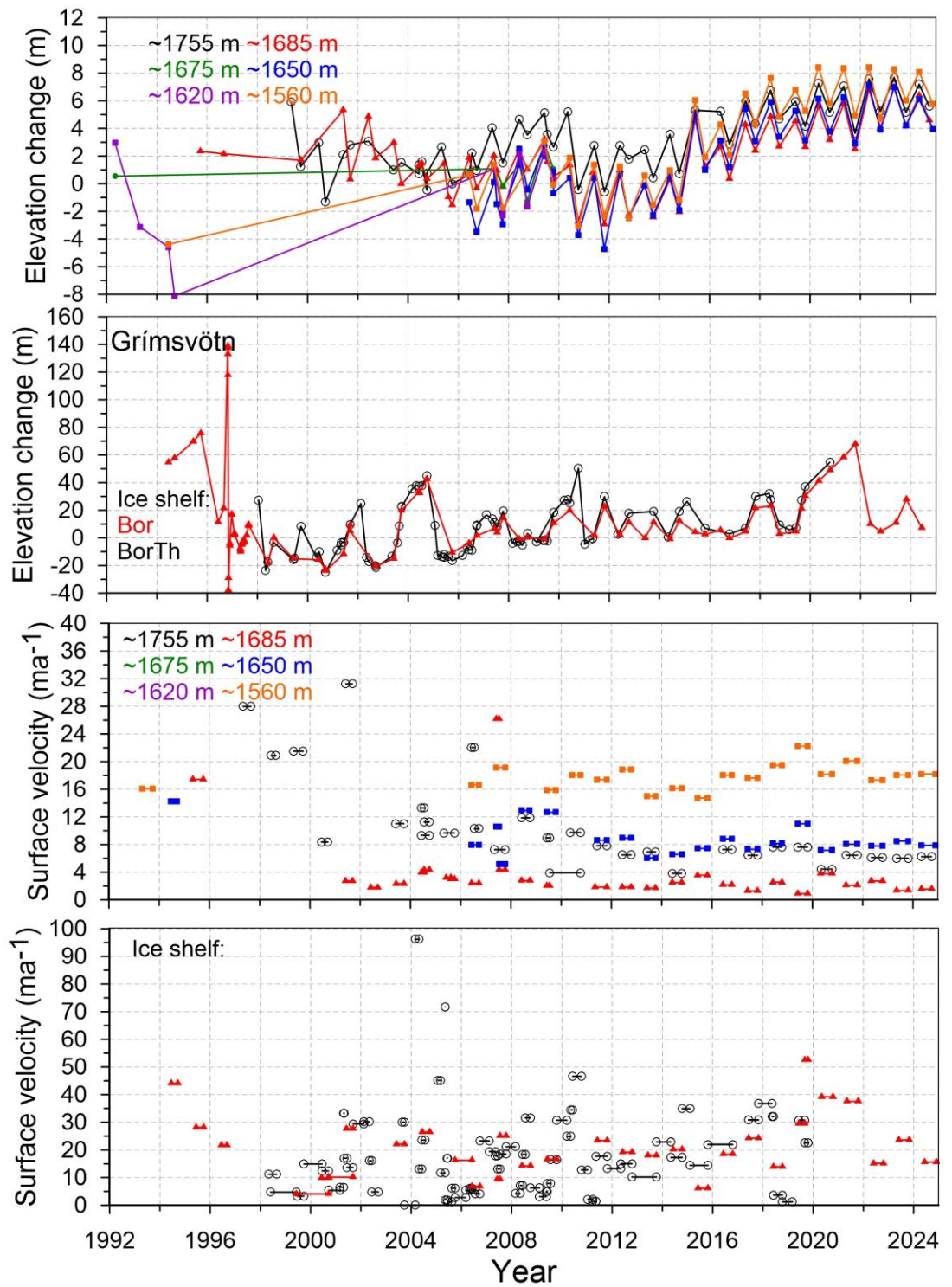
Surface elevation change relative to summer 2010 (upper panel) and average surface velocity at mb sites (lower panel) on Breiðamerkurjökull in 1993 to 2024.



Surface elevation change relative to summer 2012 (upper panel) and average surface velocity at mb sites (lower panel) on Síðujökull in 1992 to 2024.



Surface elevation change relative to summer 2011-12 (upper panel) and average surface velocity at mb sites (lower panel) on Skeiðarárjökull in 2017 to 2024.



Surface elevation change relative to summer 2012 (upper panels) and average surface velocity at mb sites (lower panels) in Grímsvötn ice catchment in 1993 to 2024.